NATIONAL ADVISORY COMMITTEE FOR AERONAUTICS

ADVANCE [redacted] REPORT

HIGH-SPEED WIND-TUNNEL TESTS OF A 0.3-SCALE MODEL OF THE P-47D AIRPLANE

By William T. Hamilton and Lee E. Boddy

Ames Aeronautical Laboratory
Moffett Field, Calif.

Washington
May 1945

NACA ACR No. 5D20 [redacted]

NATIONAL ADVISORY COMMITTEE FOR AERONAUTICS

ADVANCE [redacted] REPORT

HIGH-SPEED WIND-TUNNEL TESTS OF A 0.3-SCALE MODEL OF THE P-47D AIRPLANE

By William T. Hamilton and Lee E. Boddy

SUMMARY

Presented in this report are the results of high-speed wind-tunnel tests of a 0.3-scale model of the P-47D airplane. Included are the aerodynamic characteristics of the model, pressure distributions on the wing and horizontal tail, elevator hinge moments, and tuft photographs showing the flow over the wing and horizontal tail.

The results indicate that, at level-flight lift coefficients, the P-47D airplane will not exhibit a diving tendency below a Mach number of 0.78 at an altitude of 20,000 feet or below a Mach number of 0.72 at an altitude of 40,000 feet. The Mach number at which the lift, drag, and pitching-moment coefficients diverged rapidly from the low-speed values is about 0.15 higher than the critical Mach number. This is an unusually large margin.

INTRODUCTION

As the speed of an airplane approaches the speed of sound, drastic changes in its aerodynamic characteristics generally take place. In order to approach logically the problems encountered in high-speed flight, it is necessary to determine these high-speed characteristics and the degree to which they vary from those at low speed.

This report presents the results of tests of a 0.3-scale model of the P-47D airplane which were carried out in the Ames 16-foot wind tunnel in order to obtain information concerning the high-speed characteristics, especially the longitudinal stability, trim, and control. Reference 1

[redacted]

[redacted]

presents the results of tests of this same model to determine the usefulness of dive-recovery flaps under the wing in gaining additional longitudinal control.

MODEL AND APPARATUS

The 0.3-scale model of the P-47D airplane was designed and built by the Ames Aeronautical Laboratory. The wing, fuselage, vertical fin, and horizontal stabilizer were each constructed of a steel spar covered with mahogany. The rudder and elevator were cast of aluminum and the engine cowl was formed from sheet aluminum. The elevator deflection was controlled remotely through a unit which incorporated an electric motor for power, an electric strain gage for measuring the elevator hinge moments, and a selsyn motor for indicating the elevator angle.

Figure 1 is a three-view drawing of the model. The more important dimensions are as follows:

Wing area, sq ft	27.000
Wing span, ft	12.233
Mean aerodynamic chord, ft	2.187
Wing section	Republic S-3
Wing thickness at root, percent chord	15.0
Wing incidence at root, deg	1.00
Wing incidence at tip, deg	-2.96
Horizontal-tail area, sq ft	4.95
Horizontal-tail length (c.g. to elevator hinge line), ft	6.786
Horizontal-tail incidence, deg	2.8

The wing and horizontal-tail stations are denoted by their distances in inches along the surface from the center line of the model.

The model was supported in the wind tunnel by three

[redacted]

struts as shown in figure 2. Angle-of-attack variation was obtained by vertical movement of the rear strut. The forces and moments were recorded by self-balancing, recording, beam scales.

SYMBOLS

The symbols used in this report are defined as follows:

V	free-stream velocity, feet per second
q	free-stream dynamic pressure $\left(\frac{1}{2}\rho V^2\right)$, pounds per square foot
M	Mach number $\left(\frac{V}{\text{velocity of sound}}\right)$
S	wing area, square feet
M.A.C.	mean aerodynamic chord, feet
C_L	lift coefficient $\left(\frac{\text{lift}}{qS}\right)$
C_D	drag coefficient $\left(\frac{\text{drag}}{qS}\right)$
C_m	pitching-moment coefficient $\left(\frac{\text{pitching moment}}{qS\ \text{M.A.C.}}\right)$
α	angle of attack of the fuselage reference line, degrees
α_u	angle between the fuselage reference line and the tunnel center line, degrees
δ_e	elevator deflection, degrees
δ_t	elevator-tab deflection, degrees
i_T	angle between the stabilizer and the fuselage reference line, degrees
p_s	static pressure in free stream, pounds per square foot

[redacted]

p_L static pressure on the model surface, pounds per square foot

P pressure coefficient $\left(\frac{p_L - p_E}{q}\right)$

P_{cr} critical pressure coefficient (P at which the local velocity equals the local velocity of sound)

M_{cr} critical Mach number (free-stream Mach number at which P_{cr} is first reached on the model)

RESULTS

The model of the P-47D airplane was originally mounted on 13-percent-thick shielded struts for tests (fig. 2(a)) and later on an improved 5-percent-thick unshielded strut system (fig. 2(b)). The wing and tail tuft studies, elevator hinge moments, and horizontal-tail pressure distribution and effectiveness, presented in this report, were obtained from tests with the 12-percent-thick strut system. They have been checked and found to be essentially unaffected by the change of model-support system. All other data in this report were gained from tests with the improved 5-percent-thick strut system.

The wind-tunnel dynamic-pressure and Mach number calibrations, support-strut tares, and model-constriction correction were obtained in the manner described in reference 2.

The following corrections were applied to account for the effect of the wing-tunnel walls:

Angle-of-attack correction	$1.060\ C_L$ (deg)
Drag-coefficient correction	$0.0185\ C_L^2$
Pitching-moment coefficient correction . .	$0.0200\ C_L$

The pitching moments were referred to a center-of-gravity location 1.650 inches below the fuselage reference line and above the 27.5 percent point of the mean aerodynamic chord.

[redacted]

DISCUSSION

General Characteristics

The lift, drag, and pitching-moment characteristics of the P-47D airplane model are shown in figures 3 to 7. The lift changed only slightly with speed except that a sharp decrease in slope occurred at a successively lower lift coefficient for each higher Mach number. Up to a Mach number of 0.65 the lift-curve slope increased only half as much as predicted by Glauert's relation $\frac{1}{\sqrt{1-M^2}}$, and up to a Mach number of 0.815, the limit of the tests, the angle of attack for zero lift changed only slightly.

The drag coefficient remained essentially constant with speed up to a Mach number of 0.60, then started increasing slowly at the low lift coefficients and more rapidly at the high lift coefficients, and finally increased rapidly at all lift coefficients.

The variation of pitching-moment coefficient with Mach number was similar to that discussed in reference 3. Above the critical Mach number for each lift coefficient, the static longitudinal stability increased to three or four times the low-speed value. It should be noted that for lift coefficients of 0.1 or less, and through the range of Mach numbers included in the tests, the change in the lift coefficient for balance was small. The pitching-moment coefficients for the model without the tail indicated negative stability up to a Mach number of 0.69; then the stability increased until, at a Mach number of 0.815, it was essentially neutral. This increase of stability at high speed, due to the wing and fuselage alone, was equal to one-half the stability increase of the complete model.

Wing

The wing pressure distribution was measured at two stations, 10.80 (figs. 8 to 15) and 30.00 inches from the center of the span (figs. 16 to 23). Station 10.80 was just outboard of the wing fillet and had slightly greater negative pressure coefficients than station 30.00 until well past the critical Mach number.

[redacted]

As soon as the peak-pressure coefficient ceased to increase with speed, the pressure coefficients at station 30.00 became more negative than those at station 10.80. The pressure variation over the upper surface of the wing at constant angle of attack remained similar to that at low speed until the critical Mach number was exceeded by 15 to 20 percent, after which the peak-pressure coefficient became less negative and separation of the flow occurred at the higher angles of attack. The pressure variation changed in a like manner over the lower surface of the wing except for the formation of twin pressure peaks above the critical-pressure coefficient at high speeds and negative angles of attack.

The tuft photographs for the upper surface of the wing (figs. 24 to 26) indicated no areas of rough flow for lift coefficients below 0.7 and a Mach number of 0.59, or at a Mach number of 0.73 for lift coefficients near zero. The first area of rough flow to appear was a narrow band at about 30 percent of the chord, and it extended outward from the wing root about one-third of the semispan. This band of rough flow appeared at about 0.72 lift coefficient and 0.59 Mach number, and was found at lower lift coefficients and higher Mach numbers up to about 0.24 lift coefficient at 0.73 Mach number. The flow aft of this band was nearly as smooth as that ahead of it (fig. 26). From the pressure distribution at station 10.80 (figs. 11(a), 12(a), and 13(a)), it is apparent that this band was always at a point where the pressure coefficient suddenly dropped from a much higher negative value to a point below the critical value and then decreased over the rest of the chord about the same as at low speeds. This band of rough flow is apparently caused by a compression shock, which does not cause separation, as there is smooth flow and a complete pressure recovery aft of the shock. This pressure recovery for Mach numbers well above the critical and even above that at which a shock was well developed partially accounts for the delay of compressibility effects on the characteristics of this model. When the angle of attack or Mach number was further increased above the value at which the band of rough flow appeared, the flow aft of this band also became rough and appeared to be stalled, and the pressure recovery was not complete.

Tail

Figure 27 shows the variation of stabilizer effective-

ness with Mach number and lift coefficient, and figure 28 shows the variation of pitching-moment coefficient with elevator angle, Mach number, and lift coefficient. Increasing the Mach number had only a slight effect on the increment of pitching-moment coefficient resulting from a given increment of elevator angle, except at high speeds and high lift coefficients. It decreased 25 percent at 0.6 lift coefficient as the Mach number was increased from 0.64 to 0.68. The increase in static longitudinal stability renders the airplane more difficult to control, even though the elevator retains its ability to change the pitching moment at high speeds.

The variation of elevator hinge-moment coefficient with elevator angle is shown in figures 29 to 34. The slope of the hinge-moment curves increased from about -0.004 at 0.29 Mach number to about -0.003 at 0.73 Mach number. Varying the angle of attack had essentially no effect on the hinge-moment coefficients until high speeds and high lift coefficients were reached. Difficulty was encountered in measuring the hinge moments at Mach numbers above 0.70 due to the violent buffeting of the horizontal tail by the wing wake at angles of attack of 3° or more.

The chordwise pressure distribution over the horizontal tail is presented in figures 35 to 58 for stations 10.00 and 20.325. The peak-pressure coefficients were much less negative than the corresponding peak-pressure coefficients on the wing, indicating a higher critical Mach number for the tail. The chordwise variation of pressure coefficient maintained approximately the same pattern at high and low Mach numbers but changed with angle of attack. A small negative pressure peak near the nose of the upper surface at station 20.325 formed at the high angles of attack; this peak was also observed at 5° angle of attack and 0.73 Mach number at station 10.00.

The tuft photographs for the horizontal tail (figs. 59 to 61) show no change with Mach number or angle of attack except when the tail is in the wake of the wing at high speeds. As stated before, this occurred at about 0.70 Mach number and 3° angle of attack. When the tail was in the wing wake, it shook violently - moving up and down as much as an inch at the tips - and the tufts (fig. 61) indicated that the flow over the upper and lower surfaces were extremely rough. It would seem that the tail was not stalled, since the pitching-moment curves show no decrease in stability for these conditions.

[redacted]

Limiting Conditions

Figure 62 shows a summary of the limiting Mach numbers for the P-47D airplane as indicated by the tests of the 0.3-scale model. Also shown in this figure are the lift coefficients required for level flight with a wing loading of 45 pounds per square foot. Curves (a), (b), and (c) indicate that local velocities above the speed of sound were present on the P-47D airplane model at lift coefficients that correspond to level flight for all Mach numbers at an altitude of 40,000 feet, and for Mach numbers above 0.67 at sea level, and 0.60 at 30,000 feet. It will be noted that the Mach number at which the critical pressure coefficient on the wing was reached (curves (b) and (c)) was exceeded by about 0.08 before the peak-pressure coefficients on the wing started decreasing (curve (d)), and by about 0.15 before the sharp increase of static longitudinal stability was encountered (curve (h)). This is an unusually large difference. The changes in the general characteristics of the model occurred in the following order: (1) the drag rise (curve (f)), (2) the increase of longitudinal stability (curve (h)), and (3) the decrease in the slope of the lift curve (curve (g)). The Mach number at which the tufts first indicated that a shock wave had formed (curve (e)) was between the Mach number at which the peak-pressure coefficient on the wing decreased (curve (d)) and that at which the general aerodynamic characteristics changed (curves (f), (g), and (h)).

The diving tendency, encountered with any further increase of speed (curve (k)) is, to the pilot, the most important of the limiting conditions indicated by the curves in figure 62. This tendency appears at level-flight lift coefficients and with the elevators fixed at Mach numbers ranging from 0.78 at 20,000 feet altitude (554 mph) to 0.72 at 40,000 feet altitude (478 mph). The use of dive-recovery flaps on the wing for additional longitudinal control at high Mach numbers is discussed in reference 1.

Figure 63 shows the gliding velocity, Mach number, and elevator angle required for balance with zero elevator-tab deflection for the P-47D airplane as calculated from the model test results and from an extrapolation of the drag data (fig. 5). All glides were calculated on the assumptions of a starting speed of 250 miles per hour, an initial altitude of 40,000 feet, zero propeller thrust, and a wing loading of 45 pounds per square foot. It is of interest to note that for all three angles of glide, the maximum

[redacted]

Mach number attained was above that at which the drag coefficient started its rapid increase. In the vertical dive, the predicted maximum Mach number is 0.85 at 26,000 feet altitude, while the predicted maximum speed is 617 miles per hour at sea level. The predicted elevator angle, required for balance, in the 15° and 30° dives varies only about 6°; this is not considered excessive. In the vertical dive, the lack of elevator characteristics for Mach numbers above 0.78 prohibited the prediction of the elevator angle for balance over most of the dive. Calculations based on the high-speed data should be treated with reserve, owing to the extrapolation of the drag coefficients.

CONCLUDING REMARKS

1. The P-47D airplane should not encounter a diving tendency below an altitude of 20,000 feet and a Mach number of 0.78.

2. The critical Mach number is exceeded by about 0.08 before the peak-pressure coefficient on the wing starts to become less negative.

3. The critical Mach number is exceeded by about 0.15 before the sharp increase in static longitudinal stability is encountered. This margin is unusually large.

4. The unusually large difference between the critical Mach number and the Mach number at which the aerodynamic characteristics change markedly is apparently due to the fact that separation did not immediately follow formation of the shock. As the Mach number or angle of attack further increased, the shock became more severe and separation occurred.

5. On the basis of extrapolation of test data and the assumption of zero propeller thrust, the maximum Mach number attainable in a vertical dive is 0.85 at 26,000 feet altitude, and the terminal velocity is 617 miles per hour at sea level.

Ames Aeronautical Laboratory,
National Advisory Committee for Aeronautics,
Moffett Field, Calif.

[redacted]

REFERENCES

1. Hamilton, William T., and Boddy, Lee E.: High-Speed Wind-Tunnel Tests of Dive-Recovery Flaps on a 0.2-Scale Model of the P-47D Airplane. NACA ACR No. 5D19, 1945.

2. Nissen, James M., Gadeberg, Burnett L., and Hamilton, William T.: Correlation of the Drag Characteristics of a P-51B Airplane Obtained from High-Speed Wind-Tunnel and Flight Tests. NACA ACR No. 4K02, 1945.

3. Hood, Manley J., and Allen, H. Julian: The Problem of Longitudinal Stability and Control at High Speeds. NACA CB No. 3K18, 1943.

[redacted]

[redacted]

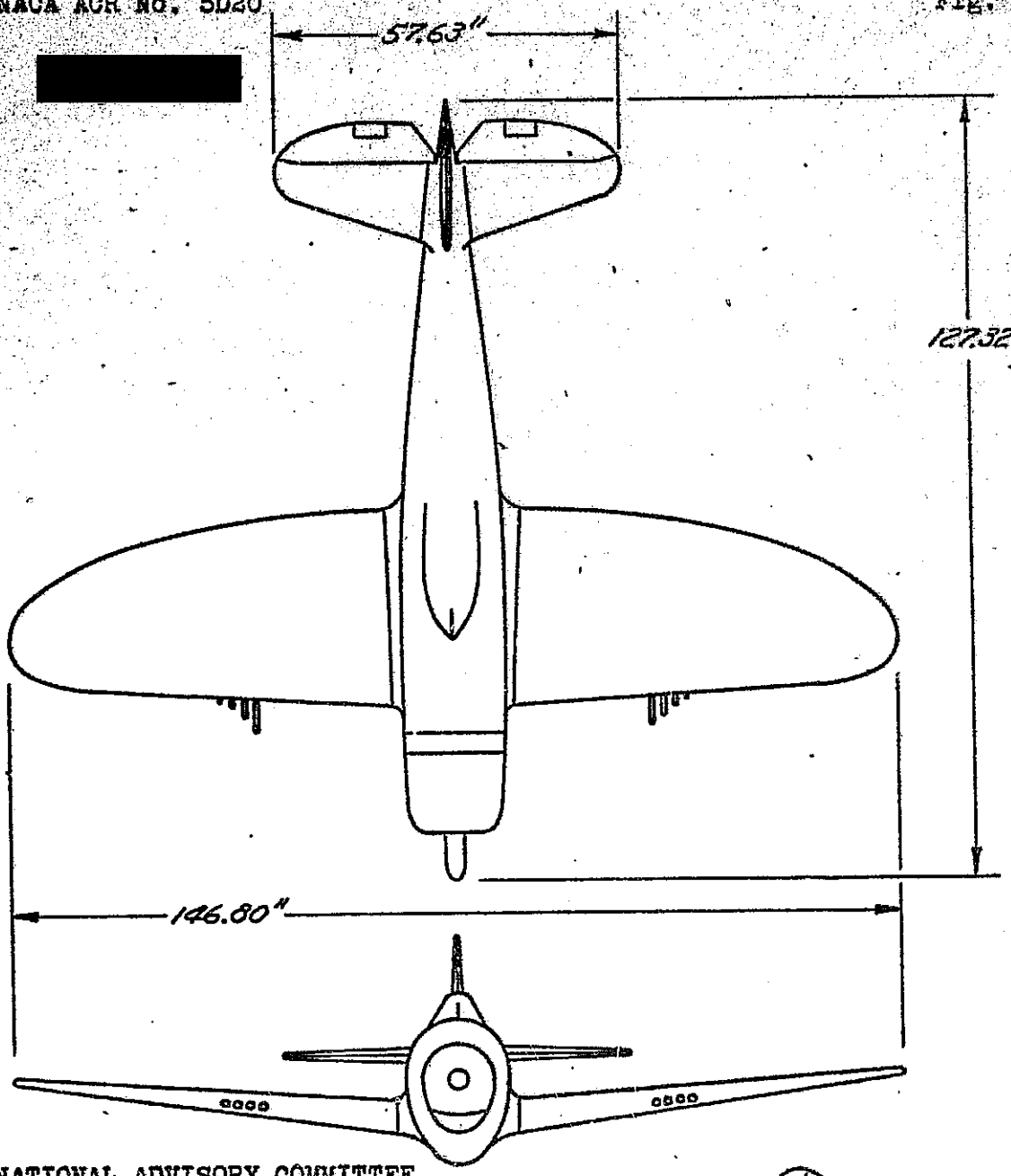

NATIONAL ADVISORY COMMITTEE
FOR AERONAUTICS

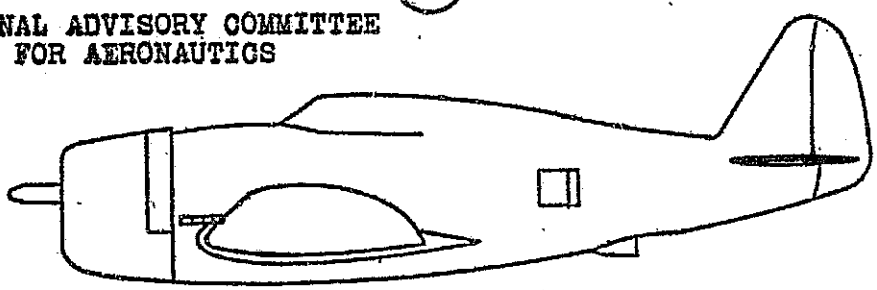

FIGURE 1.- THE 0.3-SCALE MODEL OF THE P-47D AIRPLANE

[redacted]

[redacted]

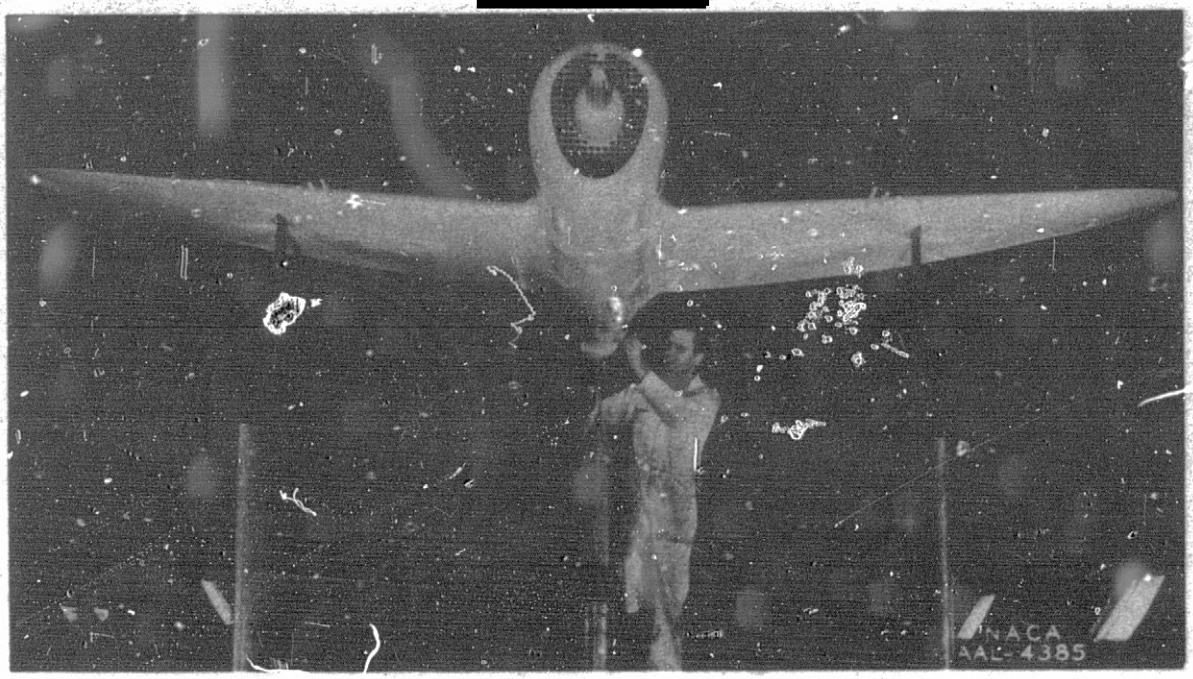

(a) Model on 12-percent-thick struts.

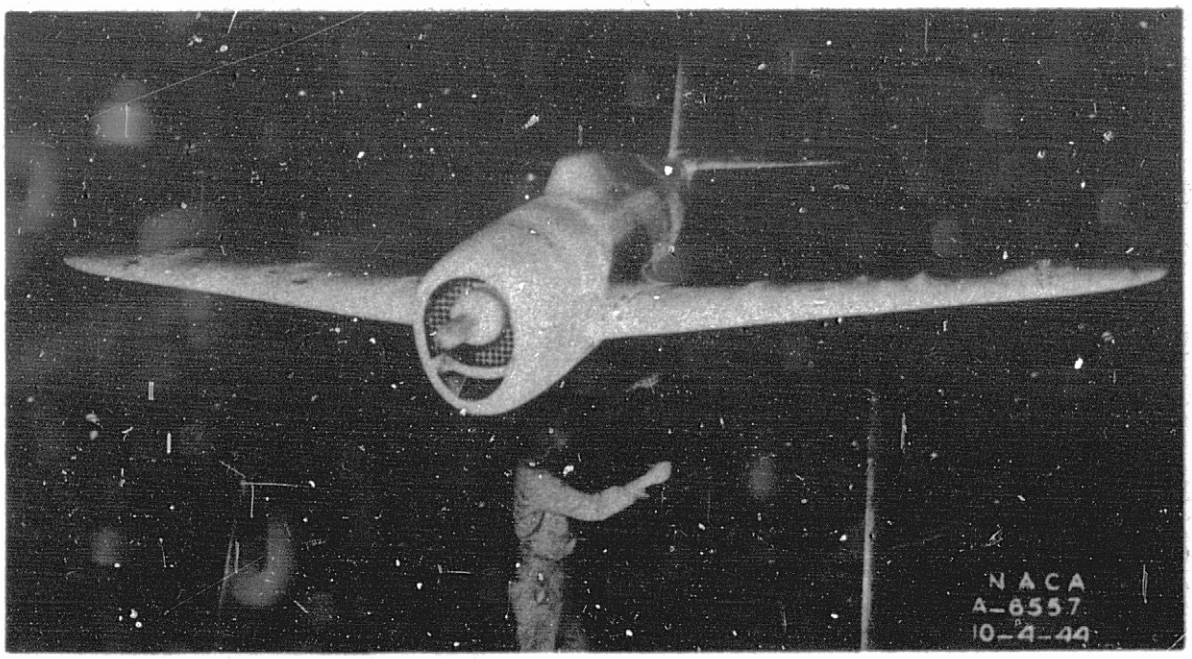

(b) Model on 5-percent-thick struts.

Figure 2.- The P-47D airplane model in the Ames 16-foot wind tunnel.

[redacted]

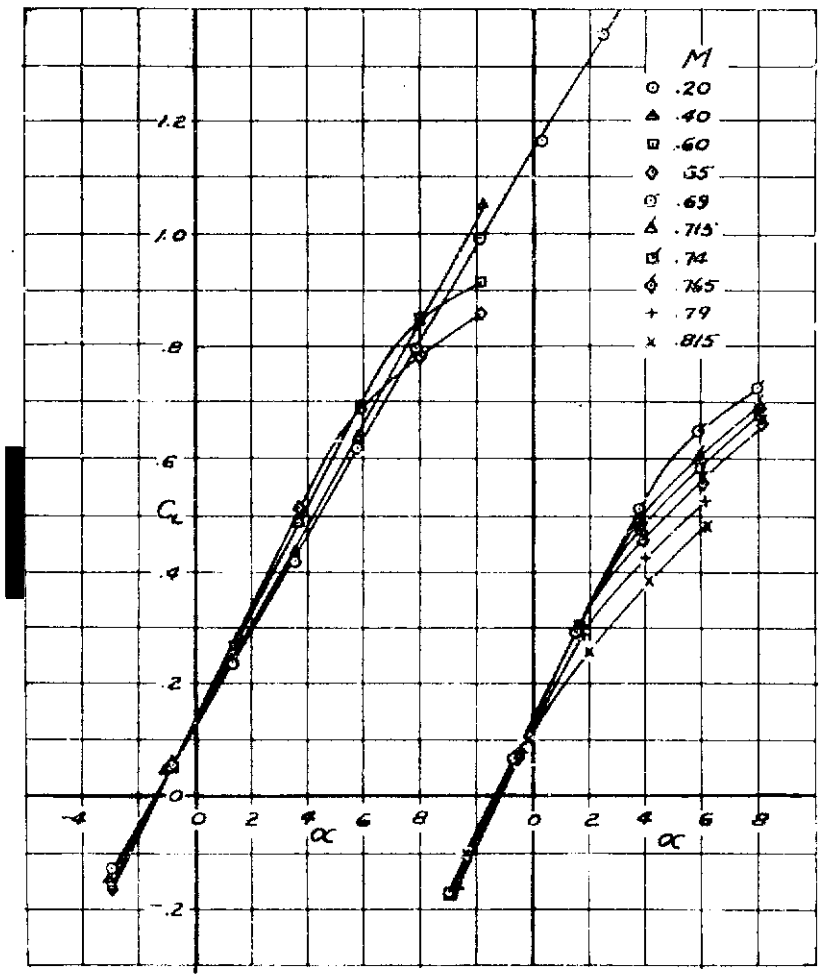

FIGURE 3.- VARIATION OF LIFT COEFFICIENT WITH ANGLE OF ATTACK OF THE P-47D AIRPLANE MODEL AT SEVERAL MACH NUMBERS.

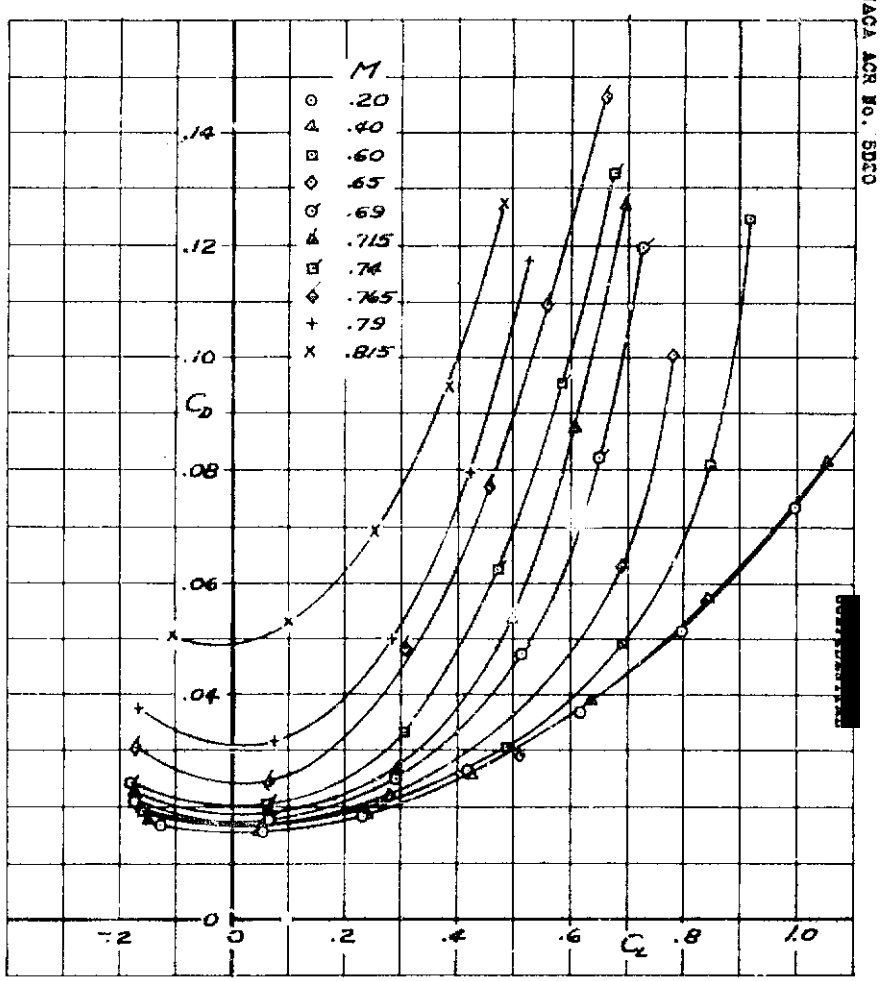

FIGURE 4.- VARIATION OF DRAG COEFFICIENT WITH LIFT COEFFICIENT OF THE P-47D AIRPLANE MODEL AT SEVERAL MACH NUMBERS.

[redacted]

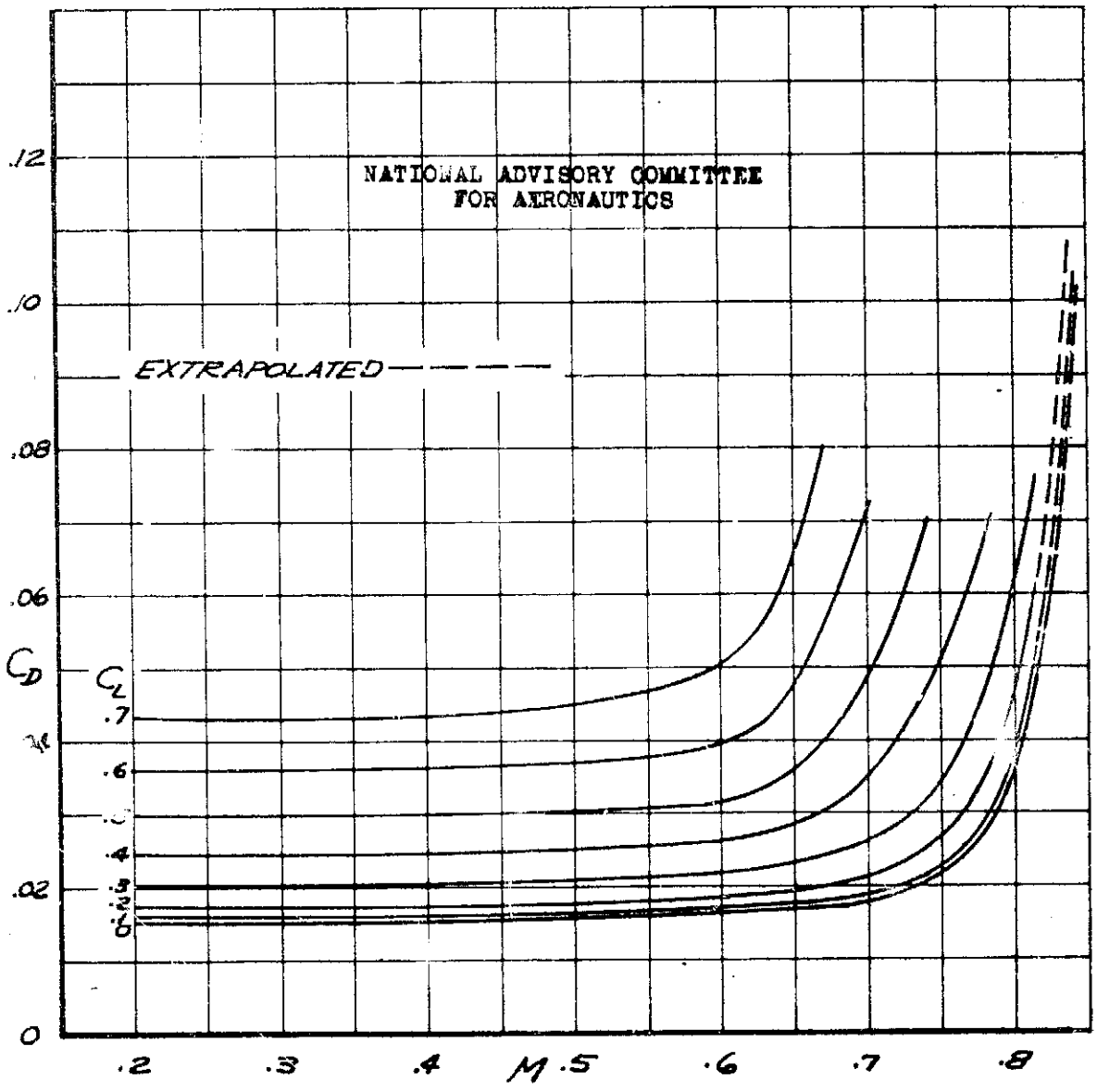

[redacted]

FIGURE 5 .— VARIATION OF DRAG COEFFICIENT WITH MACH NUMBER AT SEVERAL LIFT COEFFICIENTS. P-47D AIRPLANE MODEL.

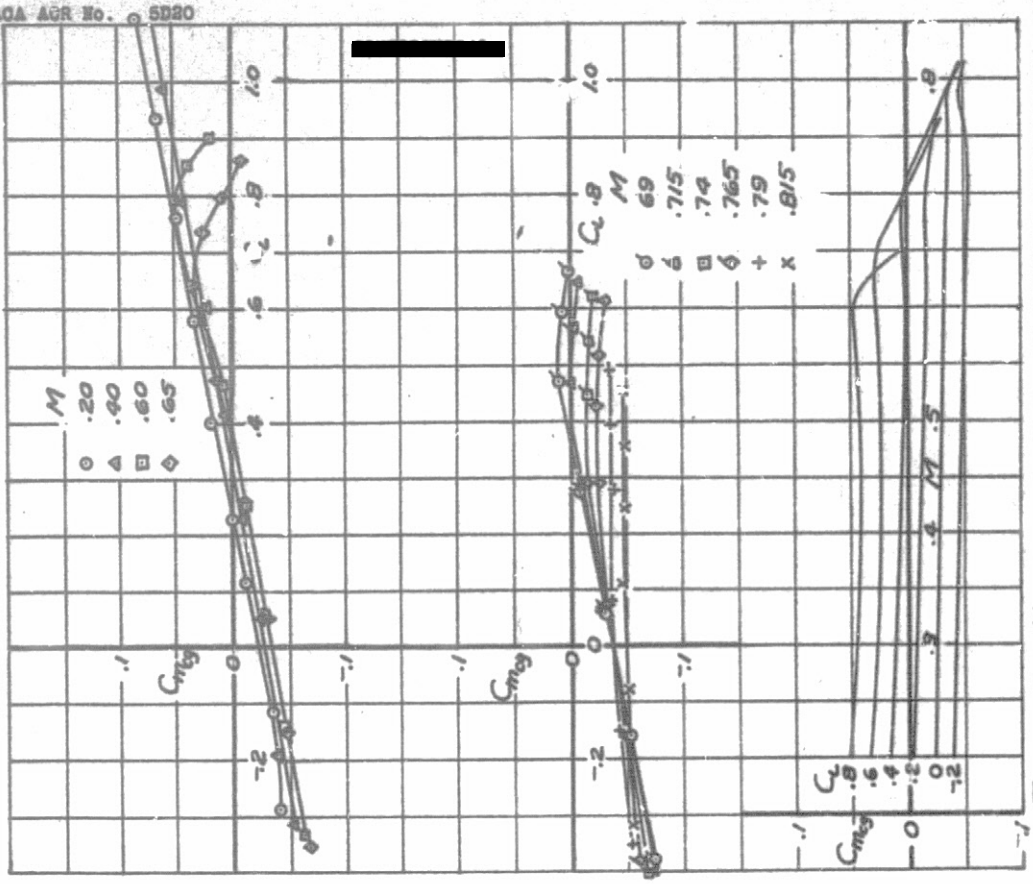

FIGURE 7.- VARIATION OF PITCHING-MOMENT COEFFICIENT WITH LIFT COEFFICIENT AND WITH MACH NUMBER. P-47D AIRPLANE MODEL, LESS TAIL.

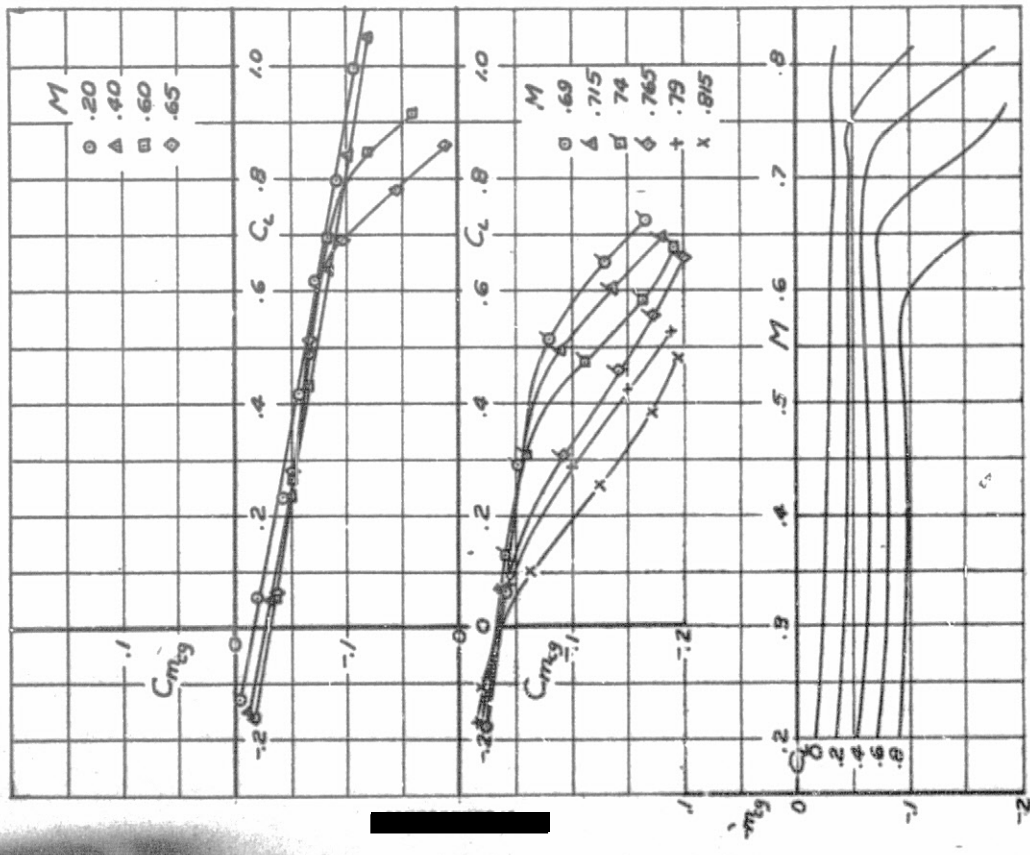

FIGURE 6.- VARIATION OF PITCHING-MOMENT COEFFICIENT WITH LIFT COEFFICIENT AND WITH MACH NUMBER. P-47D AIRPLANE MODEL.

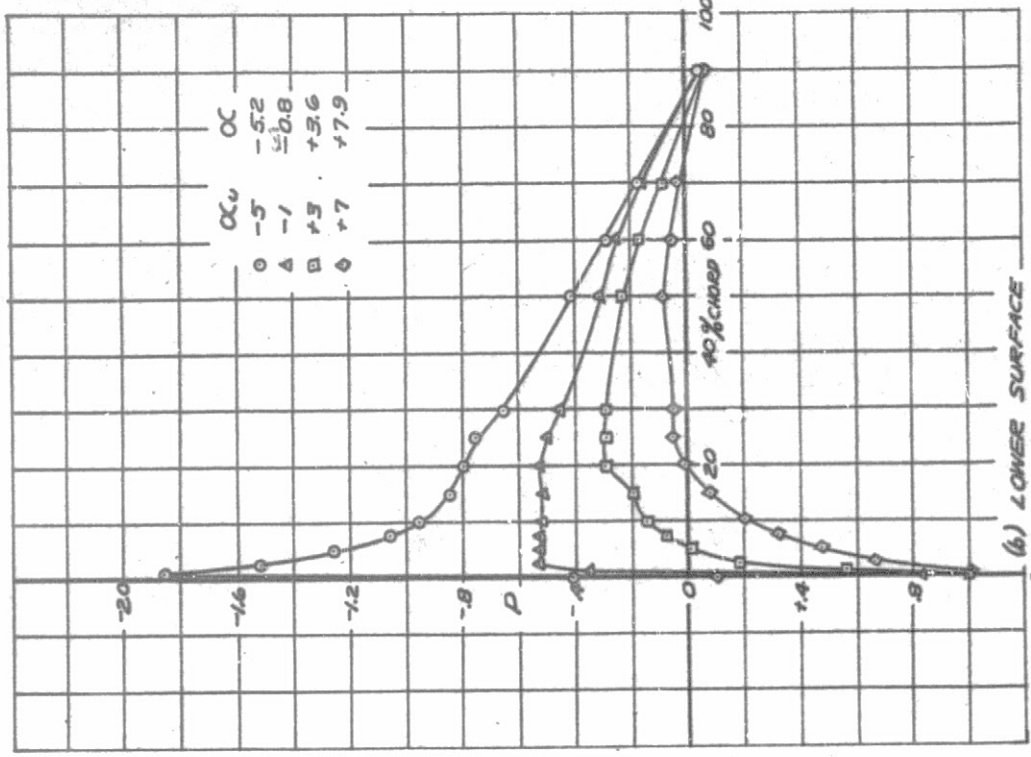

FIGURE 8(CONCLUDED).- PRESSURE DISTRIBUTION AT WING STATION 10.80 ON THE P-47D AIRPLANE MODEL. MACH NUMBER, 0.20.

(b) LOWER SURFACE

NATIONAL ADVISORY COMMITTEE
FOR AERONAUTICS

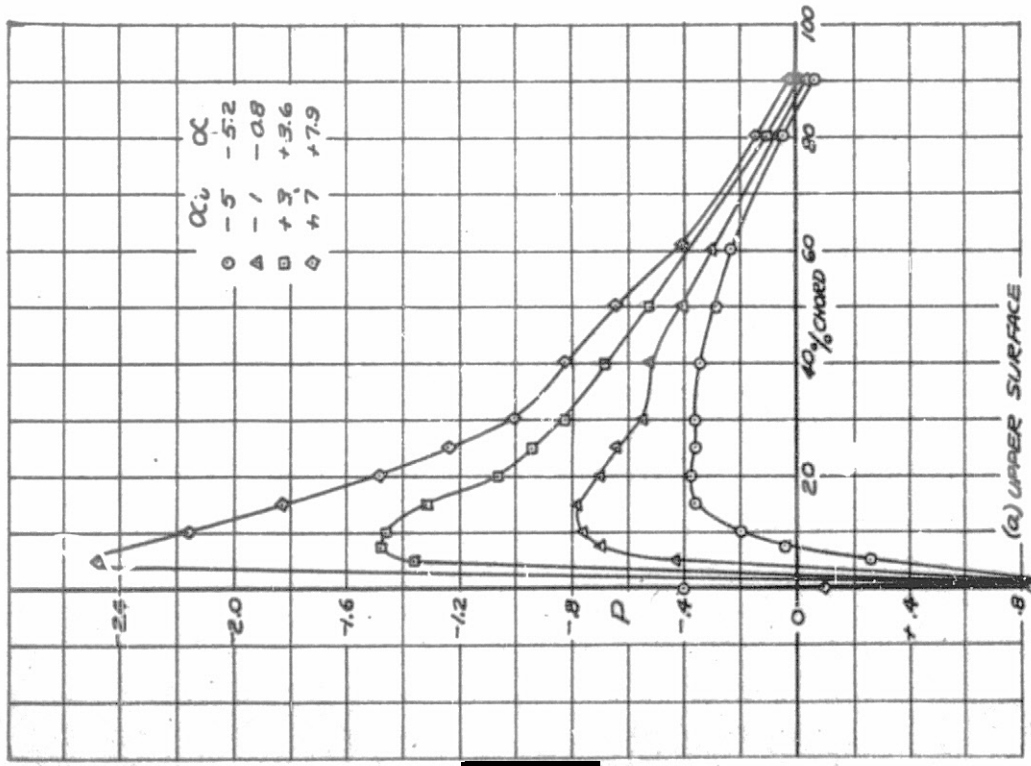

FIGURE 8.- PRESSURE DISTRIBUTION AT WING STATION 10.80 ON THE P-47D AIRPLANE MODEL. MACH NUMBER, 0.20

(a) UPPER SURFACE

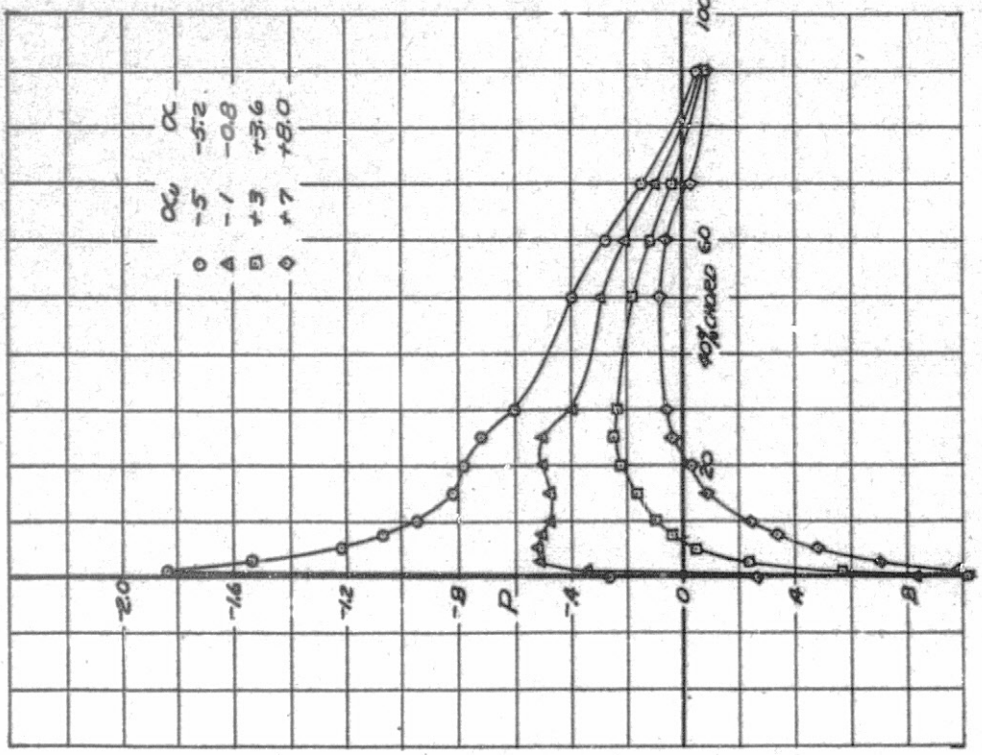

(b) LOWER SURFACE

FIGURE 9 (CONCLUDED).— PRESSURE DISTRIBUTION AT WING STATION 10.80 ON THE P-47D AIRPLANE MODEL. MACH NUMBER, 0.40.

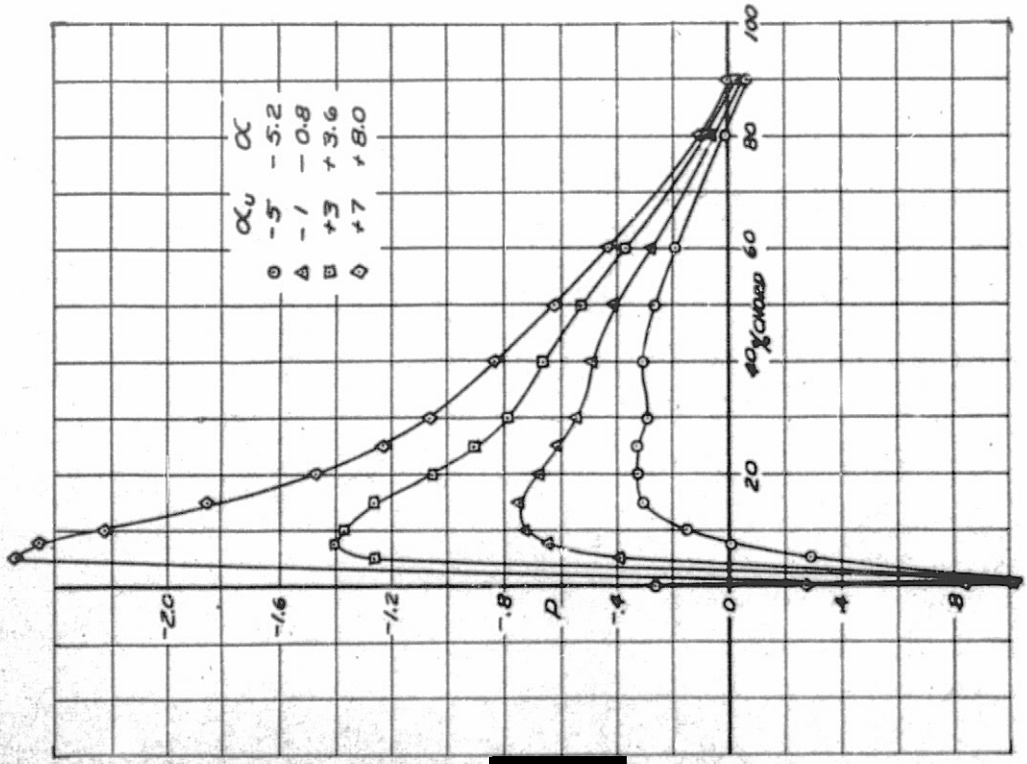

(a) UPPER SURFACE

FIGURE 9.— PRESSURE DISTRIBUTION AT WING STATION 10.80 ON THE P-47D AIRPLANE MODEL. MACH NUMBER, 0.40

[redacted]

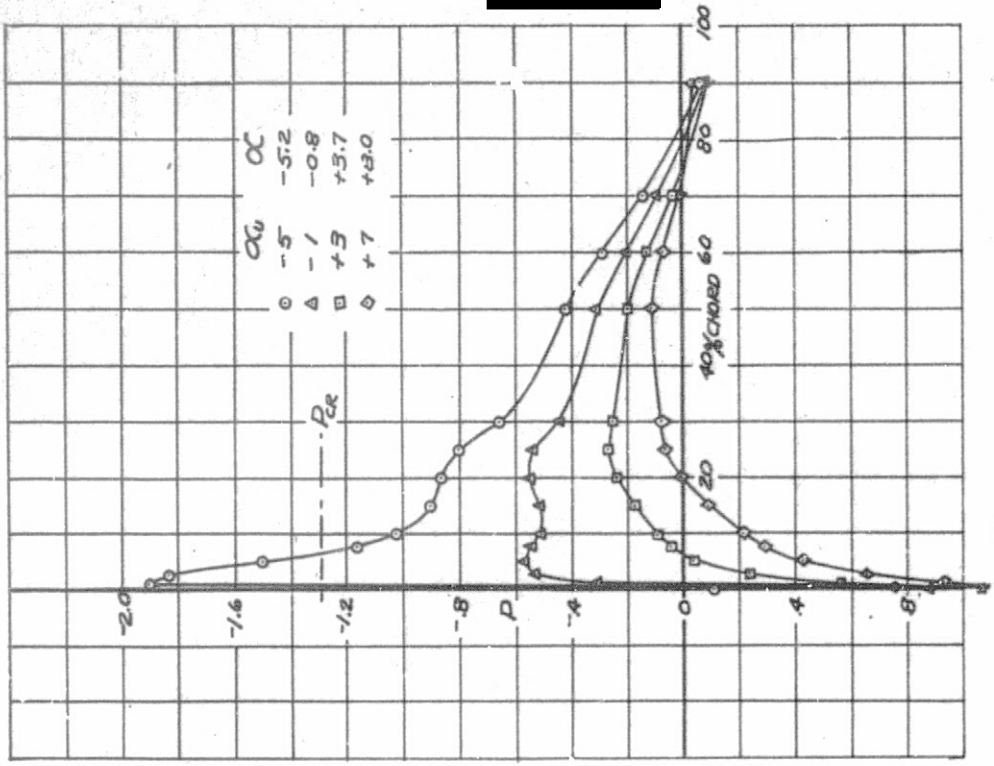

(b) LOWER SURFACE

FIGURE 10(CONCLUDED).— PRESSURE DISTRIBUTION AT WING STATION 10.80 ON THE P-47D AIRPLANE MODEL. MACH NUMBER, 0.60.

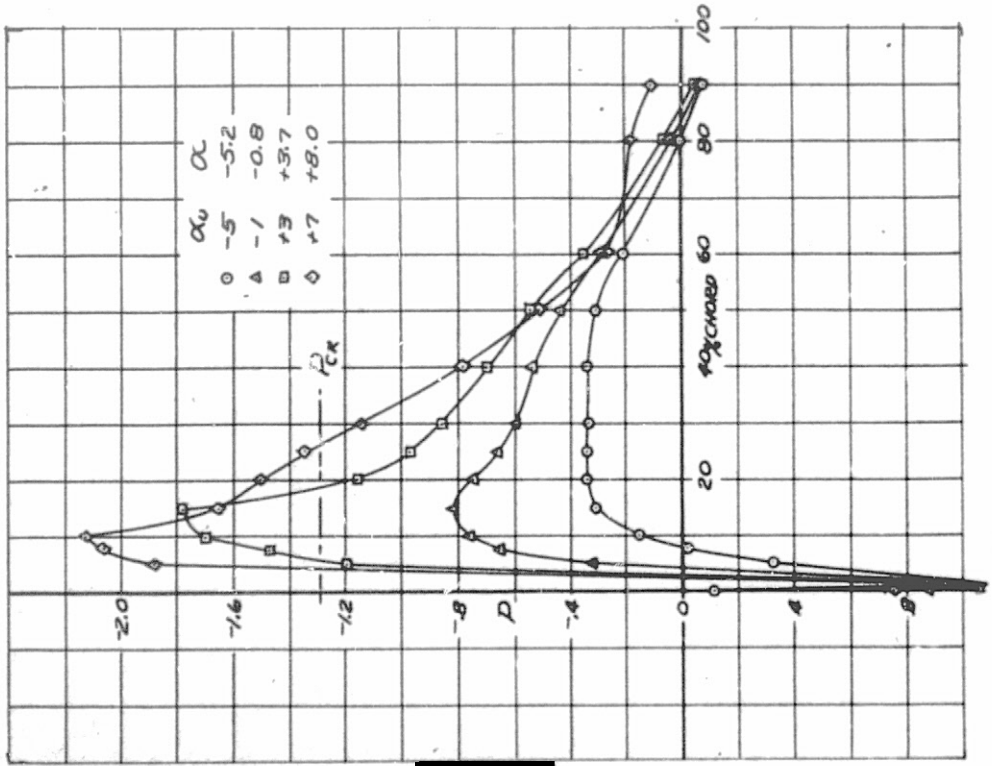

(a) UPPER SURFACE

FIGURE 10.— PRESSURE DISTRIBUTION AT WING STATION 10.80 ON THE P-47D AIRPLANE MODEL. MACH NUMBER, 0.60.

[redacted]

[redacted]

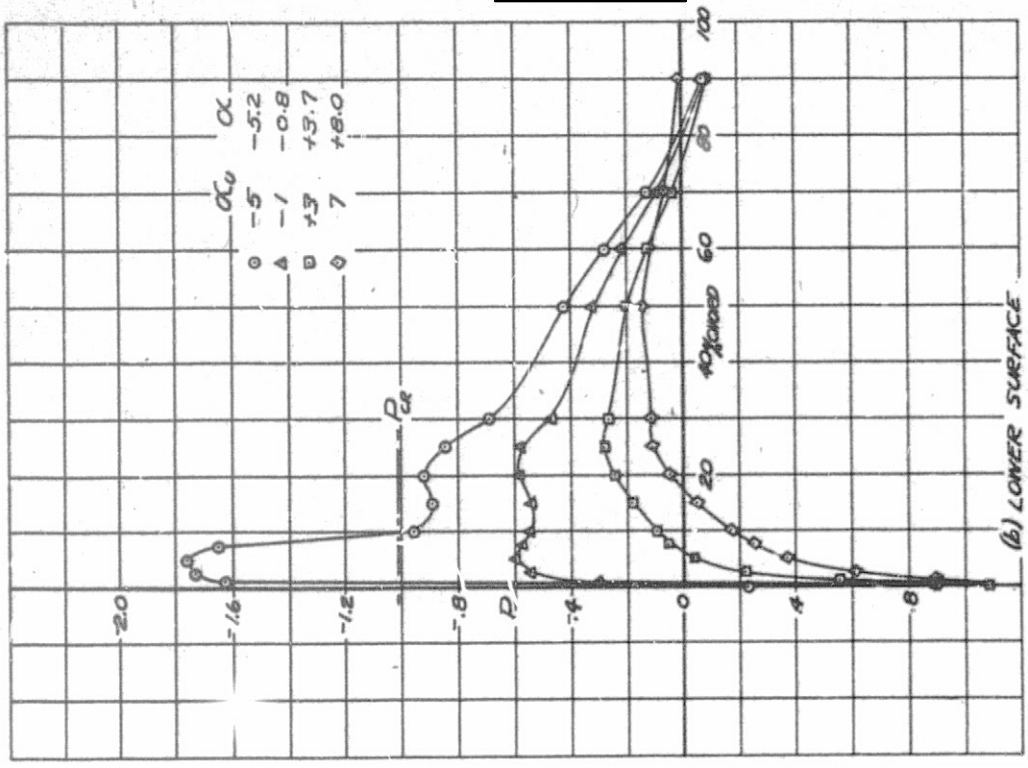

(b) LOWER SURFACE. - PRESSURE DISTRIBUTION AT WING STATION 10.80 ON THE P-47D AIRPLANE MODEL. MACH NUMBER, 0.65.

FIGURE 11 (CONCLUDED).

NATIONAL ADVISORY COMMITTEE
FOR AERONAUTICS

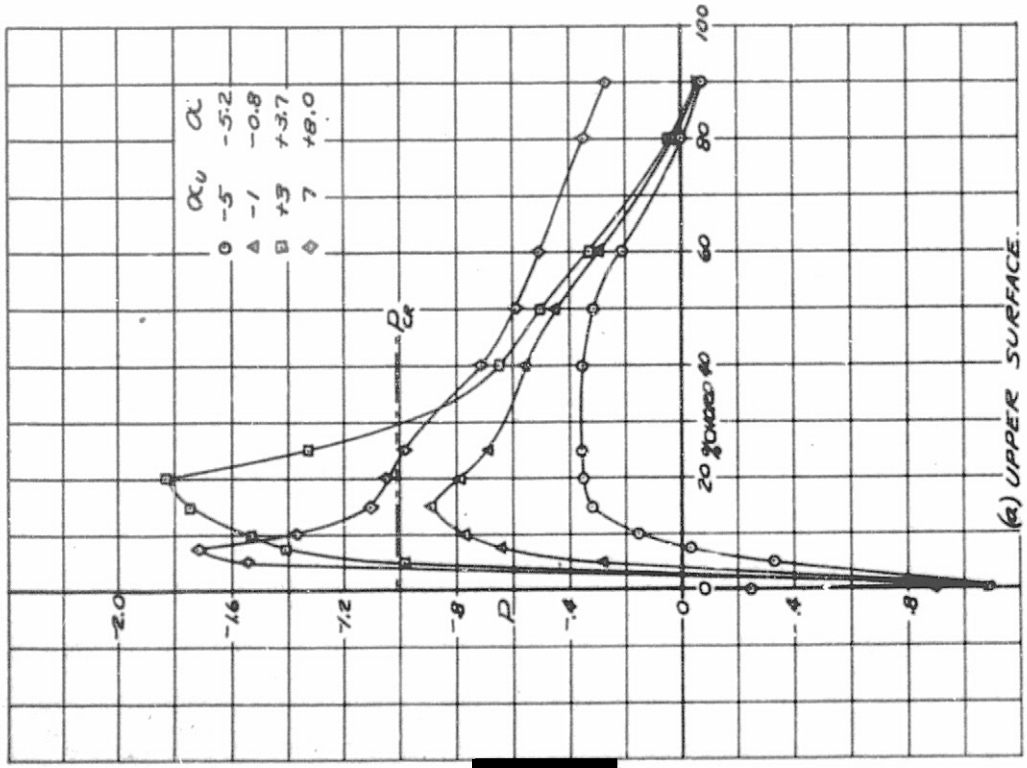

(a) UPPER SURFACE. - PRESSURE DISTRIBUTION AT WING STATION 10.80 ON THE P-47D AIRPLANE MODEL. MACH NUMBER, 0.65.

FIGURE 11. -

[redacted]

[redacted]UPDATA 1977

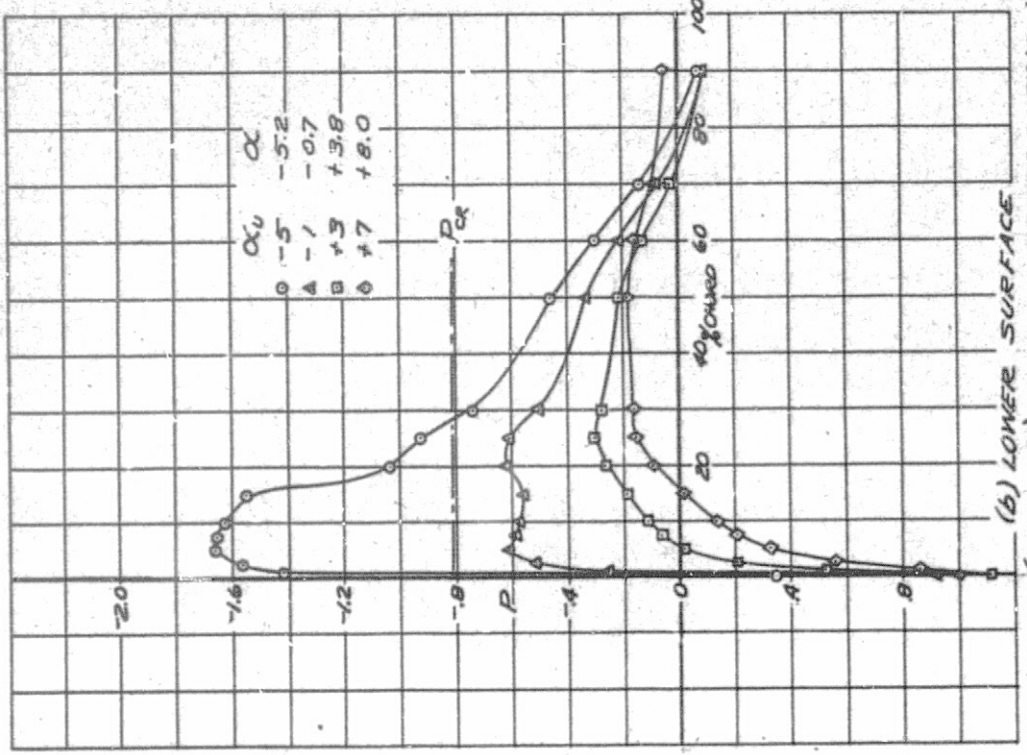

(b) LOWER SURFACE

FIGURE 12 (CONCLUDED).- PRESSURE DISTRIBUTION AT WING STATION 10.80 ON THE P-47D AIRPLANE MODEL MACH NUMBER, 0.69.

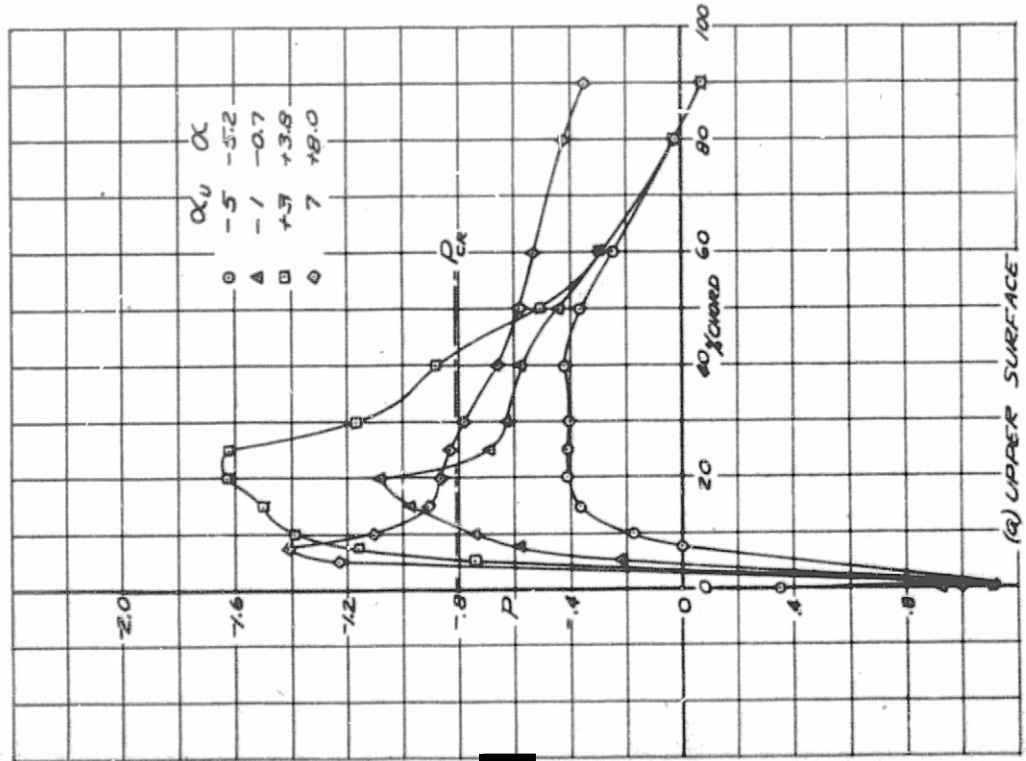

(a) UPPER SURFACE

FIGURE 12.- PRESSURE DISTRIBUTION AT WING STATION 10.80 ON THE P-47D AIRPLANE MODEL MACH NUMBER, 0.69

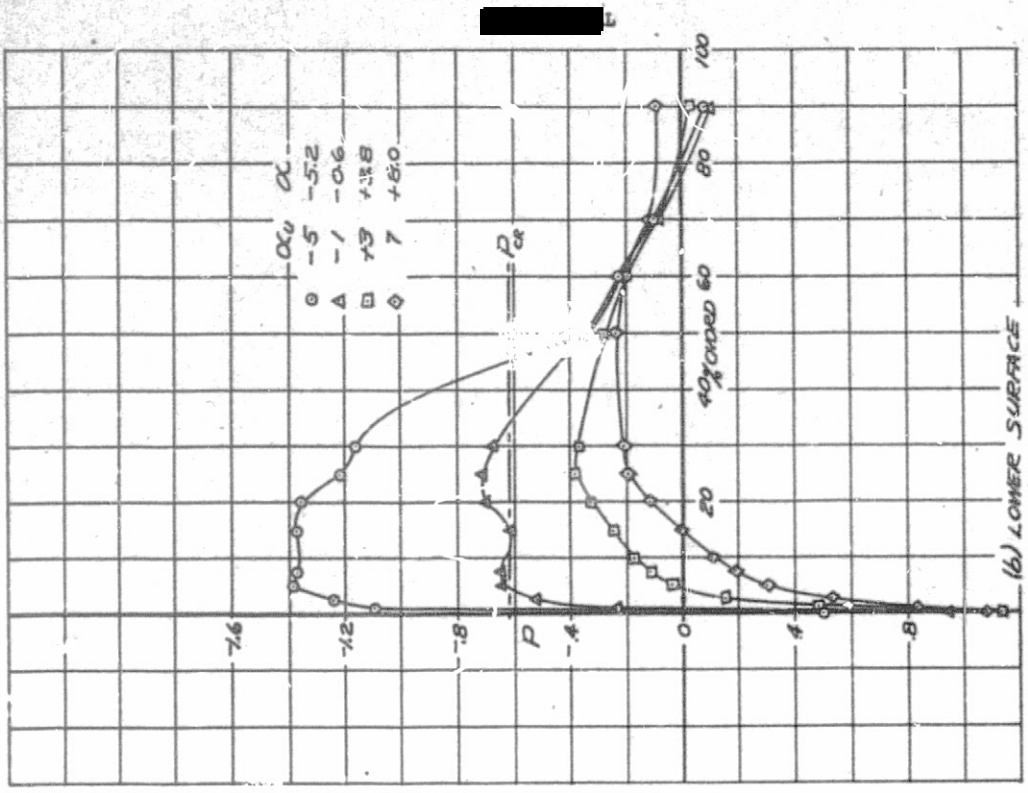

FIGURE 13 (CONTINUED).- PRESSURE DISTRIBUTION AT WING STATION 10.80 ON THE P-47D AIRPLANE MODEL. MACH NUMBER, 0.74

(b) LOWER SURFACE

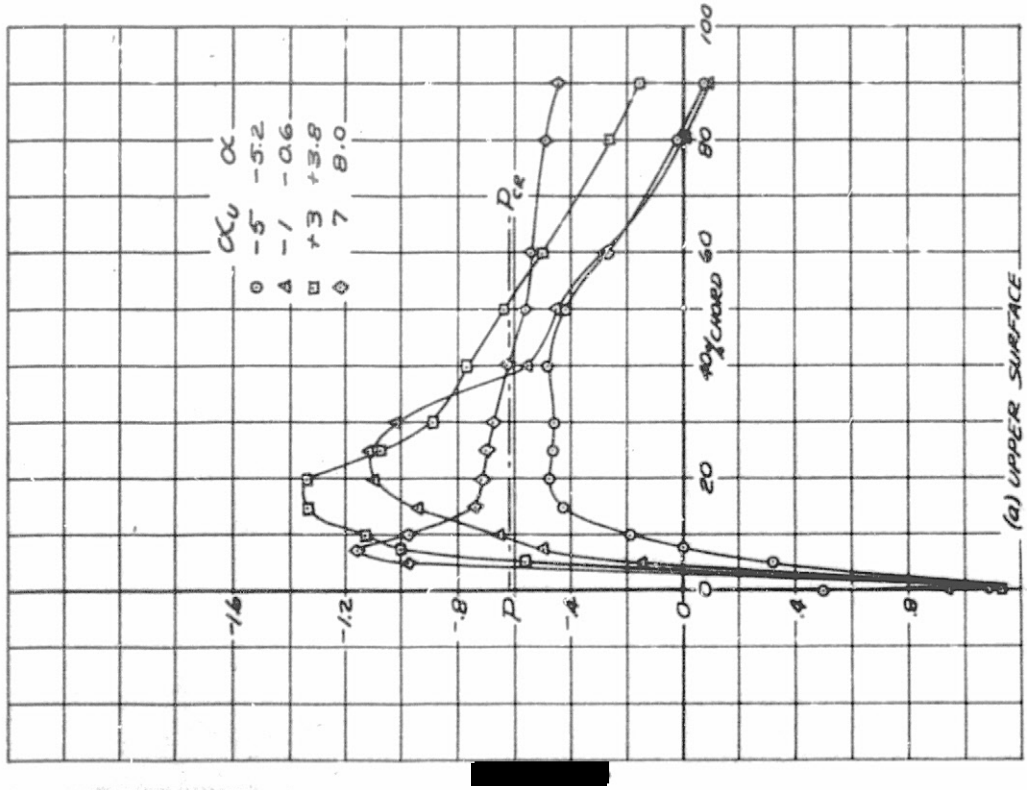

FIGURE 13.- PRESSURE DISTRIBUTION AT WING STATION 10.80 ON THE P-47D AIRPLANE MODEL. MACH NUMBER, 0.74

(a) UPPER SURFACE

Fig. 14a,b

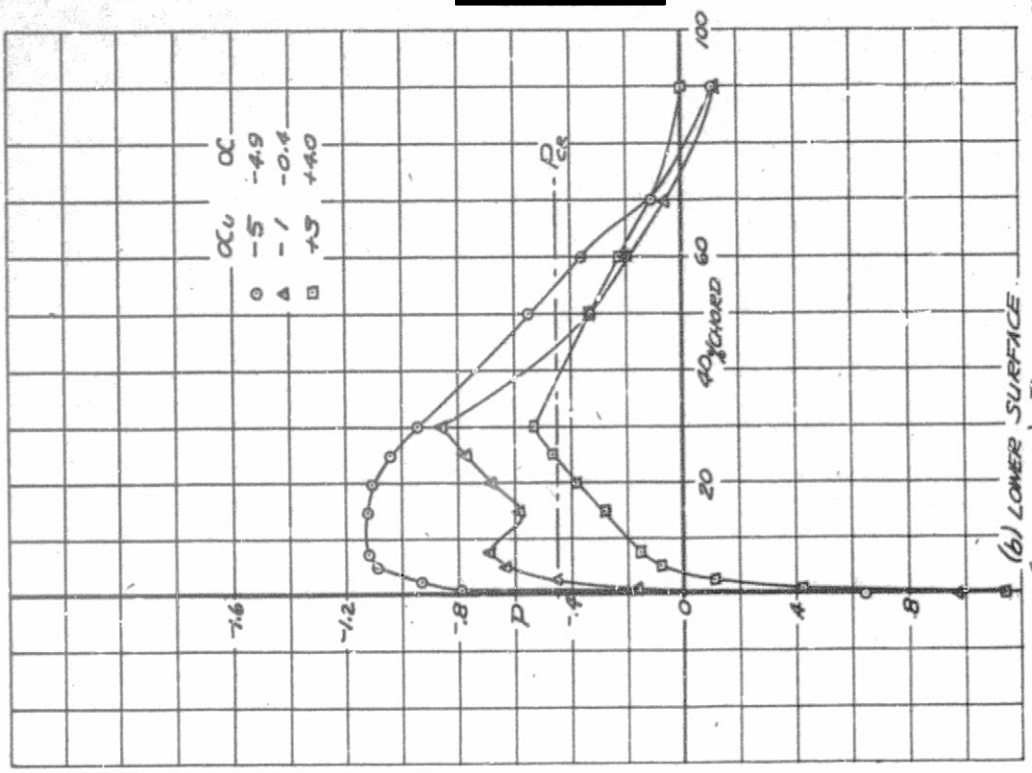

(b) LOWER SURFACE.

FIGURE 14.(CONCLUDED).- PRESSURE DISTRIBUTION AT WING STATION 10.80 ON THE P-47D AIRPLANE MODEL. MACH NUMBER, 0.79

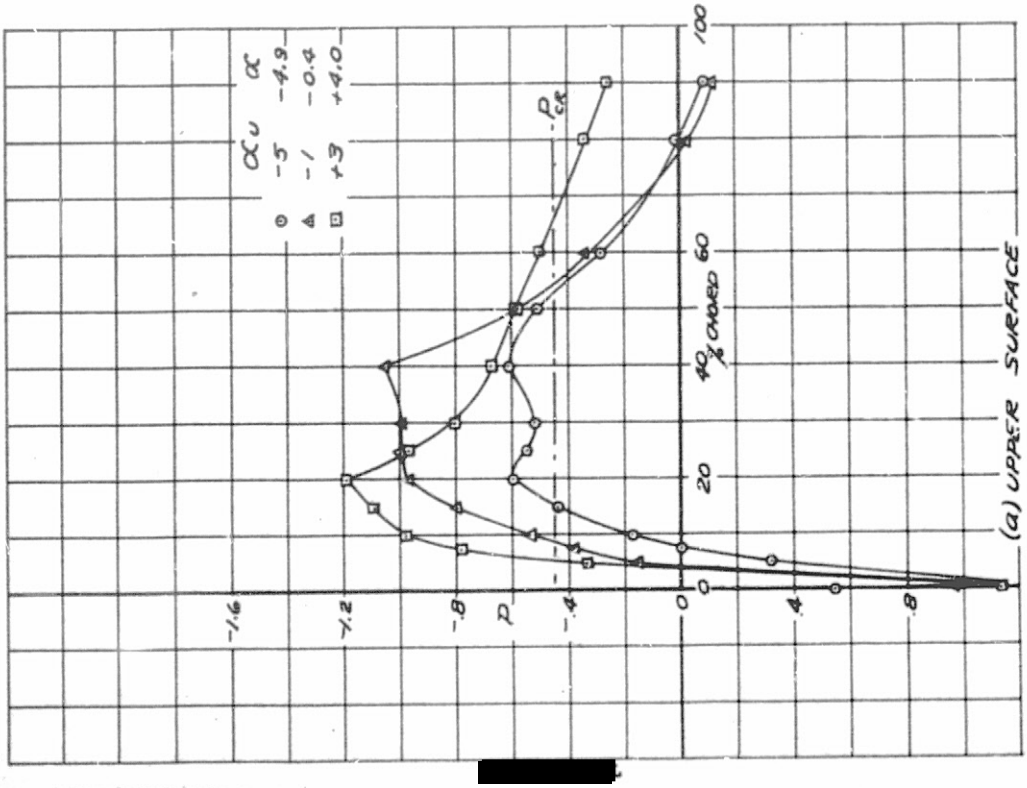

(a) UPPER SURFACE.

FIGURE 14.- PRESSURE DISTRIBUTION AT WING STATION 10.80 ON THE P-47D AIRPLANE MODEL. MACH NUMBER 0.79

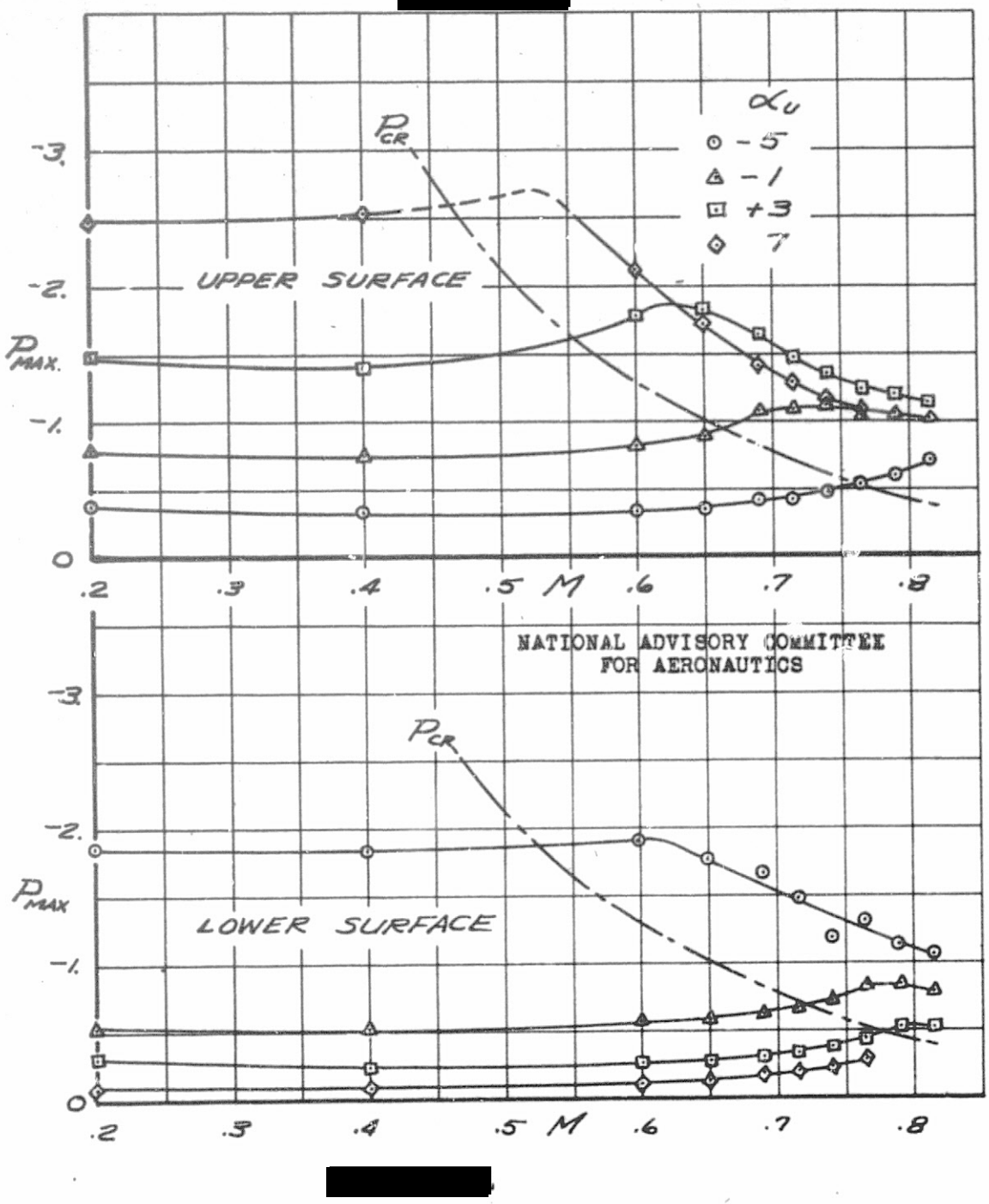

FIGURE 15.- VARIATION OF PEAK PRESSURE COEFFICIENT WITH MACH NUMBER FOR SEVERAL ANGLES OF ATTACK OF THE P-47D AIRPLANE MODEL. WING STATION, 10.80.

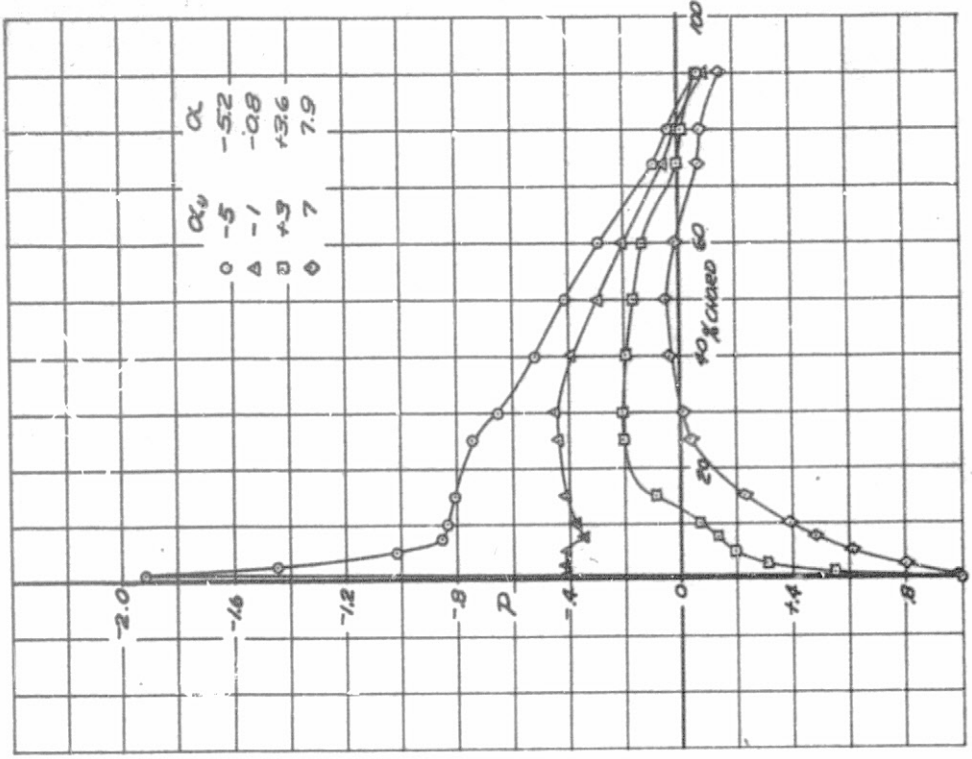

(b) LOWER SURFACE

FIGURES 16 (CONCLUDED).- PRESSURE DISTRIBUTION AT WING STATION 30.00 ON THE D-47D AIRPLANE MODEL. MACH NUMBER, 0.20

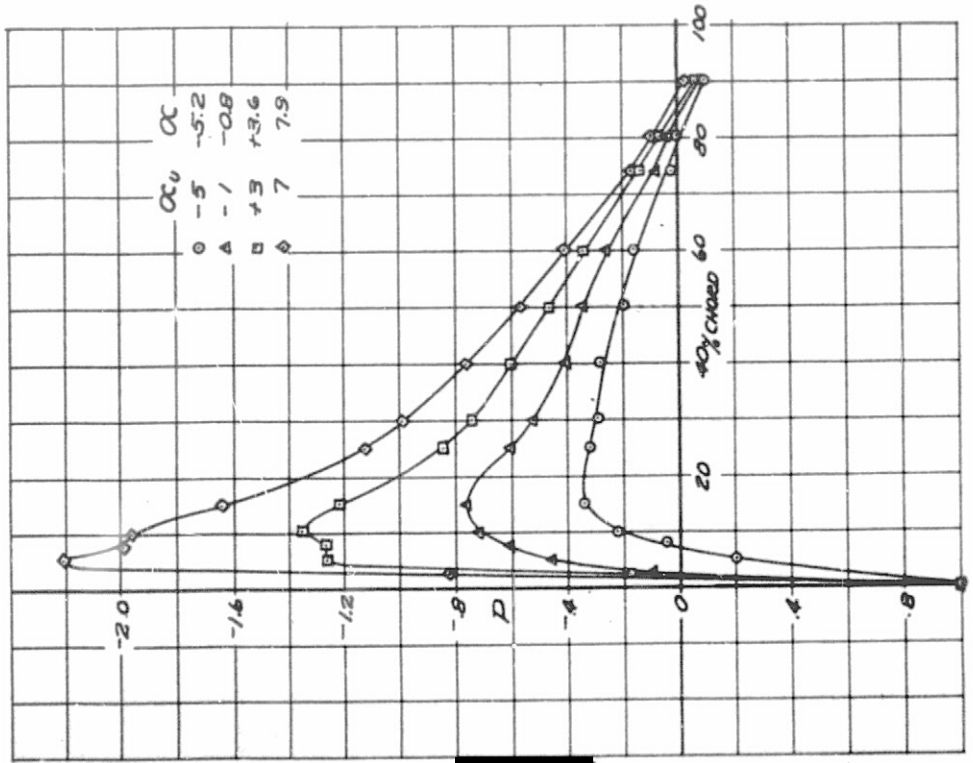

(a) UPPER SURFACE

FIGURE 16.- PRESSURE DISTRIBUTION AT WING STATION 30.00 ON THE D-47D AIRPLANE MODEL. MACH NUMBER, 0.20.

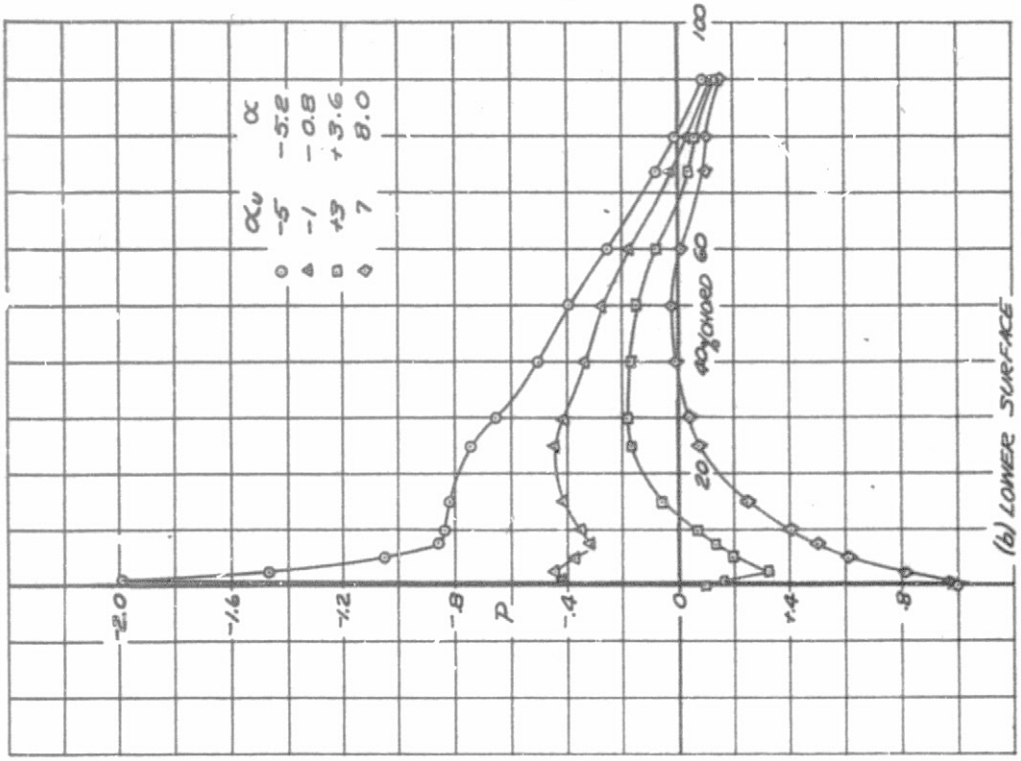

FIGURE 17 (CONCLUDED).- PRESSURE DISTRIBUTION AT WING STATION 30.00 ON THE P-47D AIRPLANE MODEL. MACH NUMBER, 0.40.

(b) LOWER SURFACE

NATIONAL ADVISORY COMMITTEE
FOR AERONAUTICS

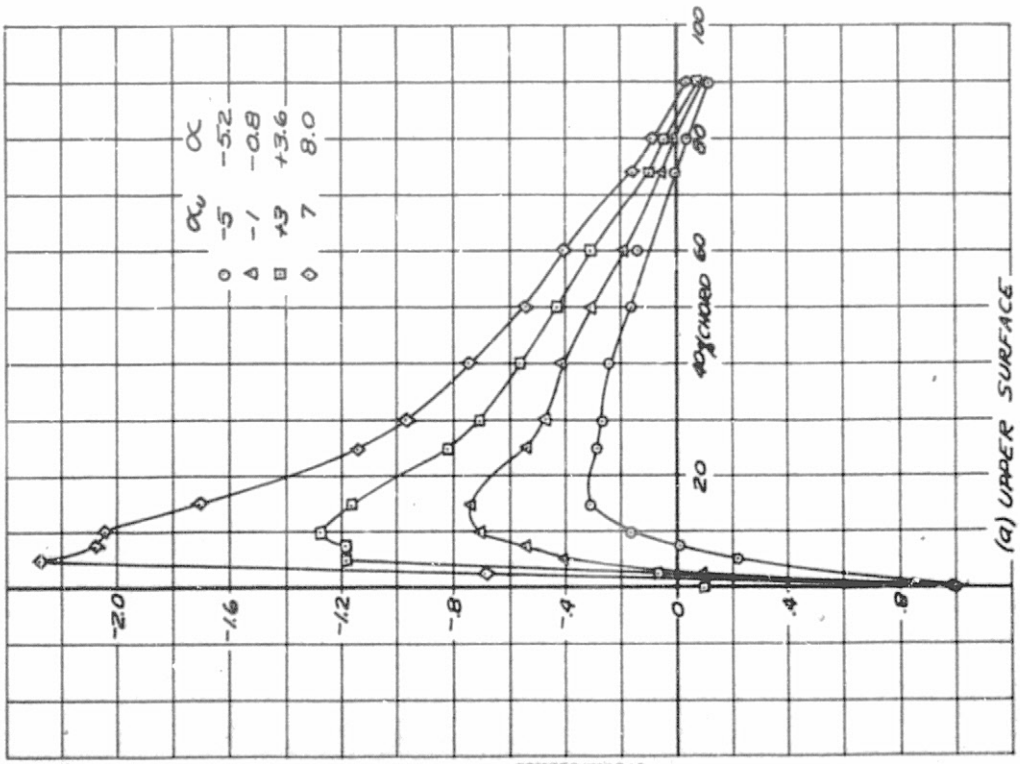

FIGURE 17.- PRESSURE DISTRIBUTION AT WING STATION 30.00 ON THE P-47D AIRPLANE MODEL. MACH NUMBER, 0.40.

(a) UPPER SURFACE

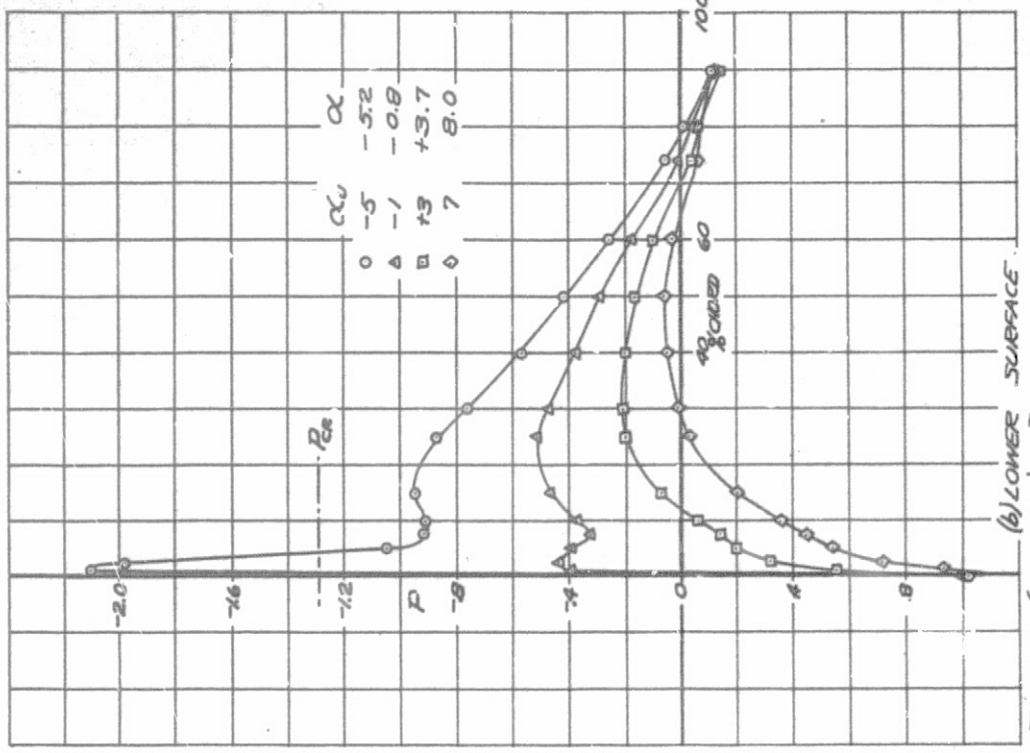

(b) LOWER SURFACE.

FIGURE 18 (CONCLUDED).— PRESSURE DISTRIBUTION AT WING STATION 30.00 ON THE P-47D AIRPLANE MODEL. MACH NUMBER, 0.60.

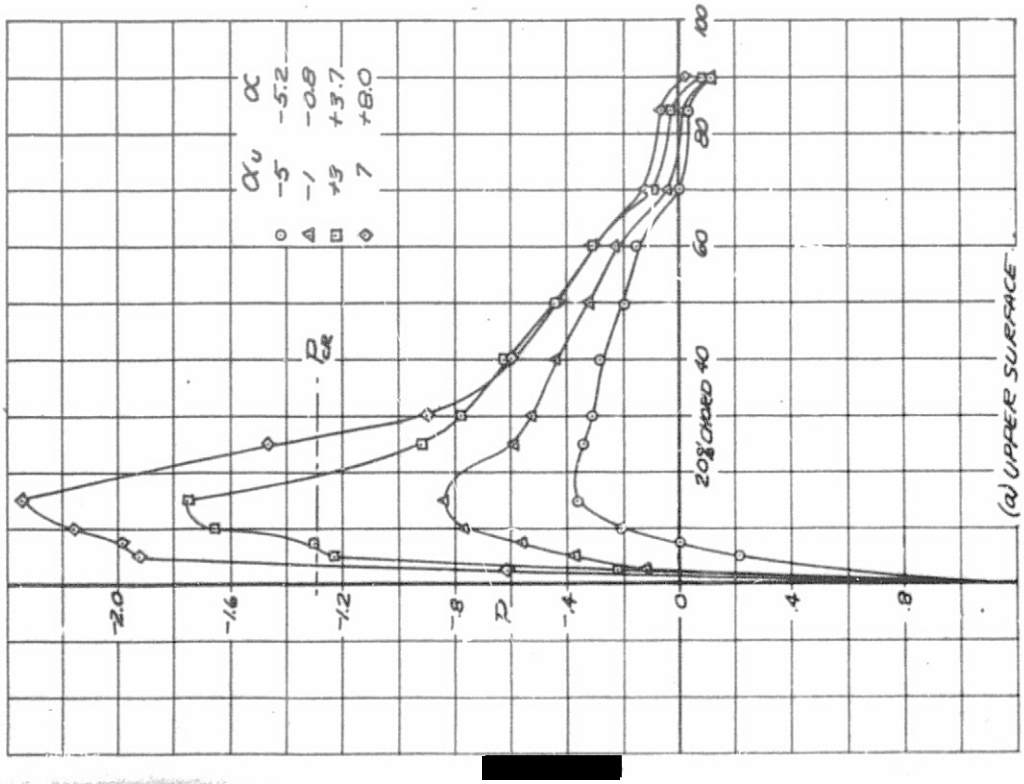

(a) UPPER SURFACE.

FIGURE 18.— PRESSURE DISTRIBUTION AT WING STATION 30.00 ON THE P-47D AIRPLANE MODEL. MACH NUMBER, 0.60.

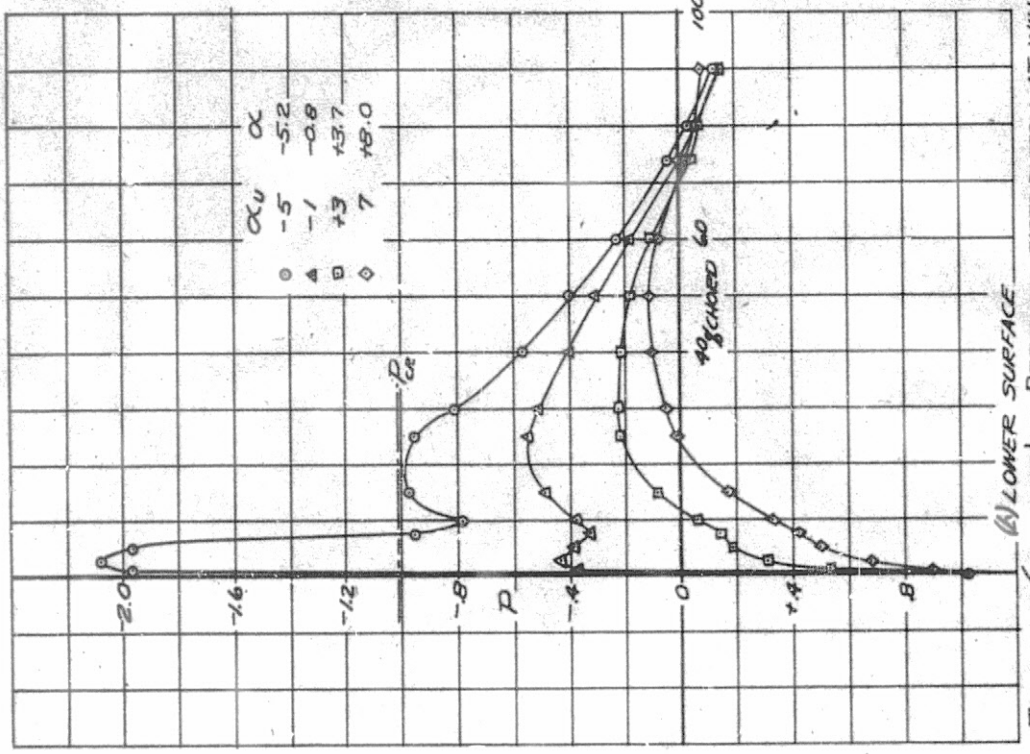

(b) LOWER SURFACE

FIGURE 19 (CONCLUDED). — PRESSURE DISTRIBUTION AT WING STATION 30.00 ON THE P-47D AIRPLANE MODEL. MACH NUMBER, 0.65.

NATIONAL ADVISORY COMMITTEE
FOR AERONAUTICS

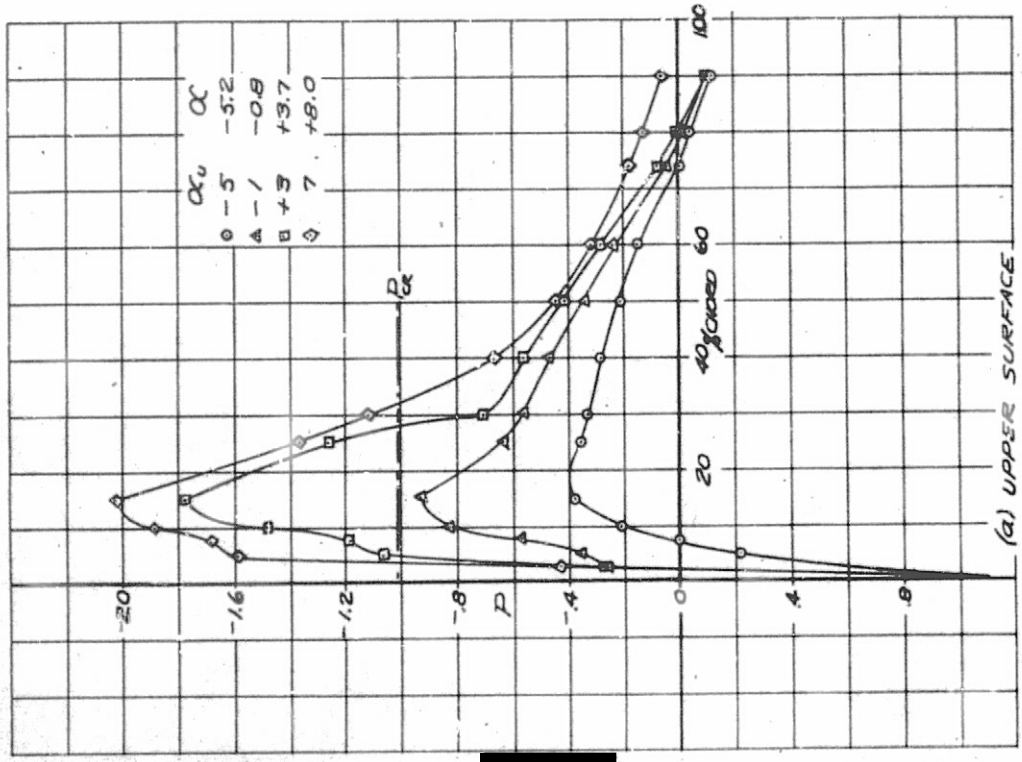

(a) UPPER SURFACE

FIGURE 19. — PRESSURE DISTRIBUTION AT WING STATION 30.00 ON THE P-47D AIRPLANE MODEL. MACH NUMBER, 0.65.

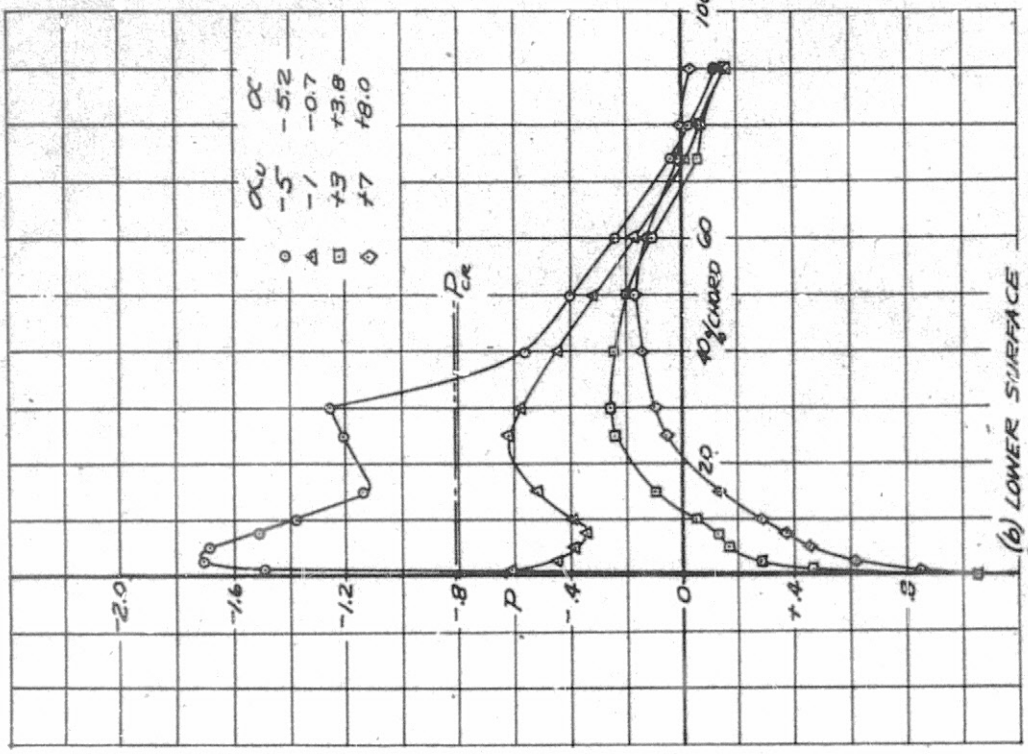

FIGURE 20 (CONCLUDED).- PRESSURE DISTRIBUTION AT WING STATION 30.00 ON THE P-47D AIRPLANE MODEL. MACH NUMBER, 0.69.

(b) LOWER SURFACE

NATIONAL ADVISORY COMMITTEE
FOR AERONAUTICS

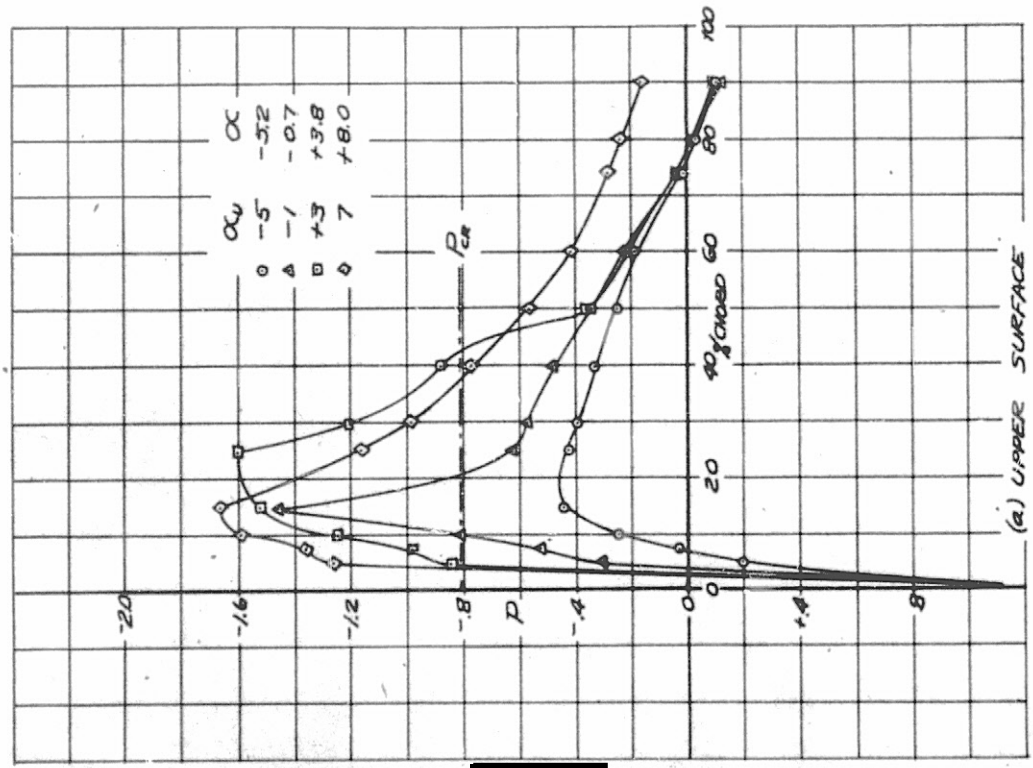

FIGURE 20.- PRESSURE DISTRIBUTION AT WING STATION 30.00 ON THE P-47D AIRPLANE MODEL. MACH NUMBER 0.69

(a) UPPER SURFACE

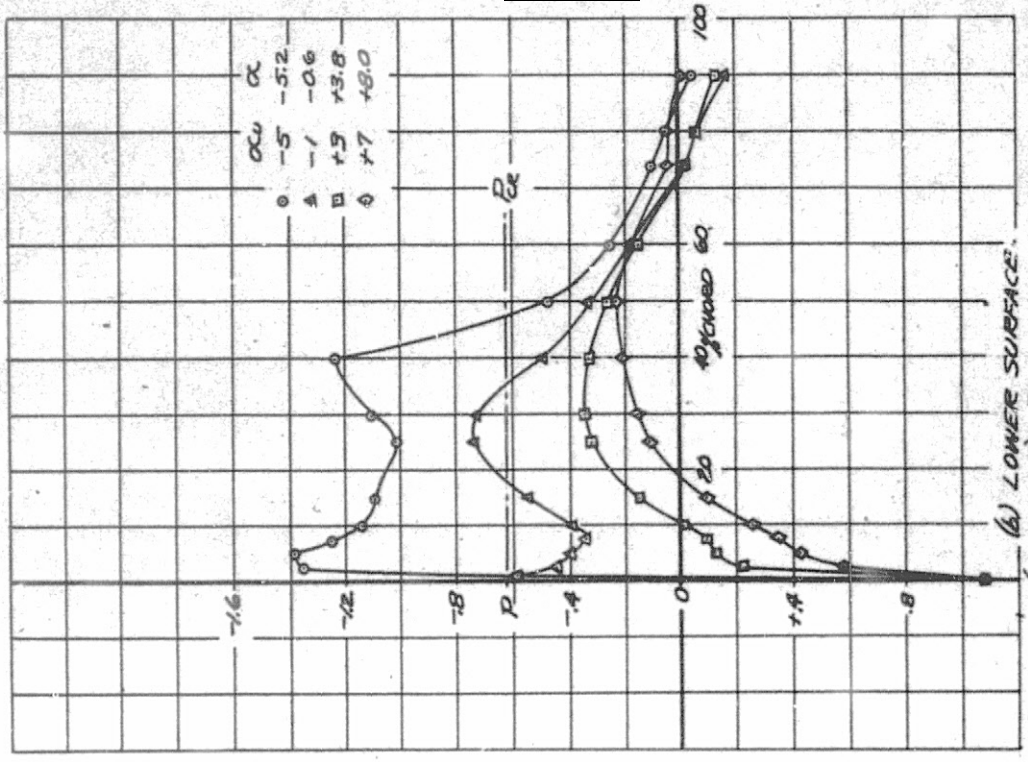

FIGURE 21 (CONCLUDED).- PRESSURE DISTRIBUTION AT WING STATION 30.00 ON THE P-47D AIRPLANE MODEL. MACH NUMBER, 0.74.

(b) LOWER SURFACE.

NATIONAL ADVISORY COMMITTEE
FOR AERONAUTICS

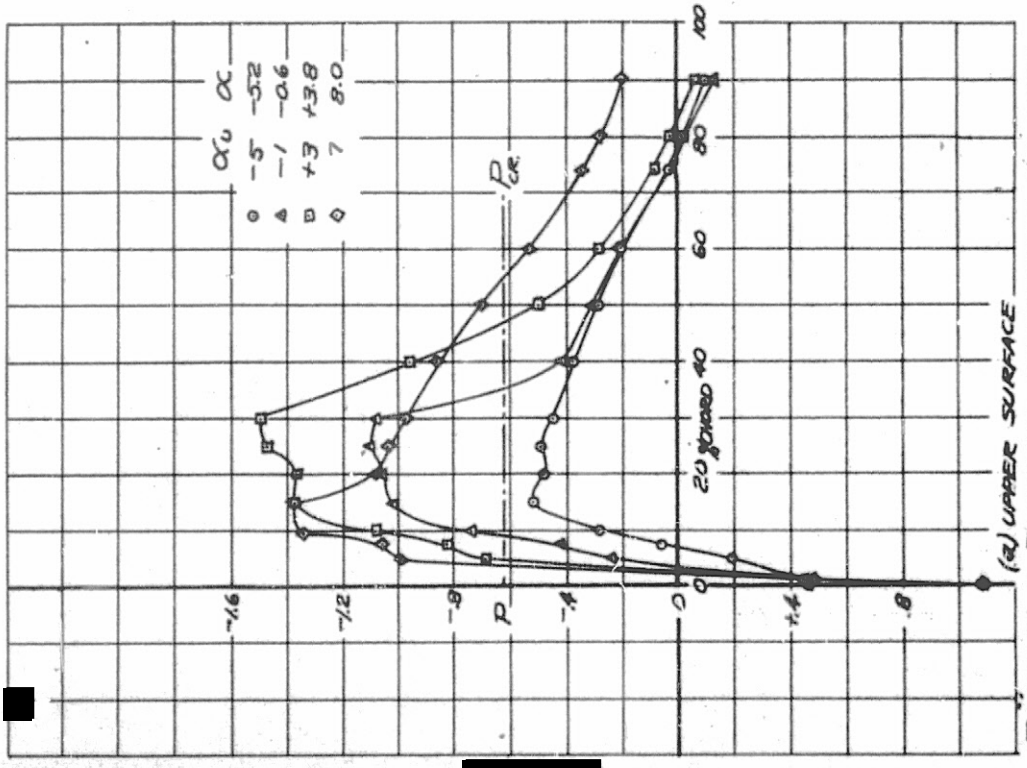

FIGURE 21.- PRESSURE DISTRIBUTION AT WING STATION 30.00 ON THE P-47D AIRPLANE MODEL. MACH NUMBER, 0.74.

(a) UPPER SURFACE

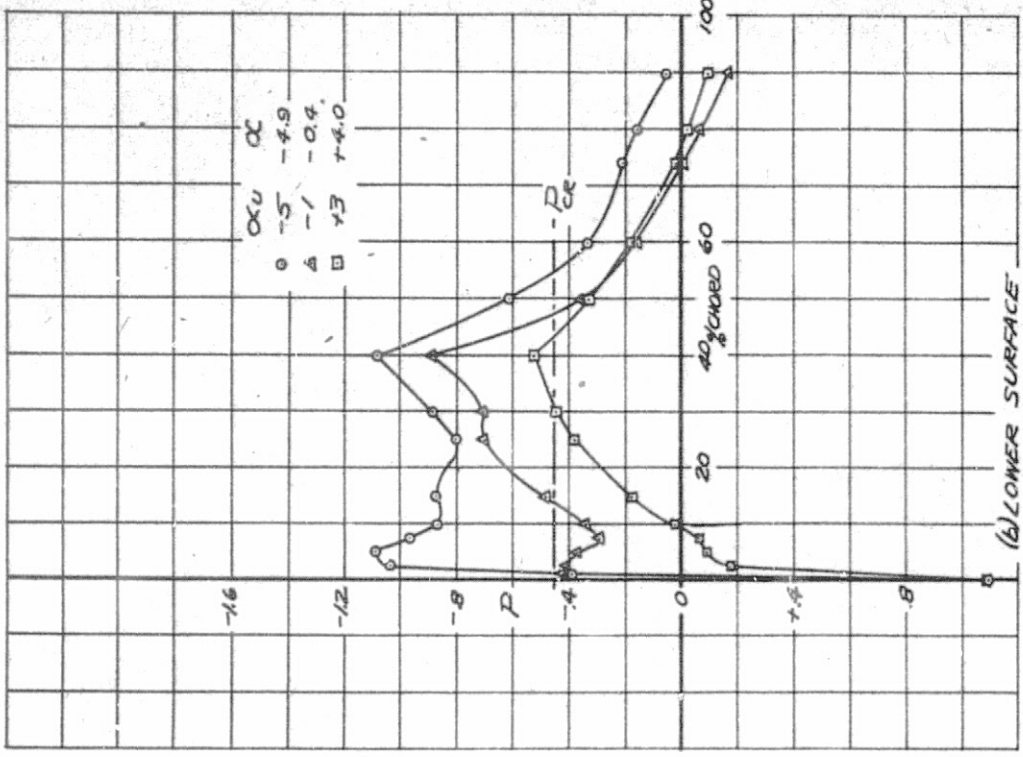

FIGURE 22.(CONCLUDED).- PRESSURE DISTRIBUTION AT WING STATION 30.00 ON THE P-47D AIRPLANE MODEL MACH NUMBER, 0.79.

(b) LOWER SURFACE

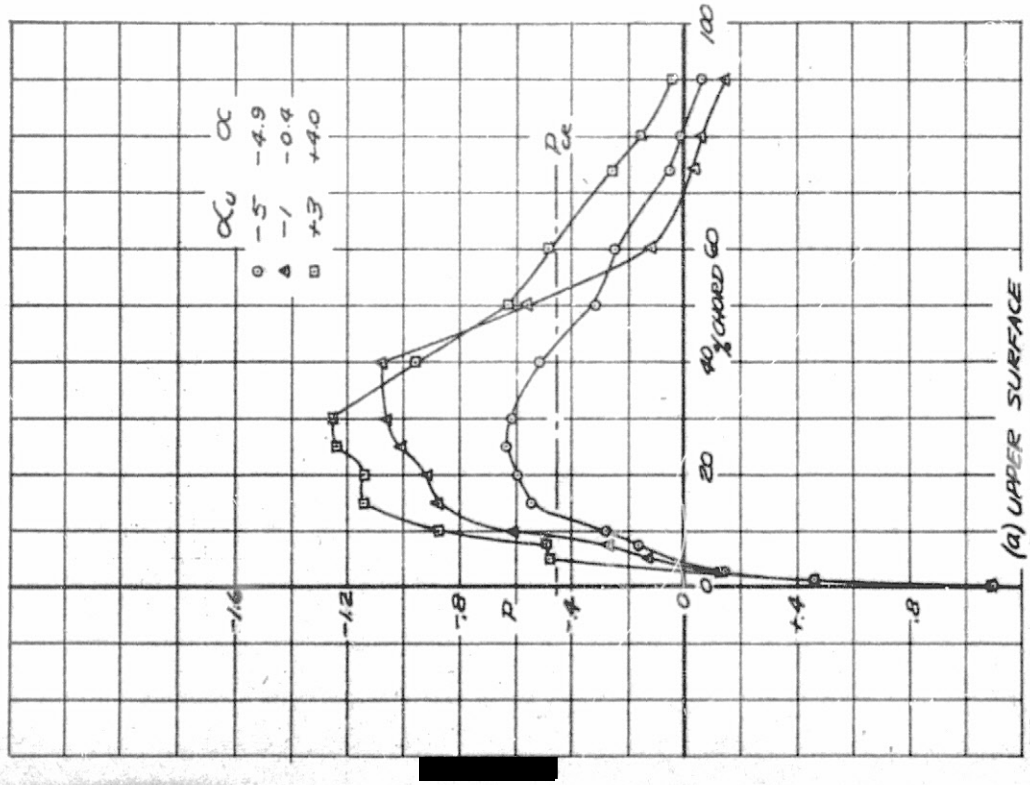

FIGURE 22.- PRESSURE DISTRIBUTION AT WING STATION 30.00 ON THE P-47D AIRPLANE MODEL MACH NUMBER, 0.79.

(a) UPPER SURFACE

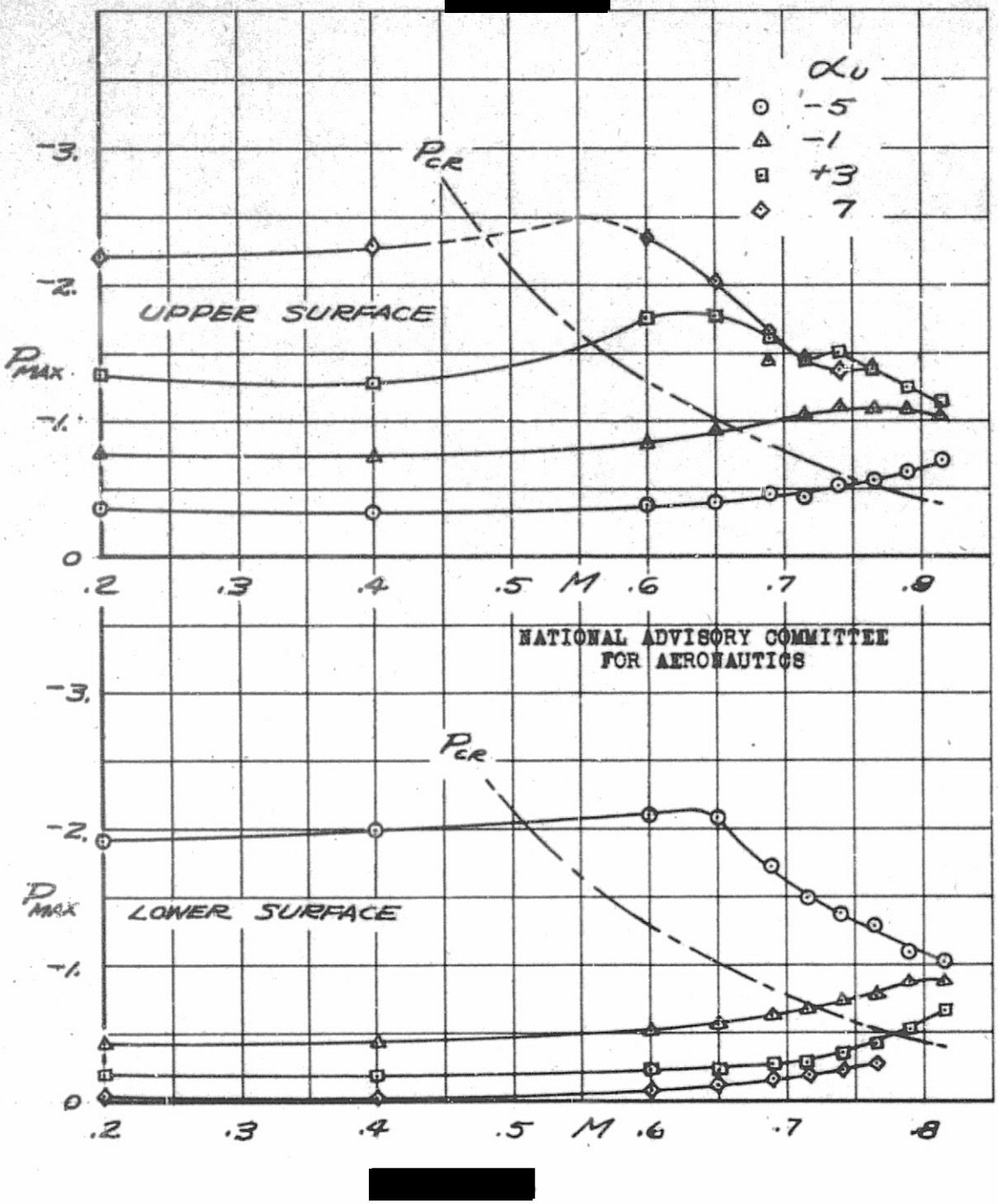

FIGURE 23.- VARIATION OF PEAK PRESSURE COEFFICIENT WITH MACH NUMBER FOR SEVERAL ANGLES OF ATTACK OF THE P-47D AIRPLANE MODEL. WING STATION, 30.00

[redacted]

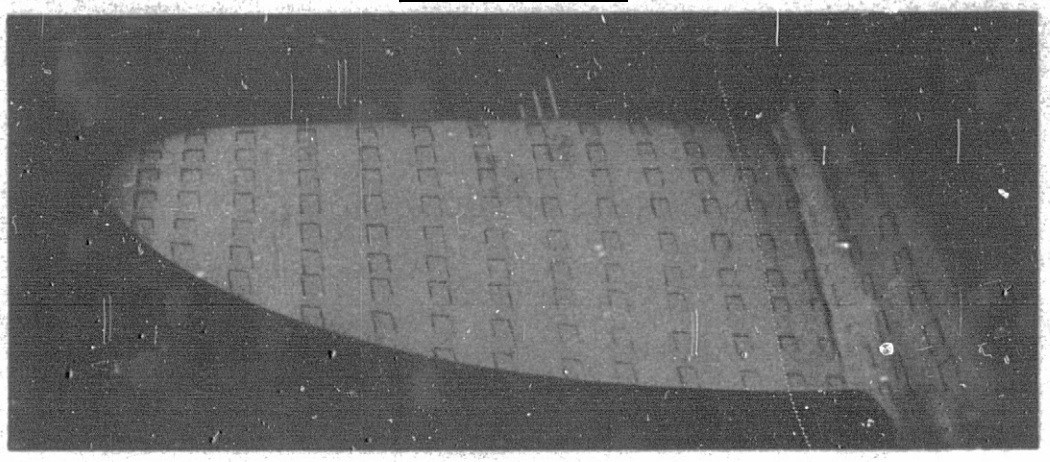

α_u, -2.5°; C_L, -.08

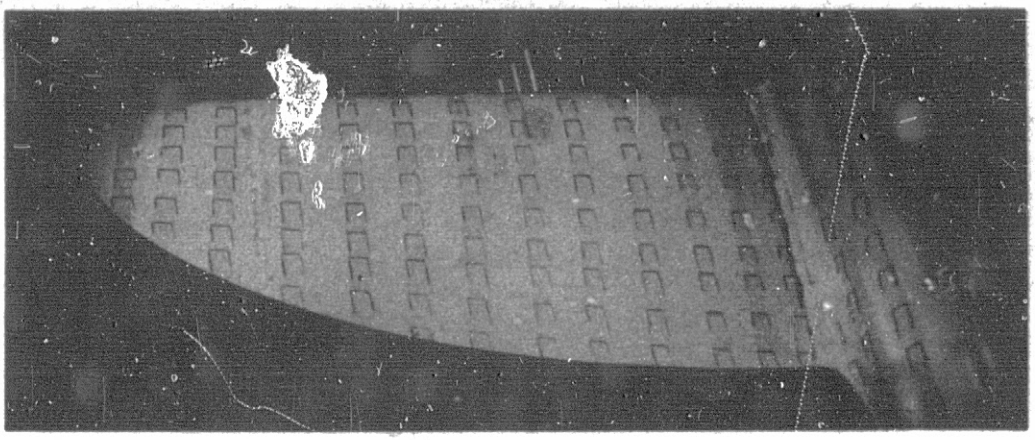

α_u, +.5°; C_L, +.21

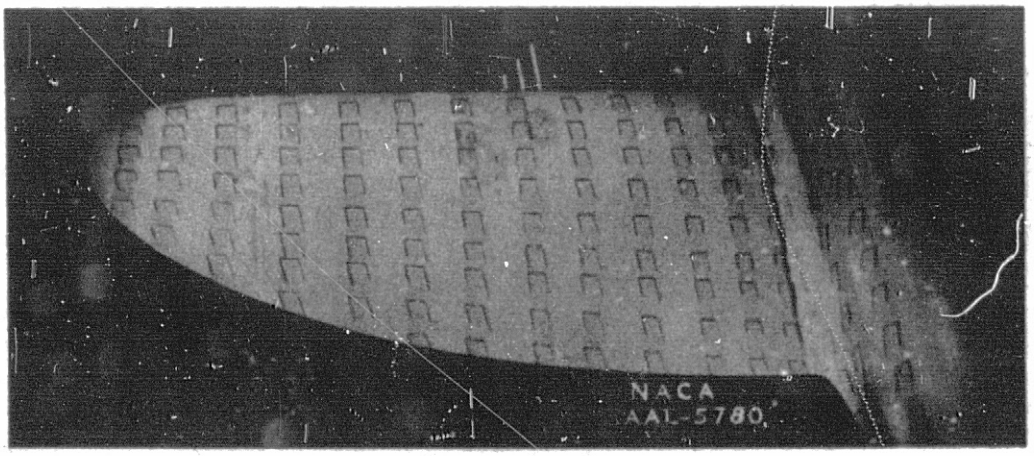

[redacted] +5°; C_L, +.65

Figure 24.- Tuft studies of flow over the upper surface of the P-47D airplane model wing. Mach number, .291.

[redacted]

[redacted]

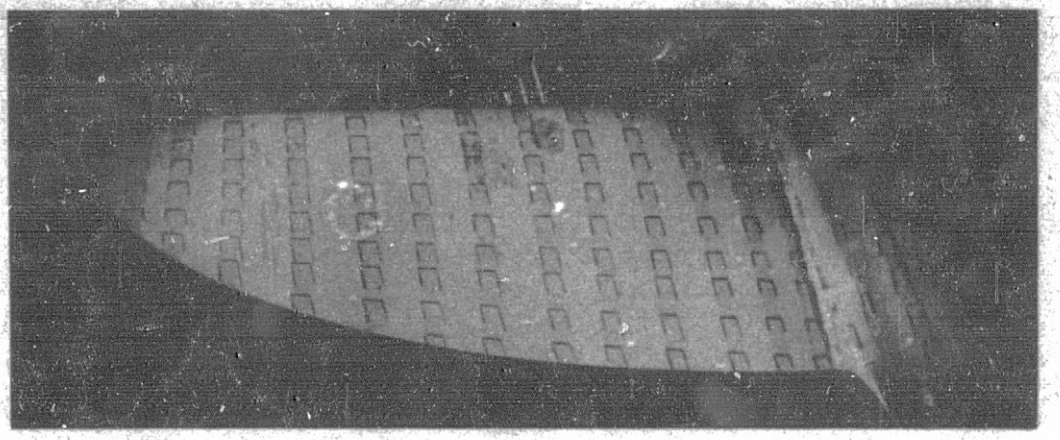

α_u, -2.5°; C_L, -.08

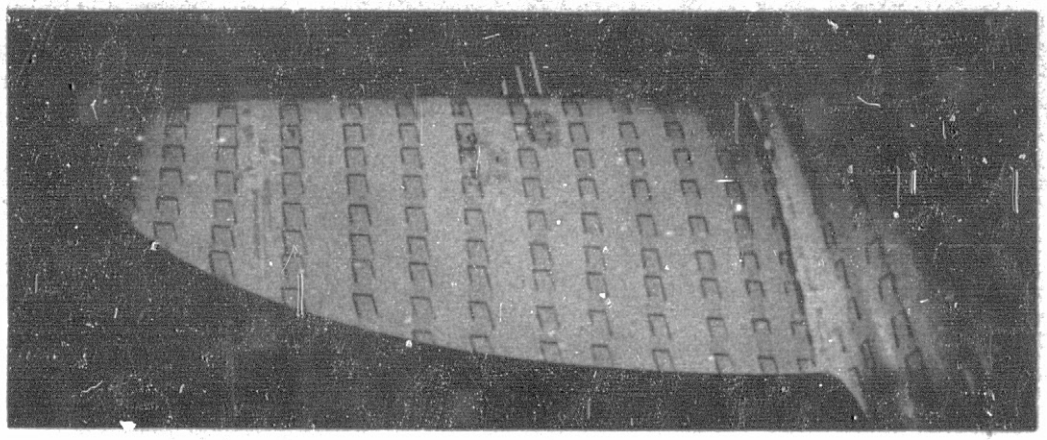

α_u, +.5°; C_L, +.24

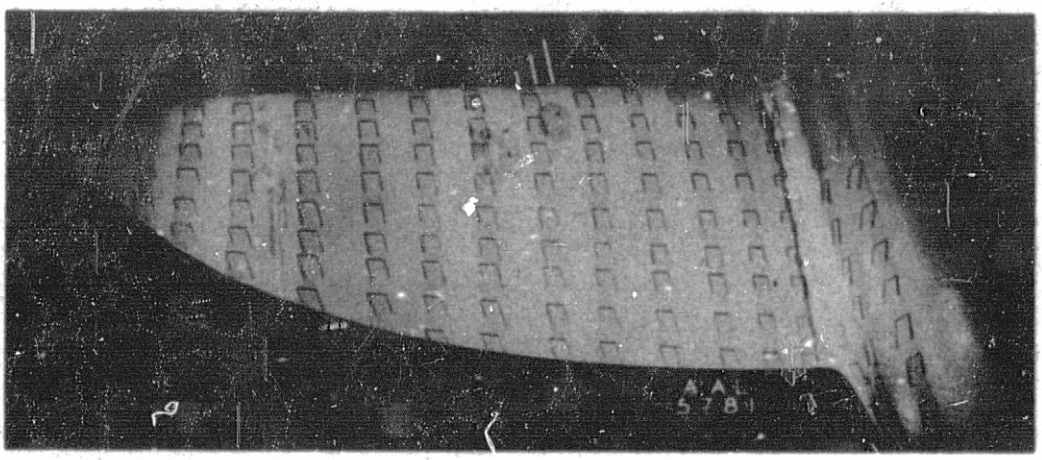

α_u, +5°; C_L, +.71

Figure 25.- Tuft studies of flow over the upper surface of the P-47D airplane model wing. Mach number, .591.

[redacted]EN[redacted]

[redacted]

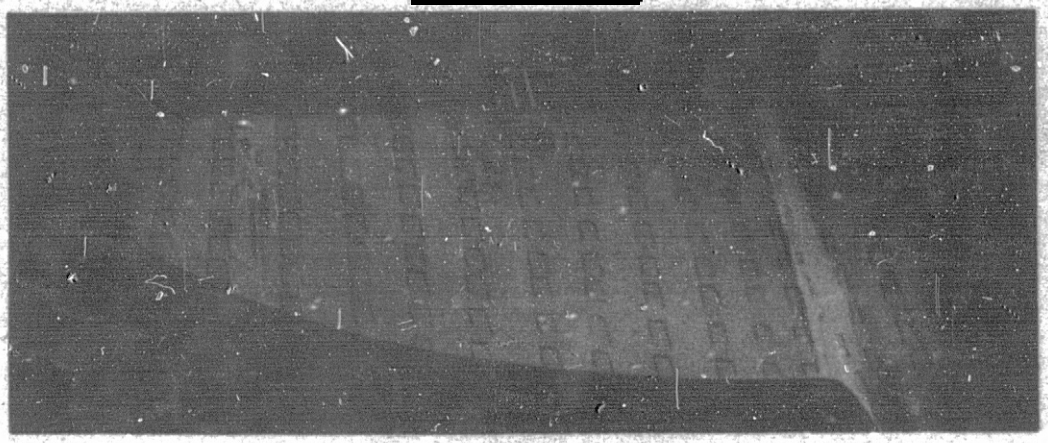

α_u, -2.5°; C_L, -.08

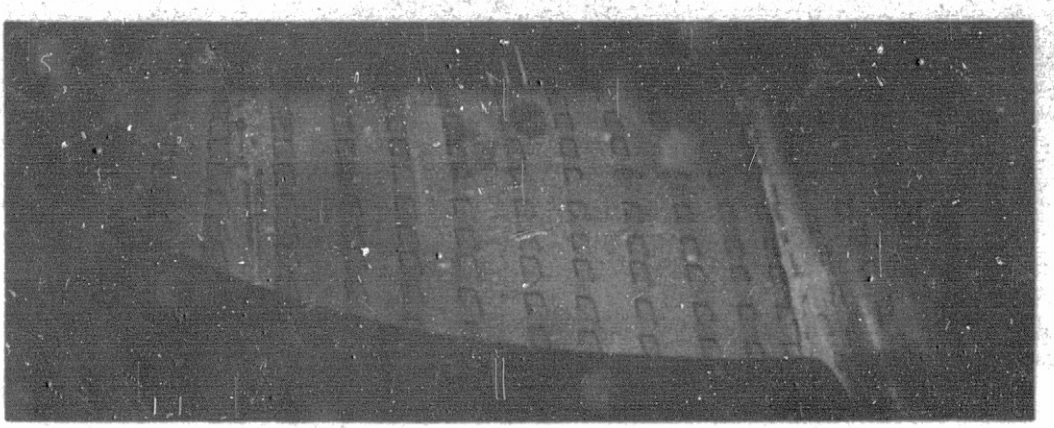

α_u, +.5°; C_L, +.25

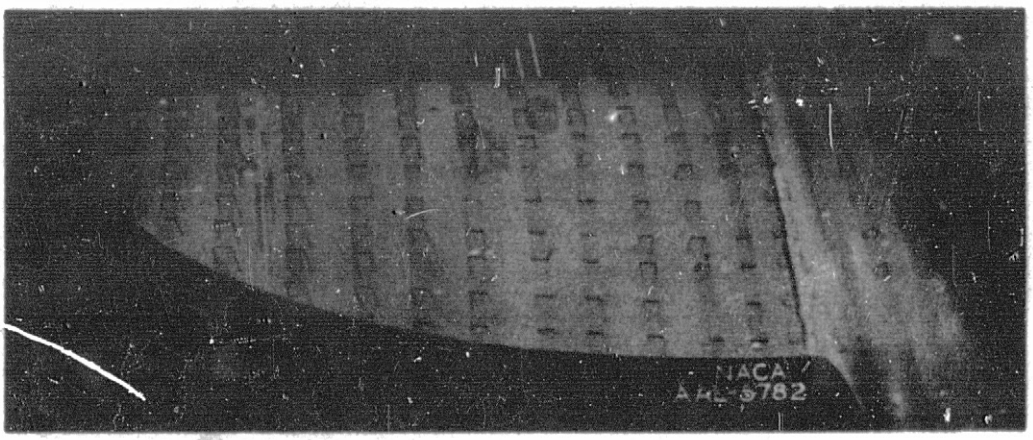

α_u, +5°; C_L, +.58

Figure 26.- Tuft studies of flow over the upper surface of the P-47D airplane model wing. Mach number, .731.

[redacted]EN[redacted]

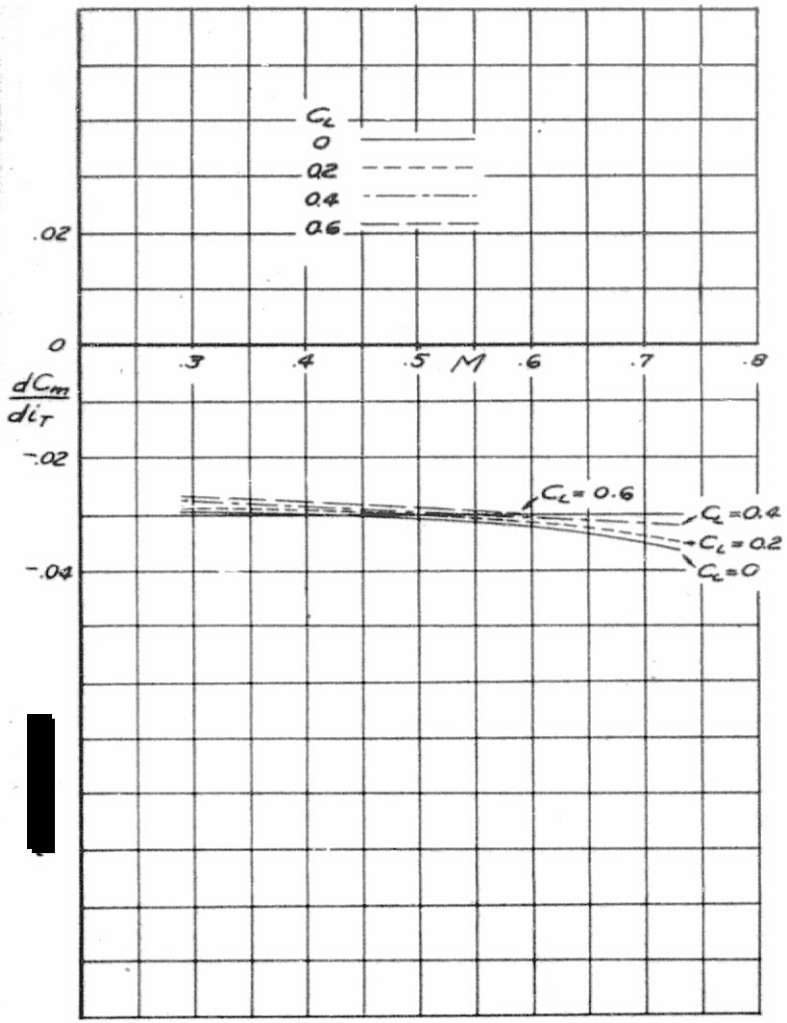

FIGURE 27.— VARIATION OF STABILIZER EFFECTIVENESS WITH MACH NUMBER FOR THE P-47D AIRPLANE MODEL

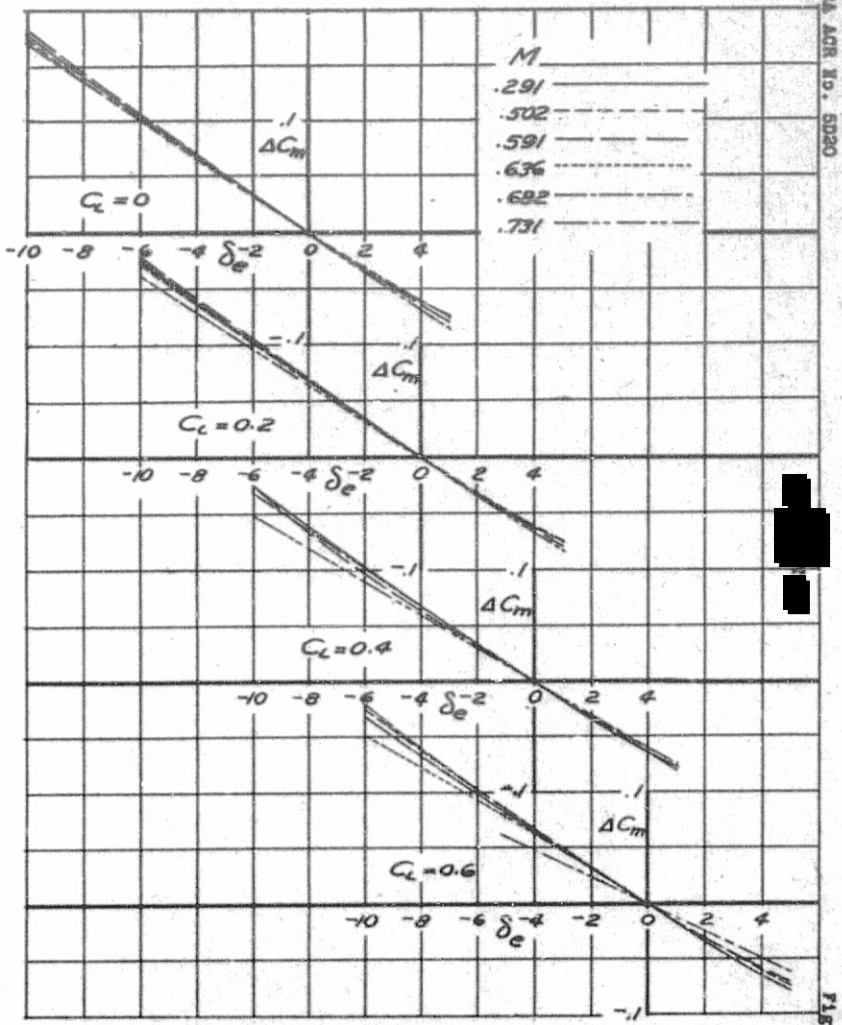

FIGURE 28.— VARIATION OF PITCHING-MOMENT COEFFICIENT WITH ELEVATOR ANGLE, FOR SEVERAL MACH NUMBERS AND LIFT COEFFICIENTS, FOR THE P-47D AIRPLANE MODEL

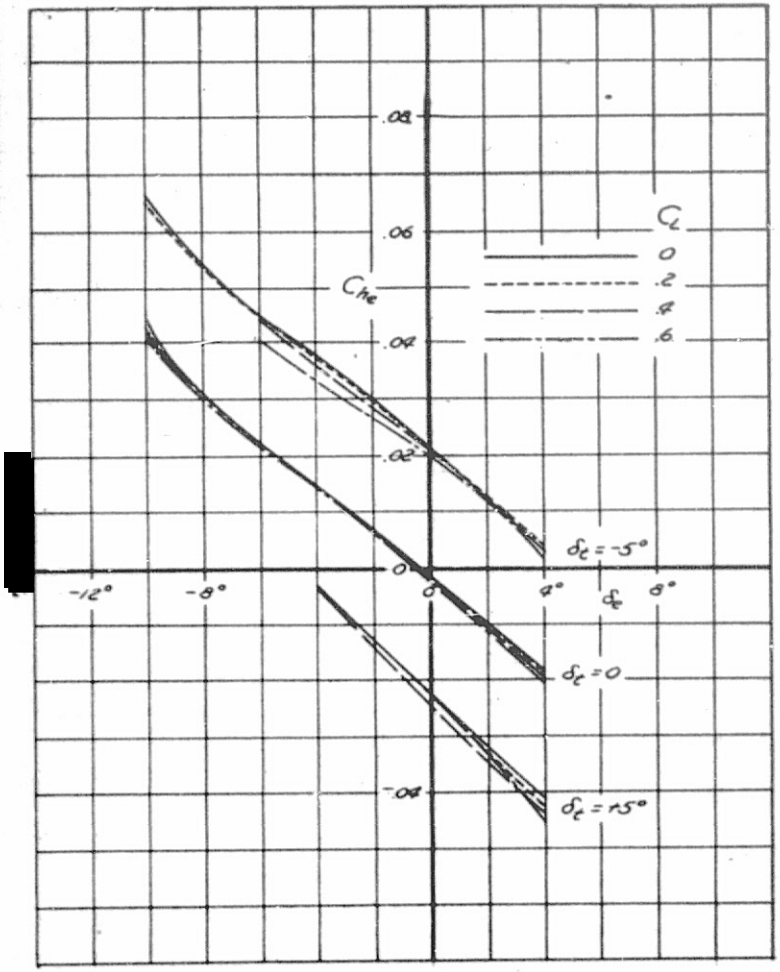

FIGURE 29.-VARIATION OF ELEVATOR HINGE-MOMENT COEFFICIENT WITH ELEVATOR ANGLE FOR THREE ELEVATOR TAB DEFLECTIONS ON THE P-47D AIRPLANE MODEL. MACH NUMBER, 0.291

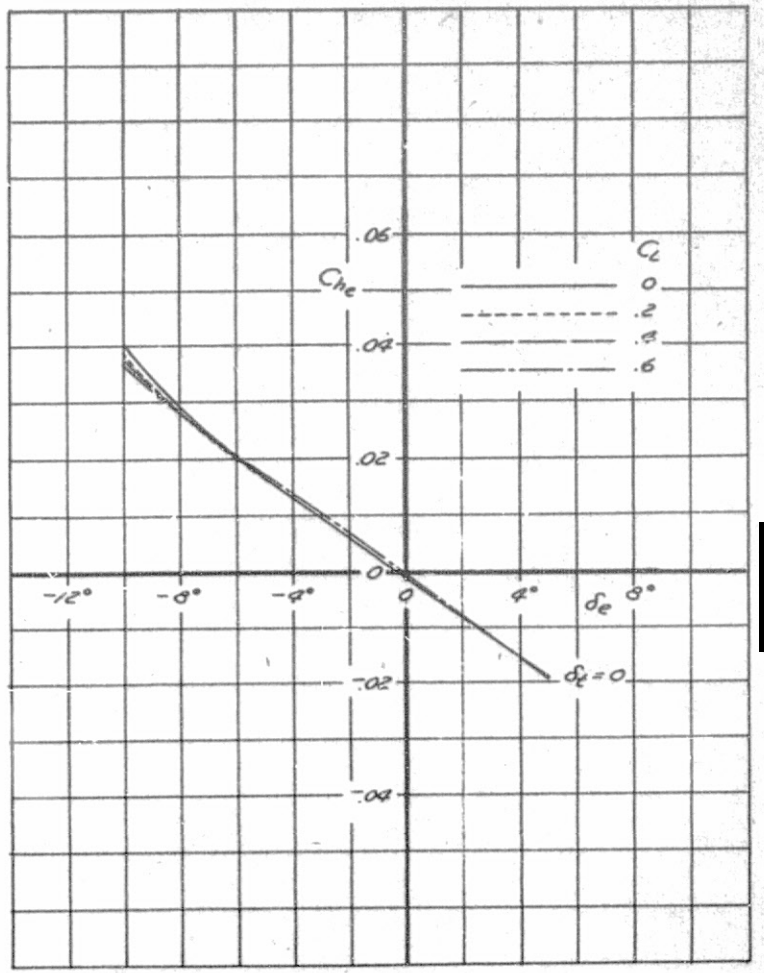

FIGURE 30.-VARIATION OF ELEVATOR HINGE-MOMENT COEFFICIENT WITH ELEVATOR ANGLE ON THE P-47D AIRPLANE MODEL. MACH NUMBER, 0.502

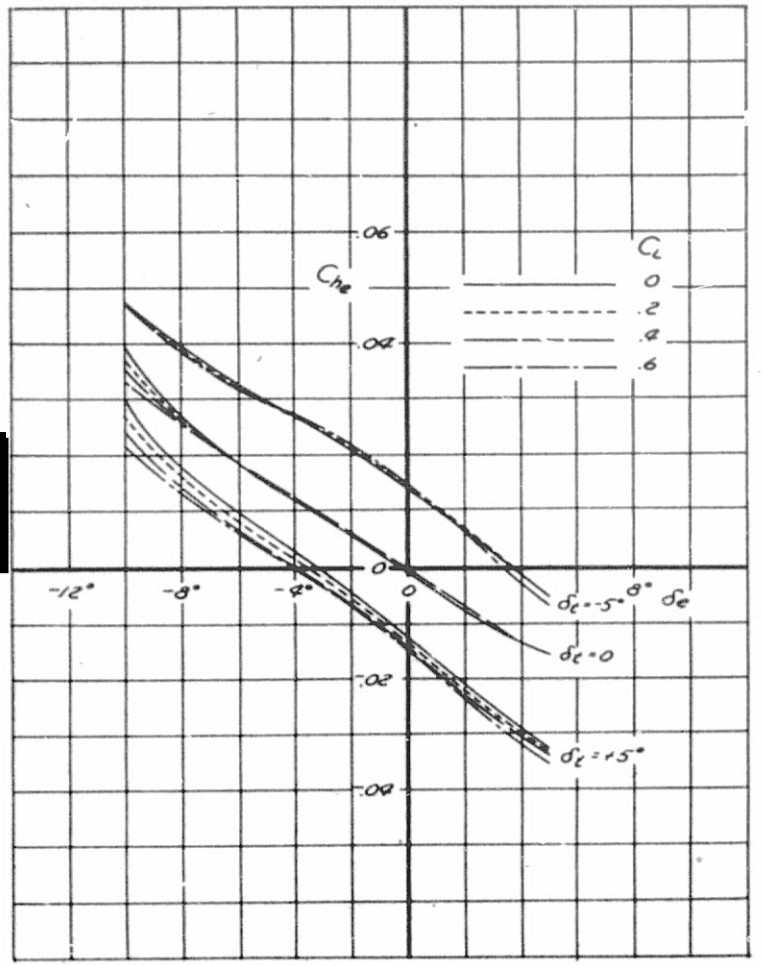

FIGURE 31.-VARIATION OF ELEVATOR HINGE-MOMENT COEFFICIENT WITH ELEVATOR ANGLE FOR THREE ELEVATOR TAB DEFLECTIONS ON THE P-47D AIRPLANE MODEL. MACH NUMBER, 0.591

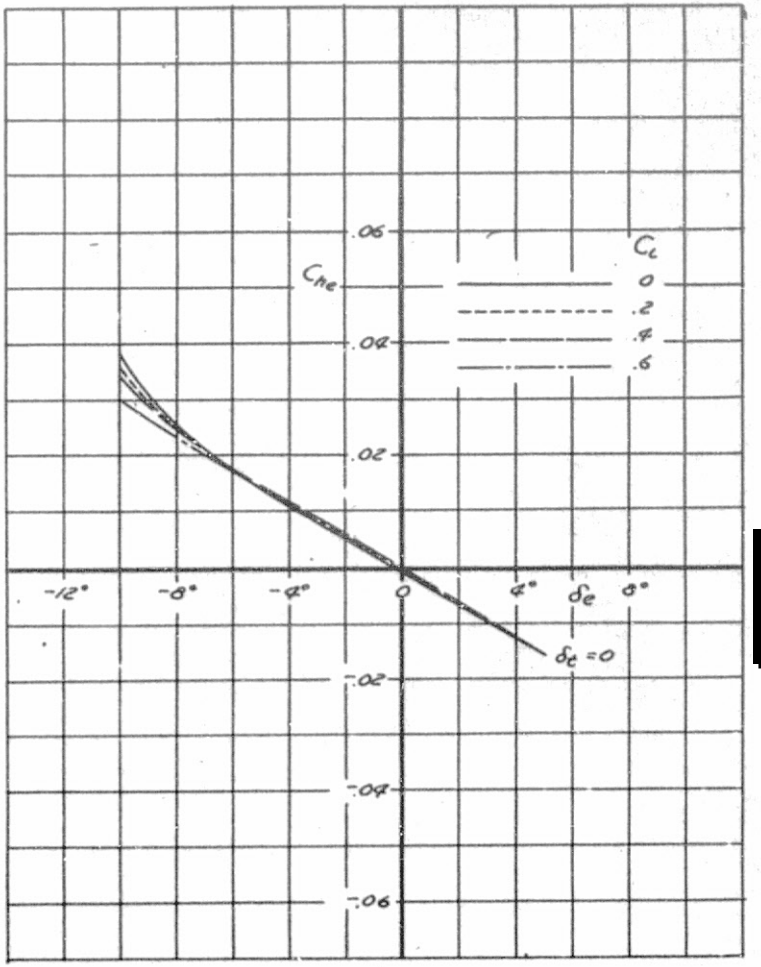

FIGURE 32.-VARIATION OF ELEVATOR HINGE-MOMENT COEFFICIENT WITH ELEVATOR ANGLE FOR THE P-47D AIRPLANE MODEL MACH NUMBER, 0.636

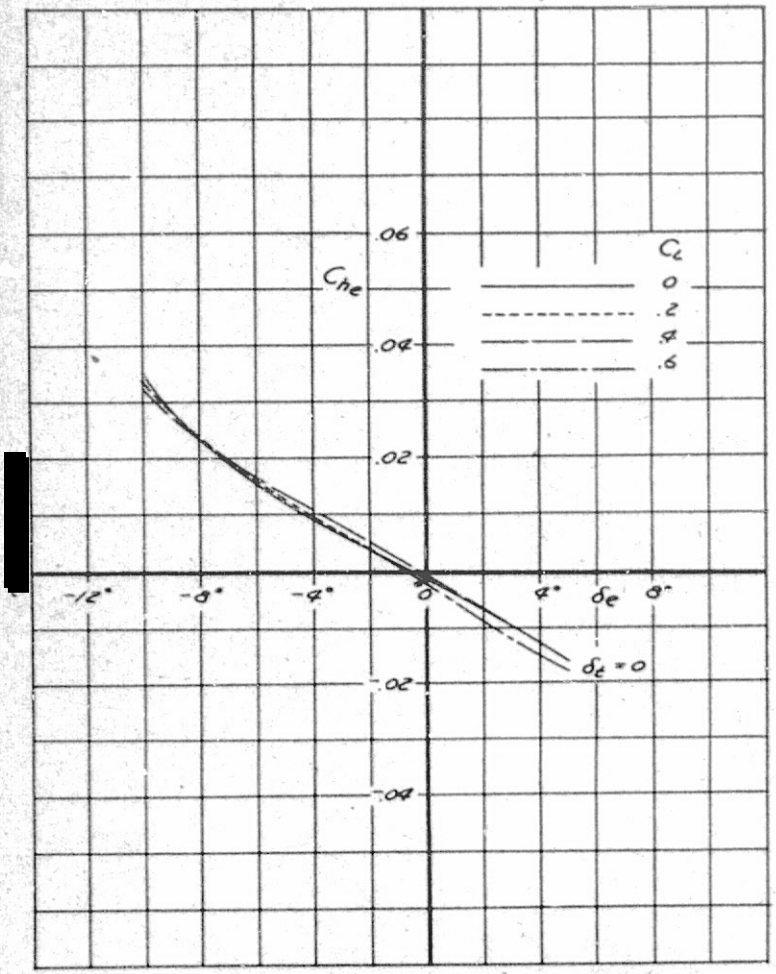

FIGURE 33.—VARIATION OF ELEVATOR HINGE-MOMENT COEFFICIENT WITH ELEVATOR ANGLE ON THE P-47D AIRPLANE MODEL. MACH NUMBER, 0.692.

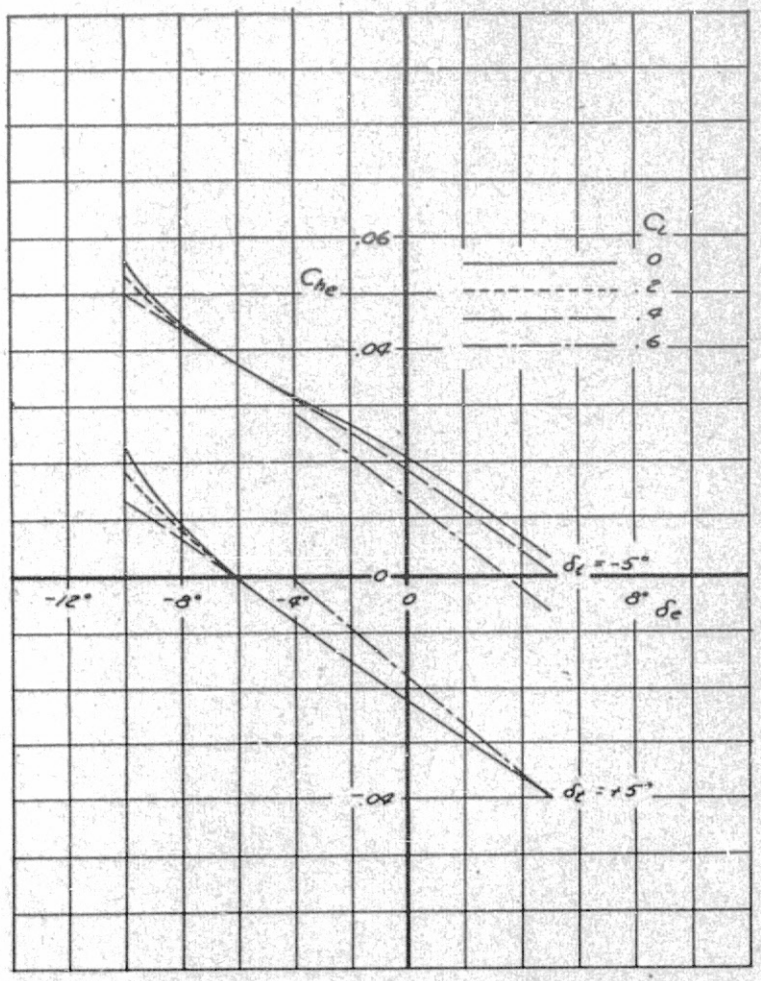

FIGURE 34.—VARIATION OF ELEVATOR HINGE-MOMENT COEFFICIENT WITH ELEVATOR ANGLE FOR TWO ELEVATOR TAB DEFLECTIONS ON THE P-47D AIRPLANE MODEL. MACH NUMBER, 0.731.

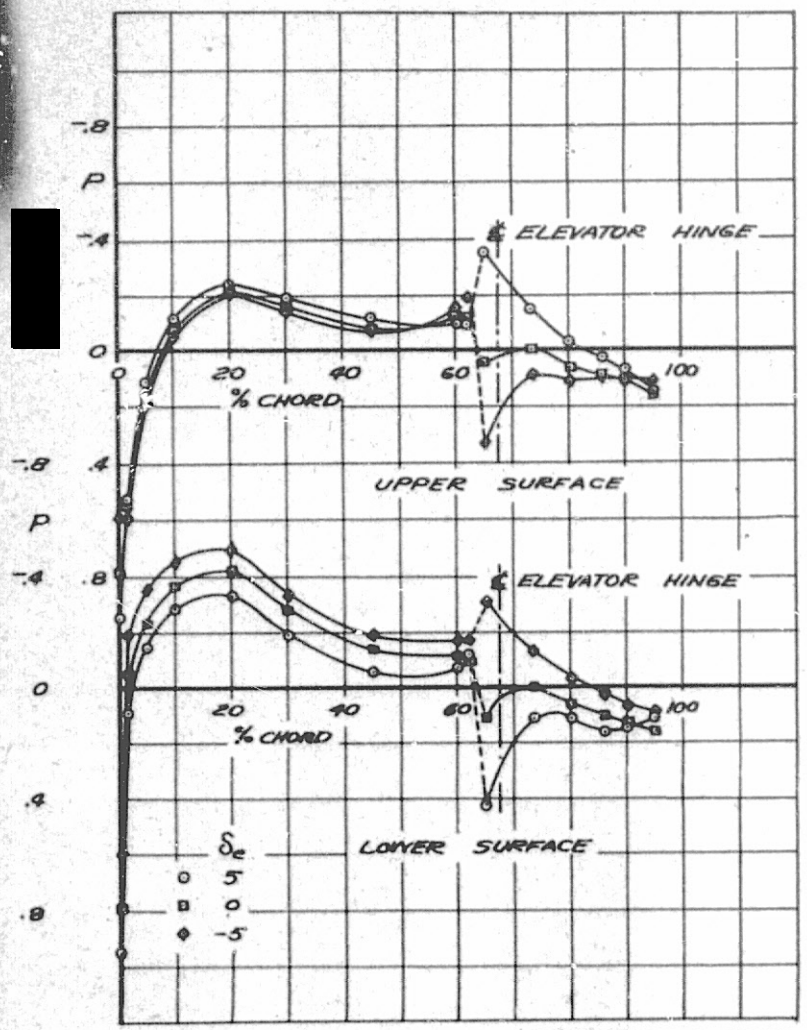

FIGURE 35.- PRESSURE DISTRIBUTION OVER THE HORIZONTAL TAIL OF THE P-47D AIRPLANE MODEL. STATION, 10.00; α, -4.3°; MACH NUMBER, 0.291

NATIONAL ADVISORY COMMITTEE FOR AERONAUTICS

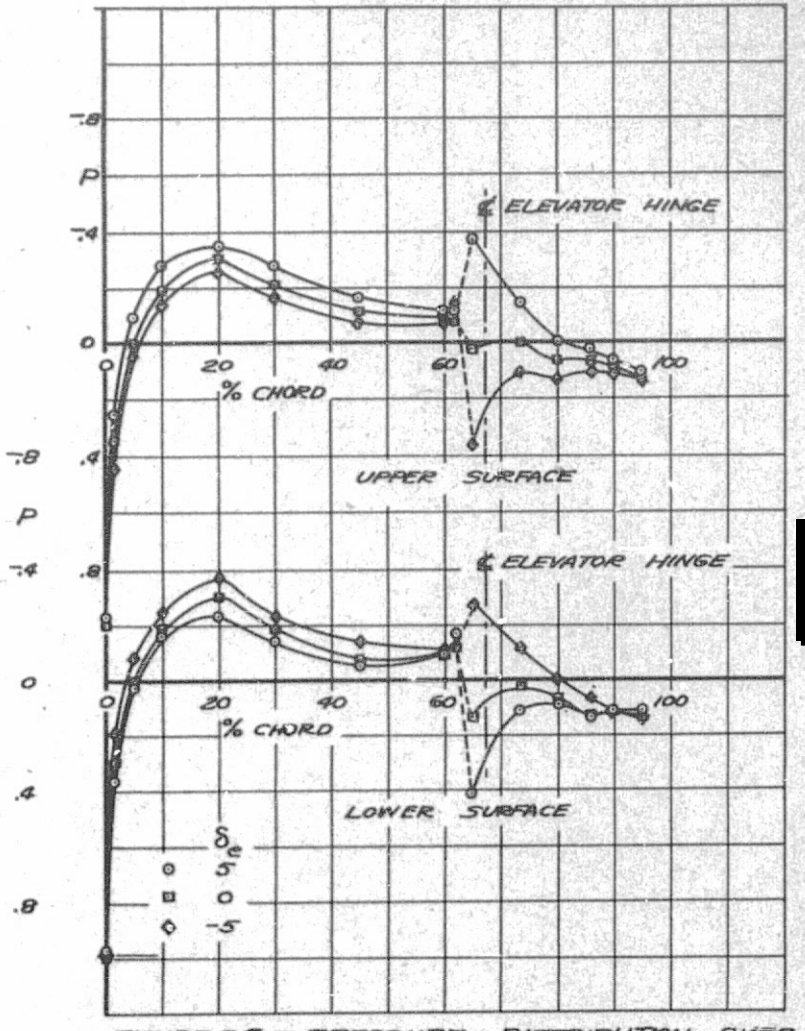

FIGURE 36.- PRESSURE DISTRIBUTION OVER THE HORIZONTAL TAIL OF THE P-47D AIRPLANE MODEL. STATION, 10.00; α, -1.0°; MACH NUMBER, 0.291

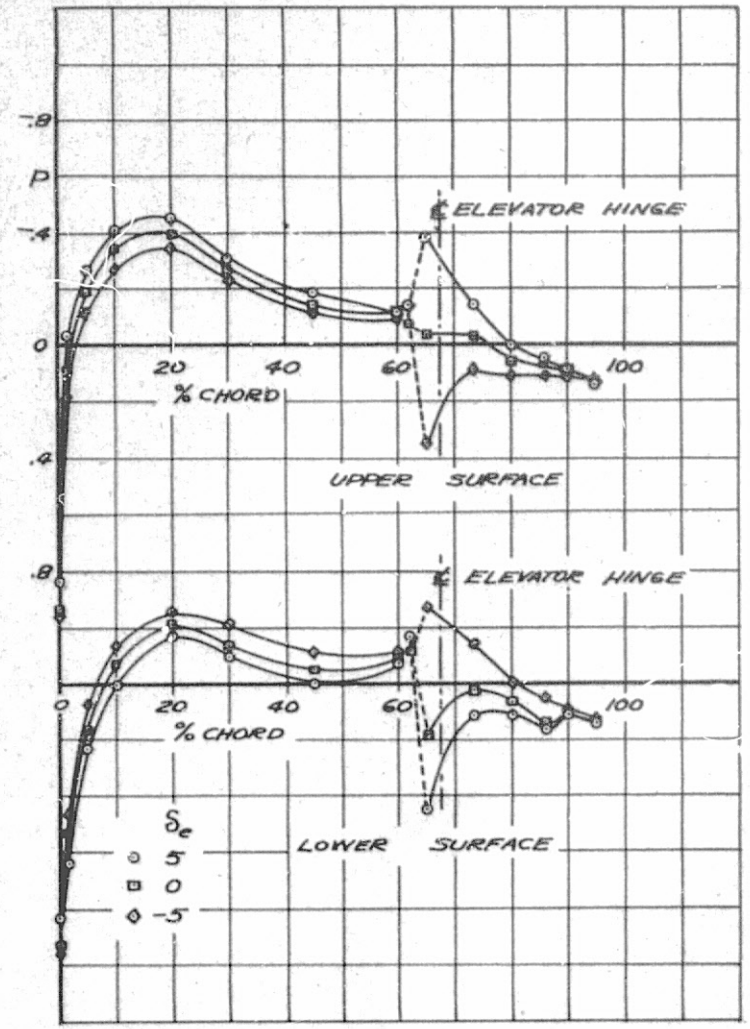

FIGURE 37.- PRESSURE DISTRIBUTION OVER THE HORIZONTAL TAIL OF THE P-47D AIRPLANE MODEL. STATION, 10.00; α, +2.16; MACH NUMBER, 0.291

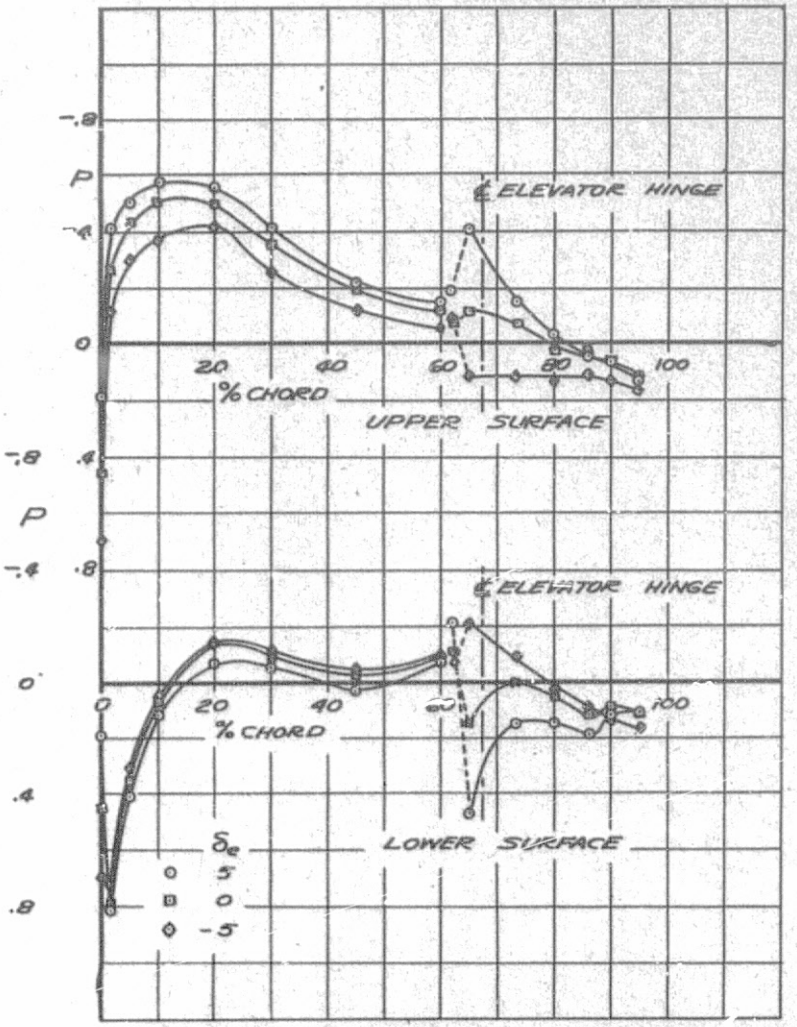

FIGURE 38.- PRESSURE DISTRIBUTION OVER THE HORIZONTAL TAIL OF THE P-47D AIRPLANE MODEL. STATION, 10.00; α, +5.37; MACH NUMBER, 0.291

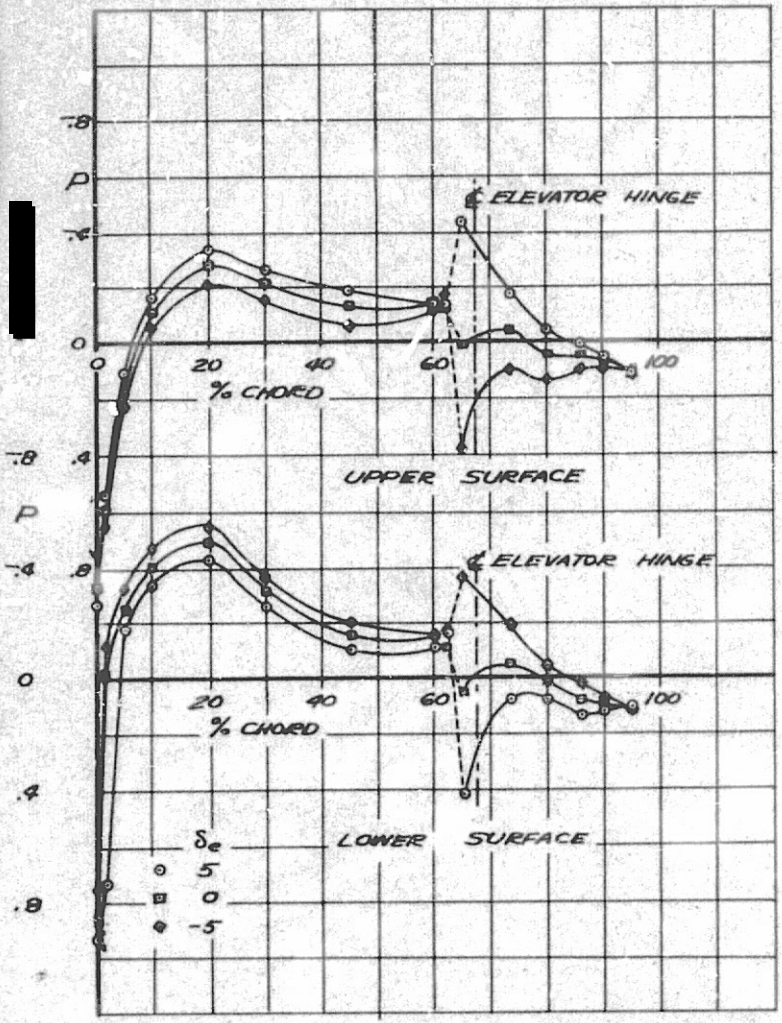

FIGURE 39.— PRESSURE DISTRIBUTION OVER THE HORIZONTAL TAIL OF THE P-47D AIRPLANE MODEL. STATION, 10.00 ; α , -4.45; MACH NUMBER, 0.591

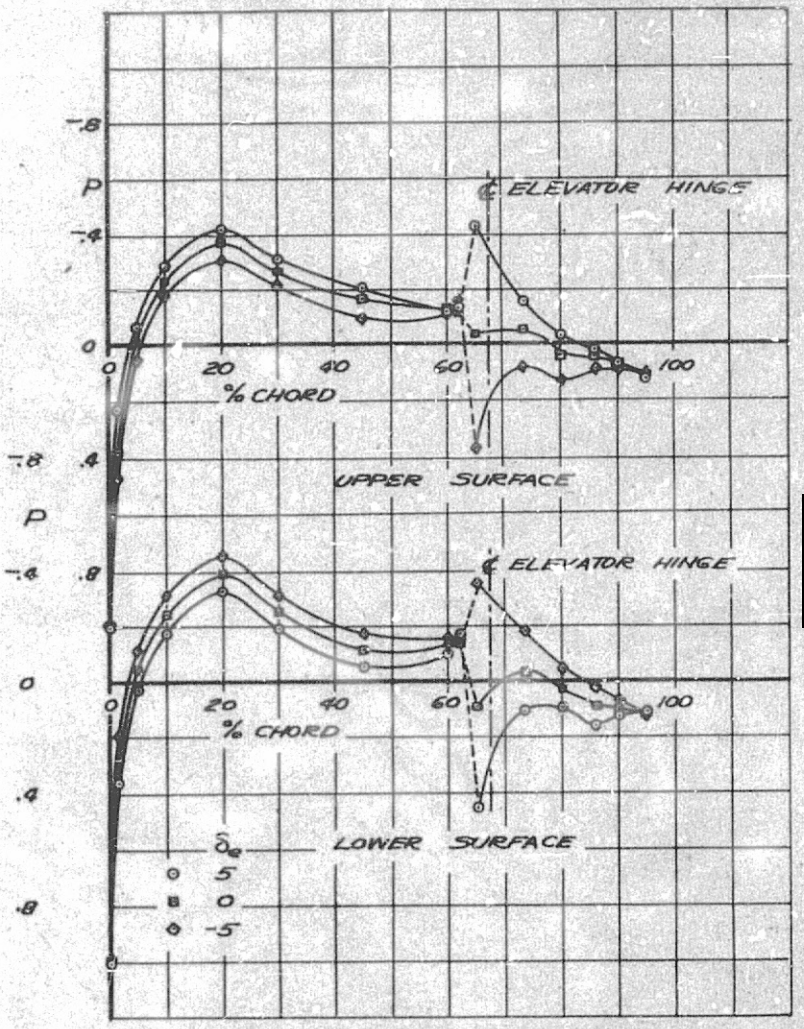

FIGURE 40.— PRESSURE DISTRIBUTION OVER THE HORIZONTAL TAIL OF THE P-47D AIRPLANE MODEL. STATION, 10.00 ; α , -1.22 MACH NUMBER, 0.591

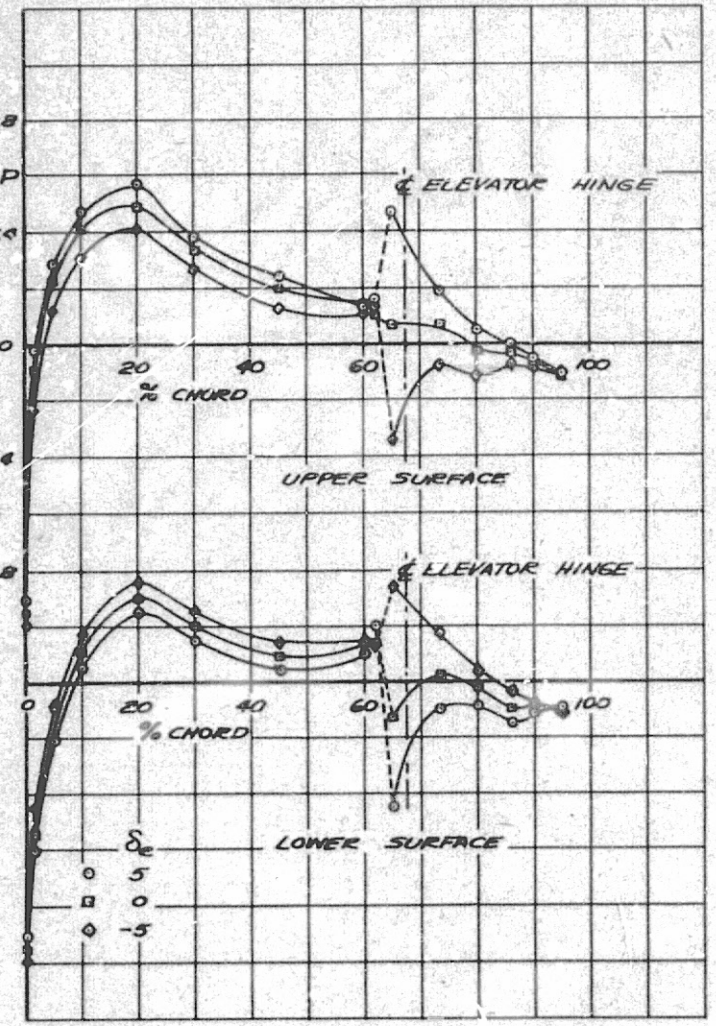

FIGURE 41 — PRESSURE DISTRIBUTION OVER THE HORIZONTAL TAIL OF THE P-47D AIRPLANE MODEL. STATION, 10.00; α, +2.01; MACH NUMBER, 0.591

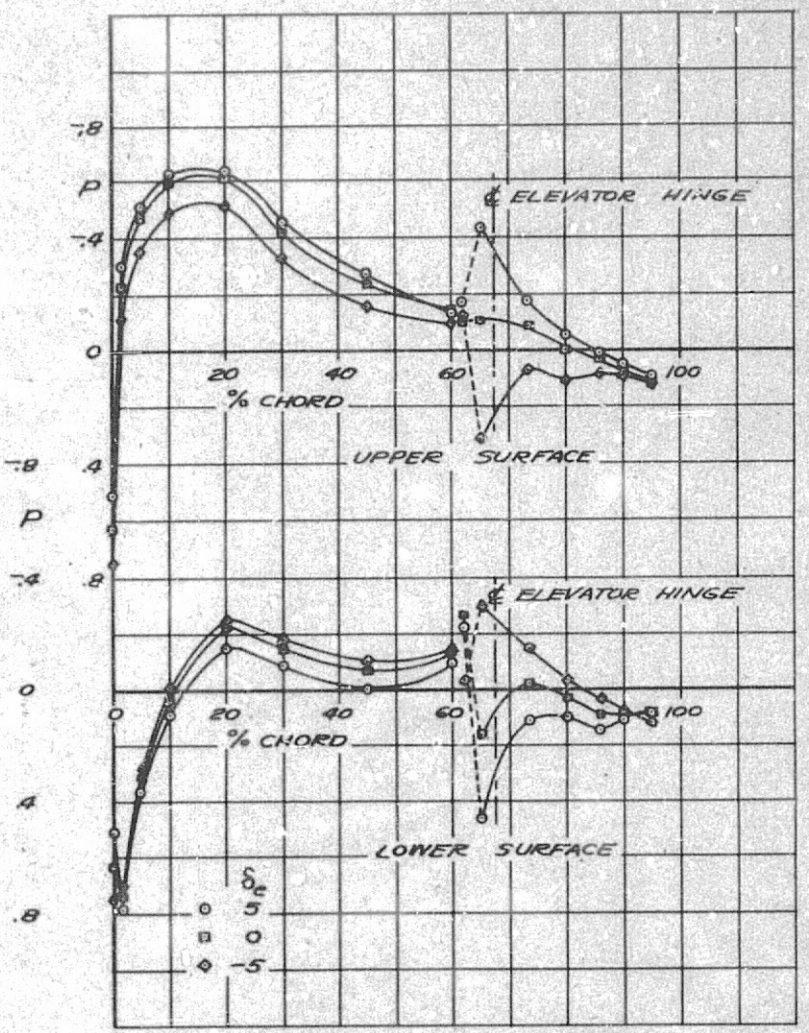

FIGURE 42 — PRESSURE DISTRIBUTION OVER THE HORIZONTAL TAIL OF THE P-47D AIRPLANE MODEL. STATION, 10.00; α, +5.18; MACH NUMBER, 0.591

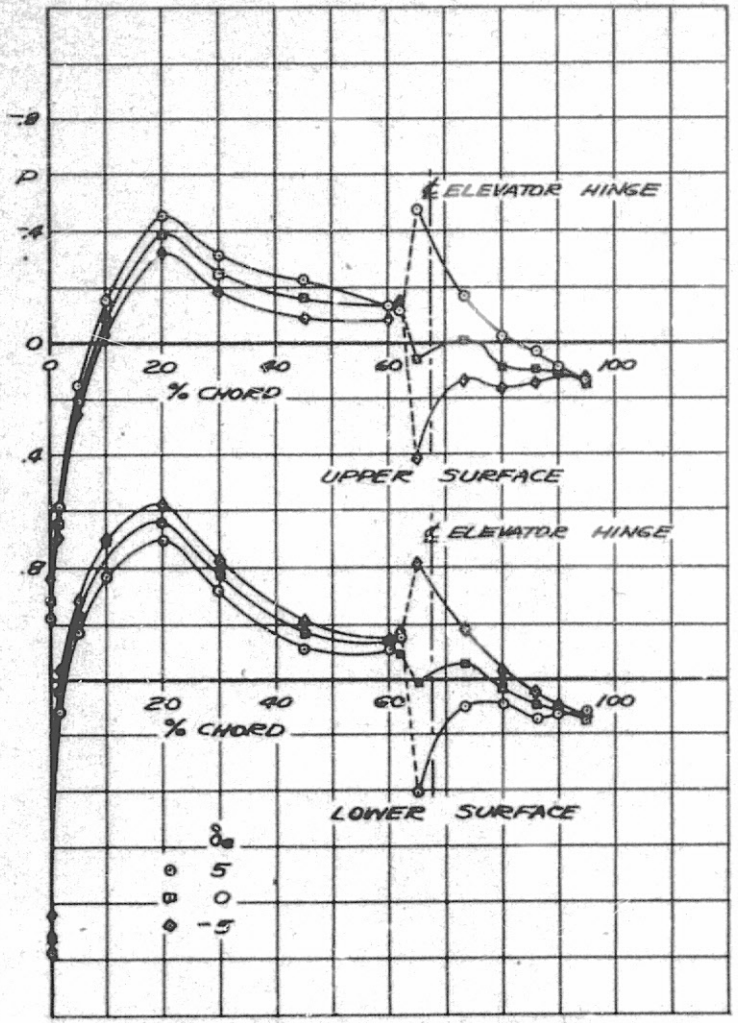

FIGURE 43 — PRESSURE DISTRIBUTION OVER THE HORIZONTAL TAIL OF THE P-47D AIRPLANE MODEL. STATION, 10.00; α -4.45°; MACH NUMBER, 0.731

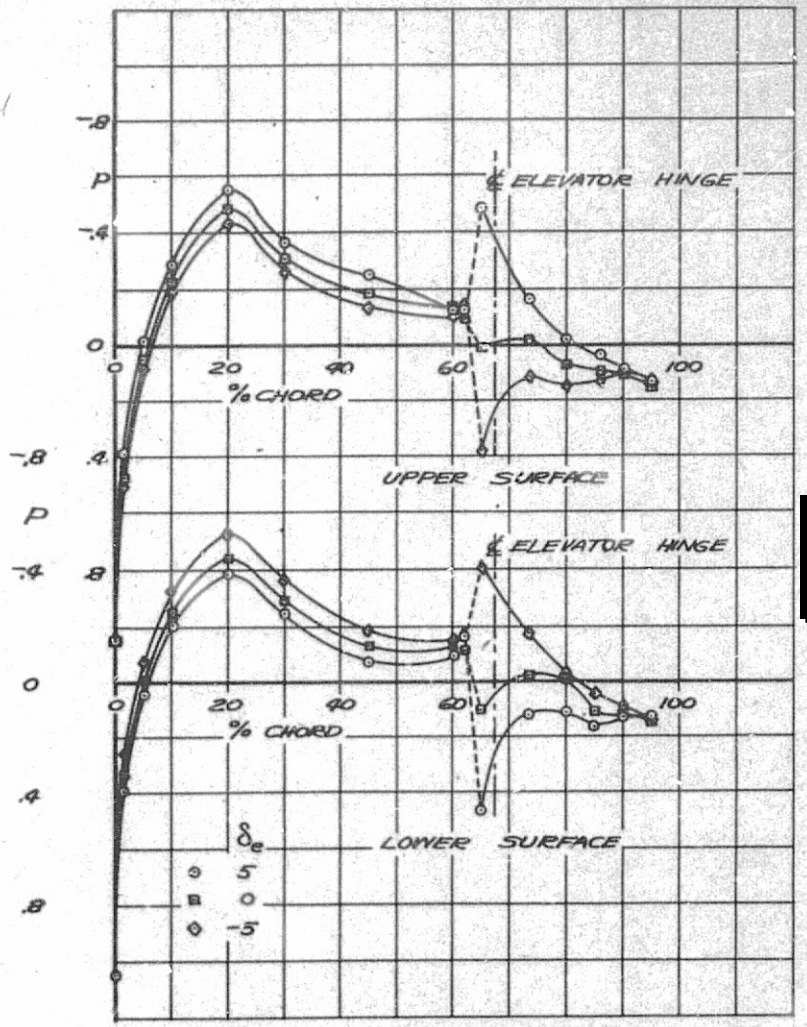

FIGURE 44 — PRESSURE DISTRIBUTION OVER THE HORIZONTAL TAIL OF THE P-47D AIRPLANE MODEL. STATION, 10.00; α -1.21°; MACH NUMBER, 0.731

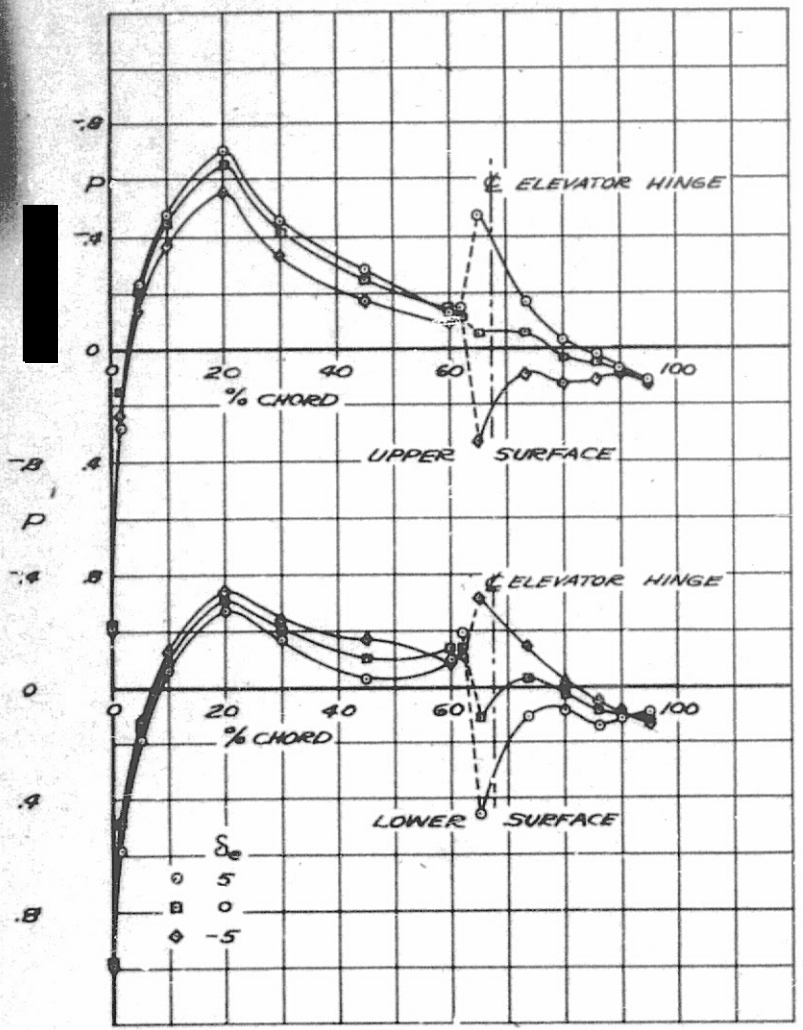

FIGURE 45.— PRESSURE DISTRIBUTION OVER THE HORIZONTAL TAIL OF THE P-47D AIRPLANE MODEL. STATION, 10.00; α, +2.02; MACH NUMBER, 0.731

NATIONAL ADVISORY COMMITTEE FOR AERONAUTICS

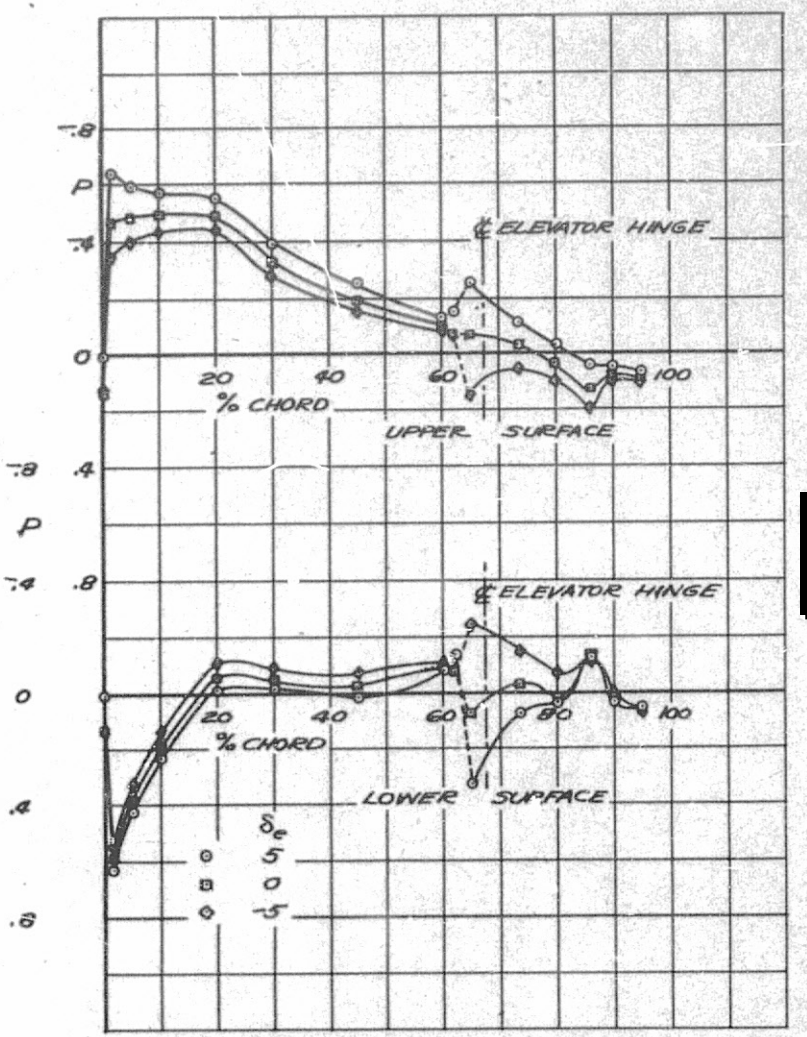

FIGURE 46.— PRESSURE DISTRIBUTION OVER THE HORIZONTAL TAIL OF THE P-47D AIRPLANE MODEL. STATION, 10.00; α, +5.04; MACH NUMBER, 0.731

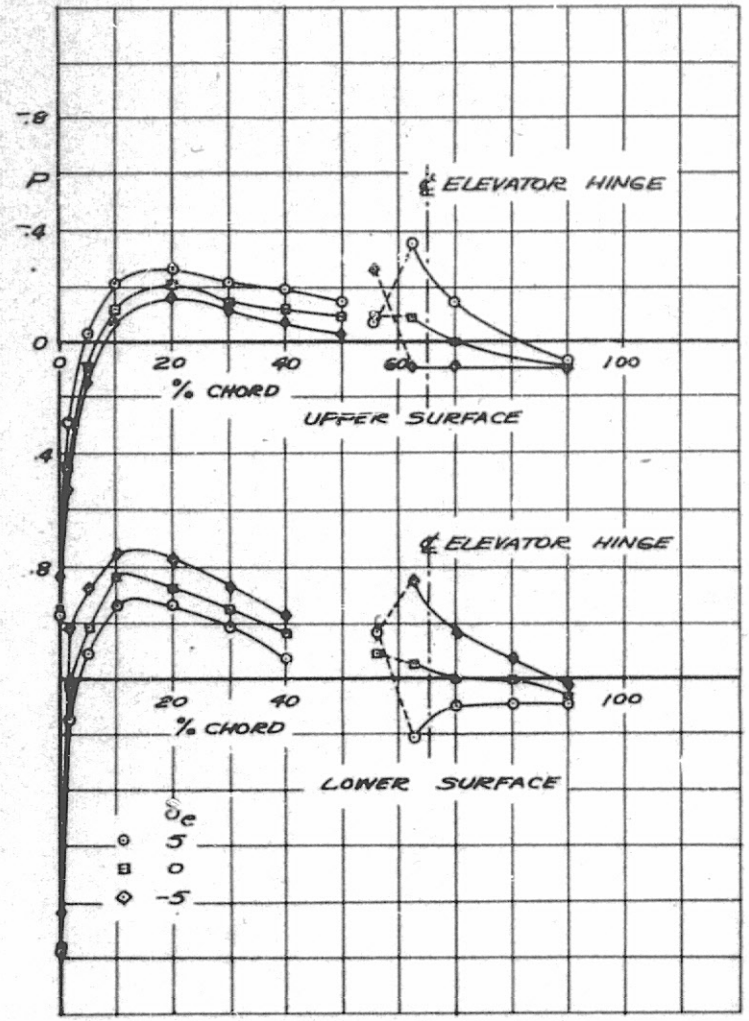

FIGURE 47.—PRESSURE DISTRIBUTION OVER THE HORIZONTAL TAIL OF THE P-47D AIRPLANE MODEL. STATION, 20.325; α, -4.3°; MACH NUMBER, 0.291

NATIONAL ADVISORY COMMITTEE FOR AERONAUTICS

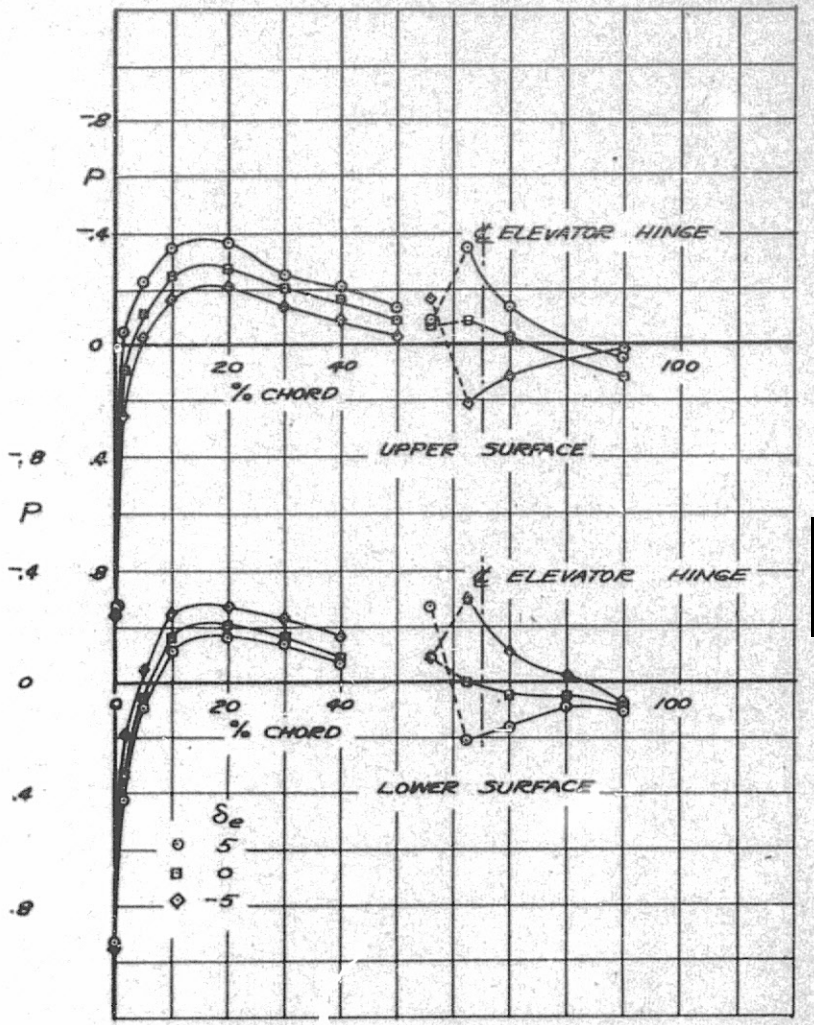

FIGURE 48.—PRESSURE DISTRIBUTION OVER THE HORIZONTAL TAIL OF THE P-47D AIRPLANE MODEL. STATION, 20.325; α, -10.3°; MACH NUMBER, 0.291

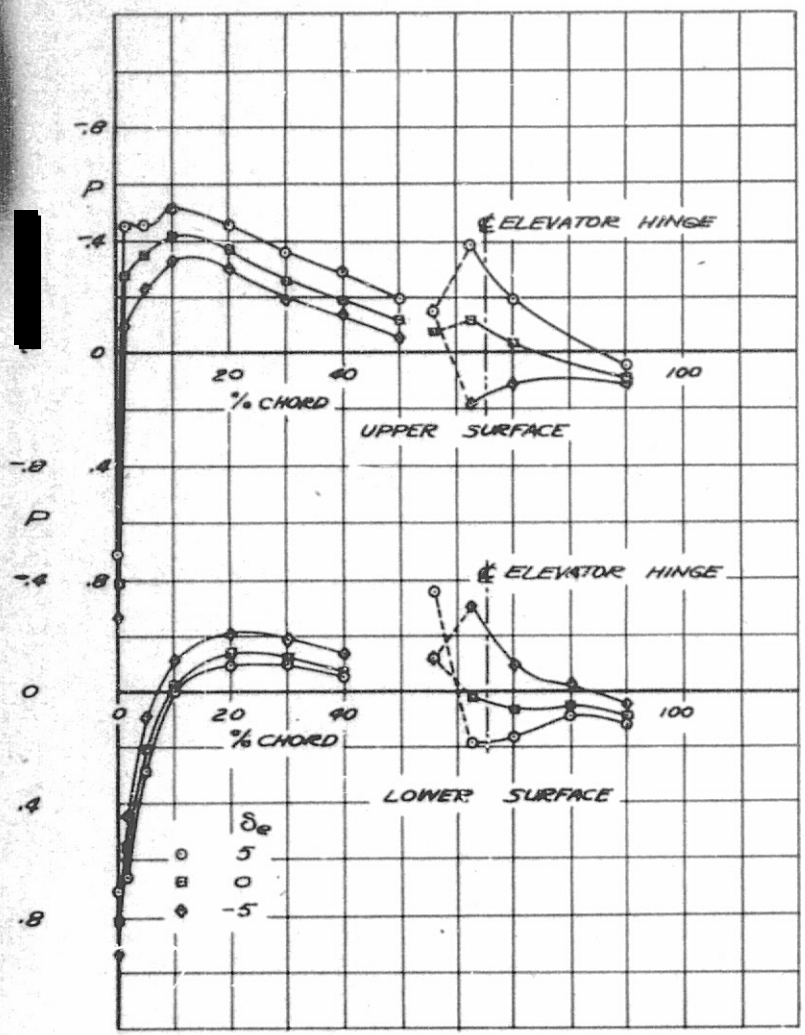

FIGURE 49 — PRESSURE DISTRIBUTION OVER THE HORIZONTAL TAIL OF THE P-47D AIRPLANE MODEL. STATION, 20.325; α, +2.1°; MACH NUMBER, 0.291

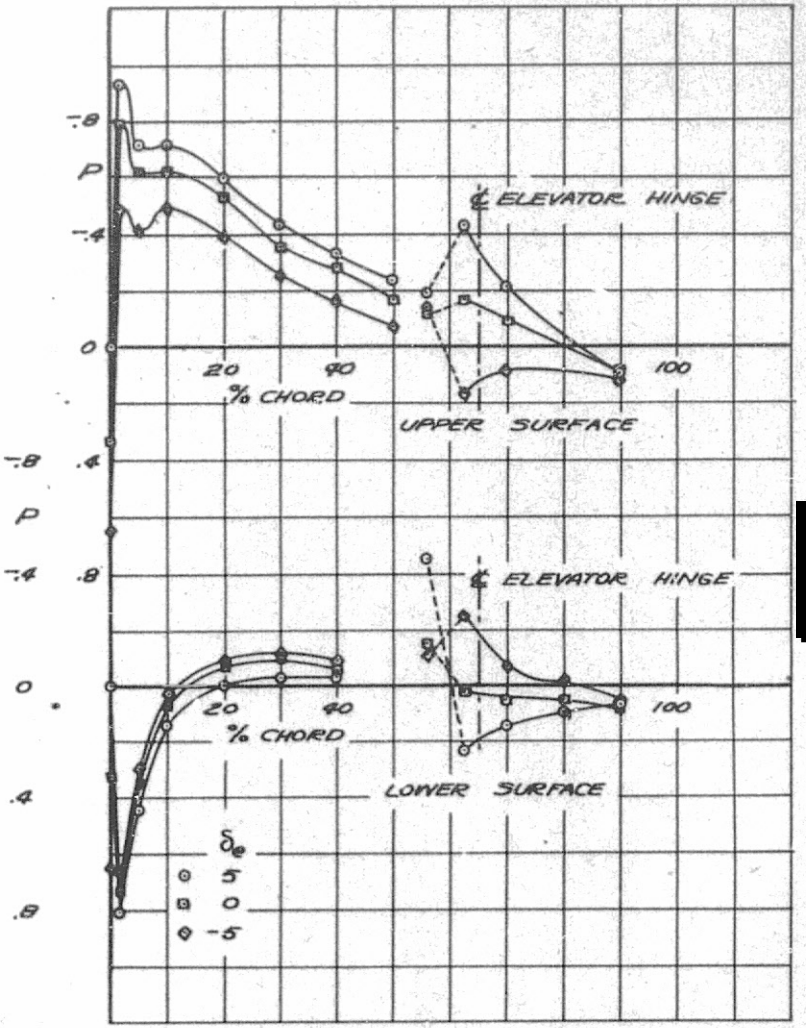

FIGURE 50 — PRESSURE DISTRIBUTION OVER THE HORIZONTAL TAIL OF THE P-47D AIRPLANE MODEL. STATION, 20.325; α, +5.3°; MACH NUMBER, 0.291

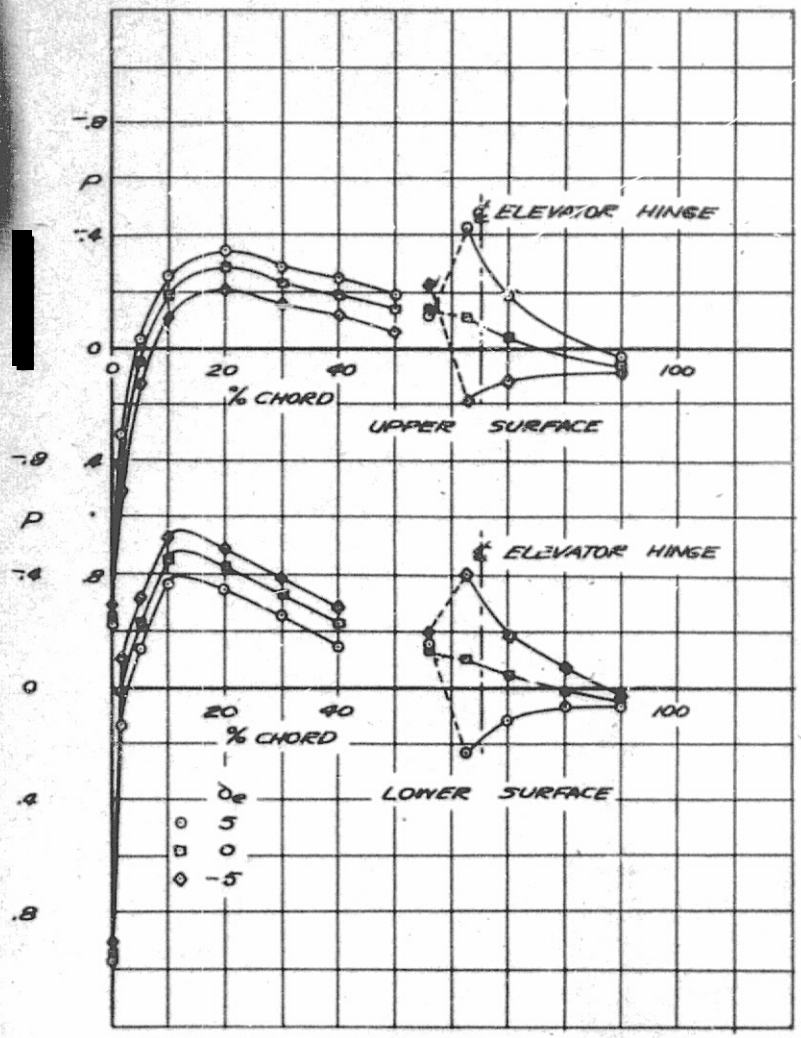

FIGURE 51.- PRESSURE DISTRIBUTION OVER THE HORIZONTAL TAIL OF THE P-47D AIRPLANE MODEL. STATION, 20.325; α, -4.45; MACH NUMBER, 0.591

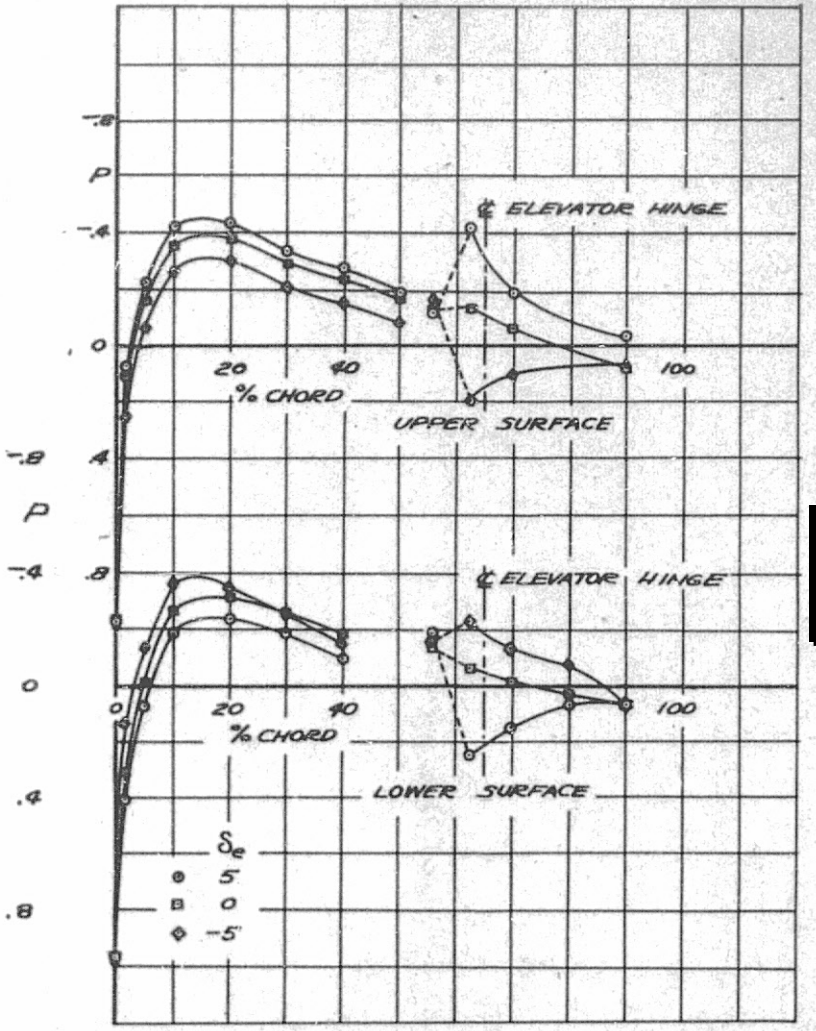

FIGURE 52 - PRESSURE DISTRIBUTION OVER THE HORIZONTAL TAIL OF THE P-47D AIRPLANE MODEL. STATION, 20.325; α, -1.22; MACH NUMBER, 0.591

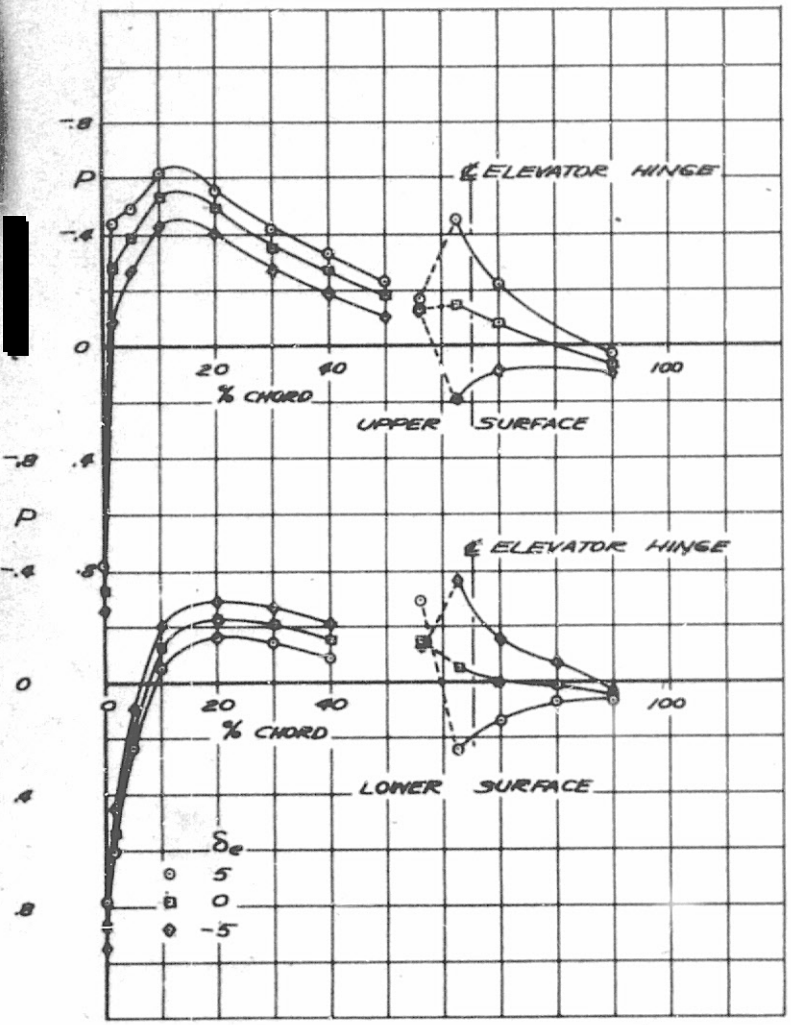

FIGURE 53.— PRESSURE DISTRIBUTION OVER THE HORIZONTAL TAIL OF THE P-47D AIRPLANE MODEL. STATION, 20.325; α, +2.01; MACH NUMBER, 0.591

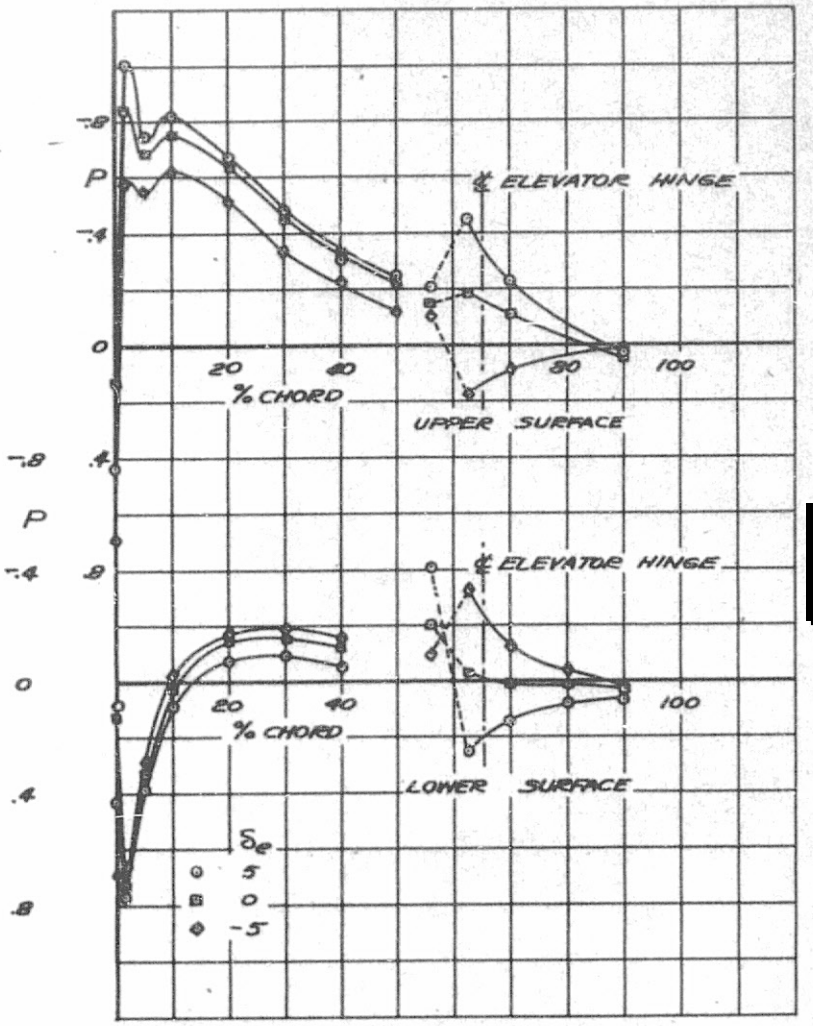

FIGURE 54.— PRESSURE DISTRIBUTION OVER THE HORIZONTAL TAIL OF THE P-47D AIRPLANE MODEL. STATION, 20.325; α, +5.18; MACH NUMBER, 0.591

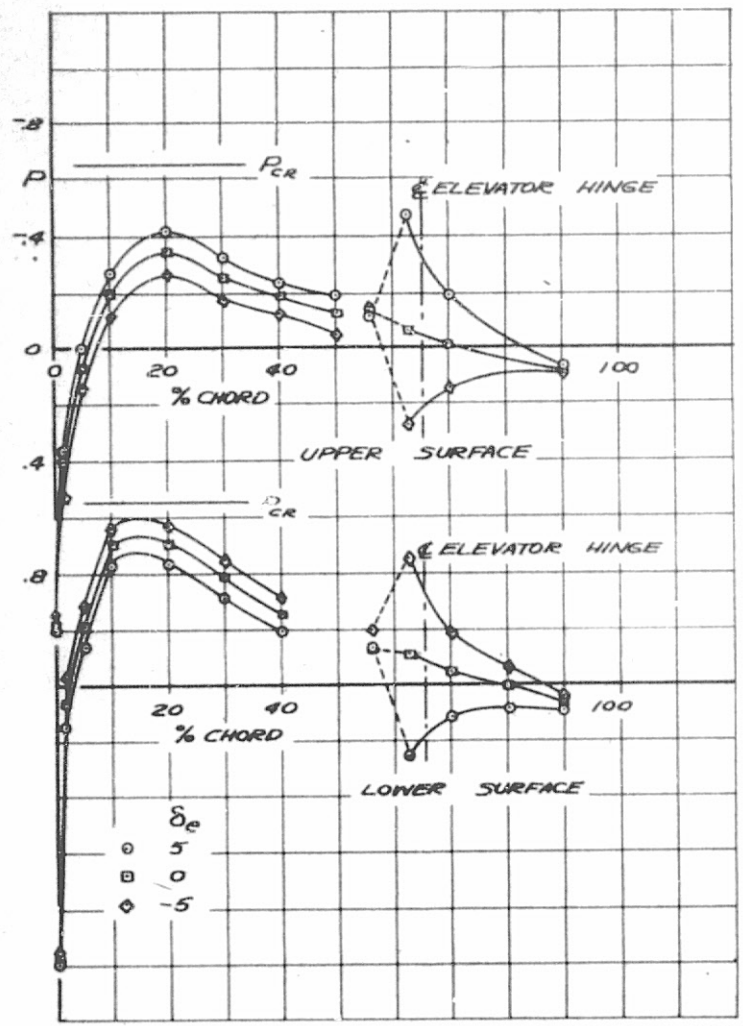

FIGURE 55.— PRESSURE DISTRIBUTION OVER THE HORIZONTAL TAIL OF THE P-47D AIRPLANE MODEL. STATION, 20.325; α, -4.45; MACH NUMBER, 0.731

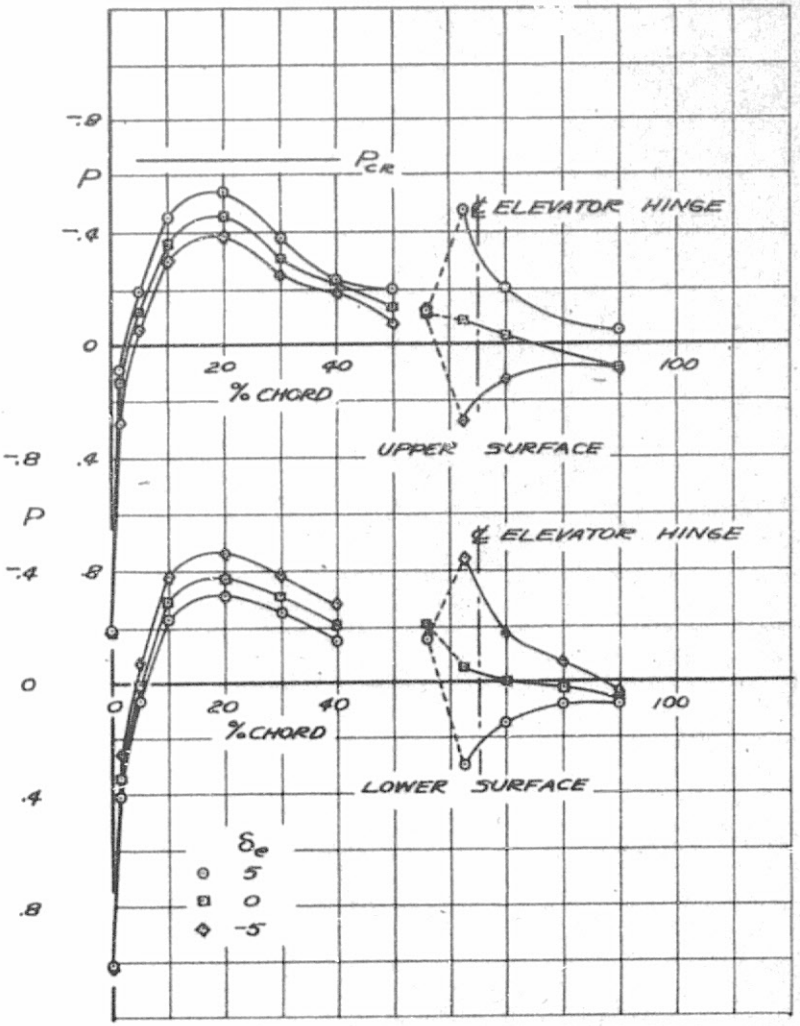

FIGURE 56.— PRESSURE DISTRIBUTION OVER THE HORIZONTAL TAIL OF THE P-47D AIRPLANE MODEL. STATION, 20.325; α, -1.21; MACH NUMBER, 0.731

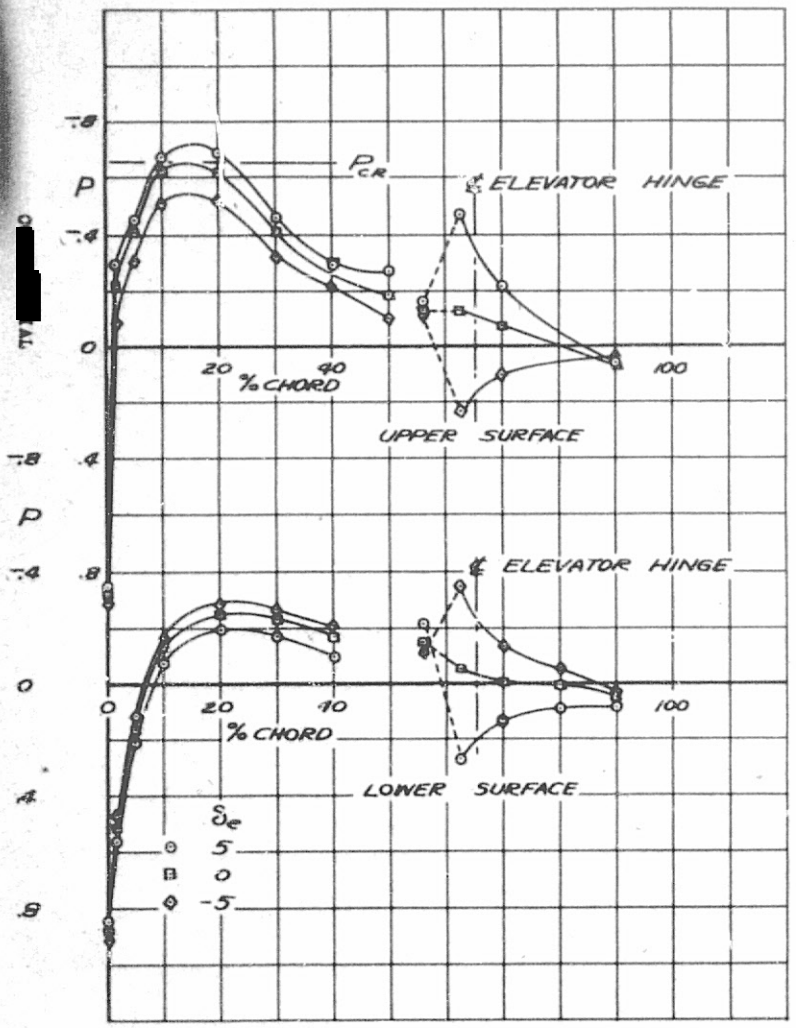

FIGURE 57 — PRESSURE DISTRIBUTION OVER THE HORIZONTAL TAIL OF THE P-47D AIRPLANE MODEL. STATION, 20.325; α, +2.02; MACH NUMBER, 0.731

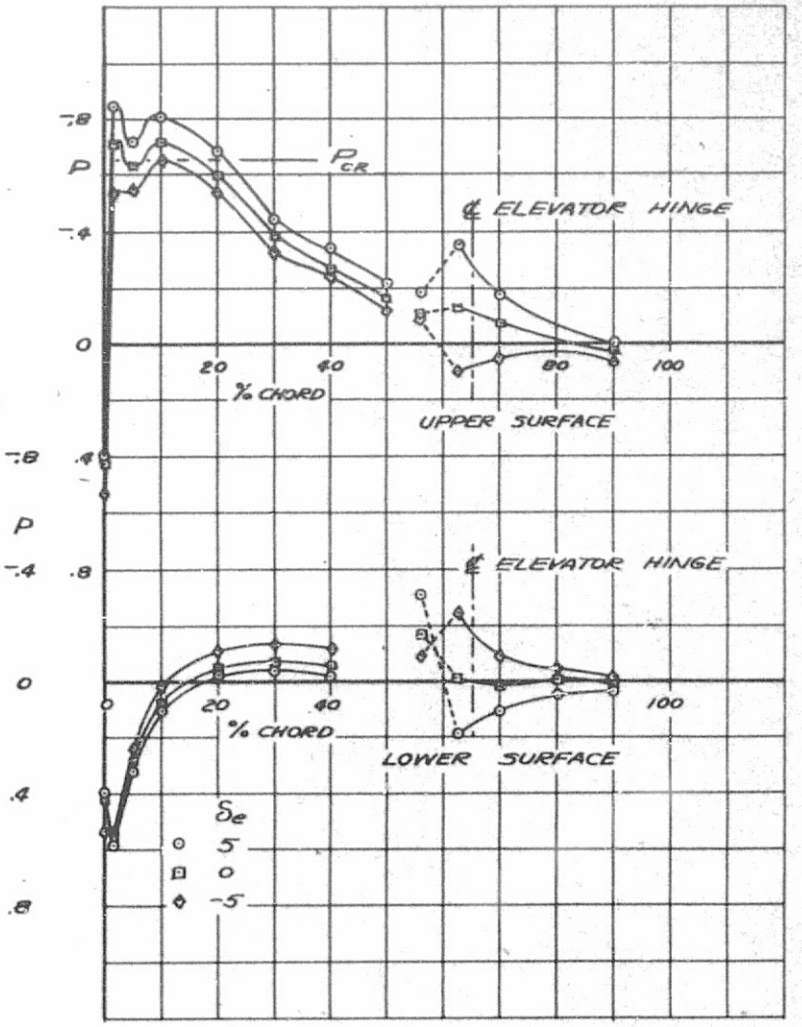

FIGURE 58 — PRESSURE DISTRIBUTION OVER THE HORIZONTAL TAIL OF THE P-47D AIRPLANE MODEL; STATION, 20.325; α, +5.04; MACH NUMBER, 0.731

[redacted]

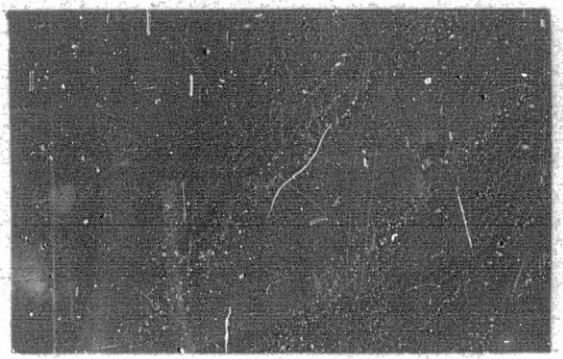

Lower surface, $\alpha_u = -2.5^\circ$

Upper surface, $\alpha_u = -2.5^\circ$

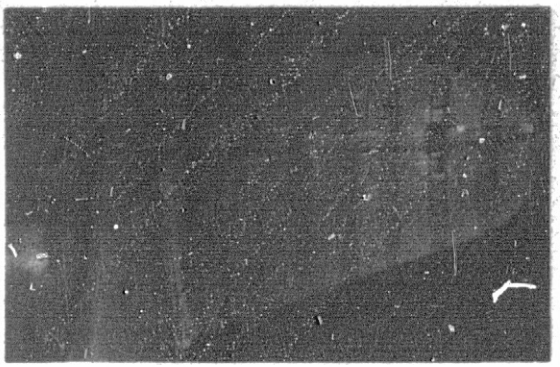

Lower surface, $\alpha_u = +.5^\circ$

Upper surface, $\alpha_u = +.5^\circ$

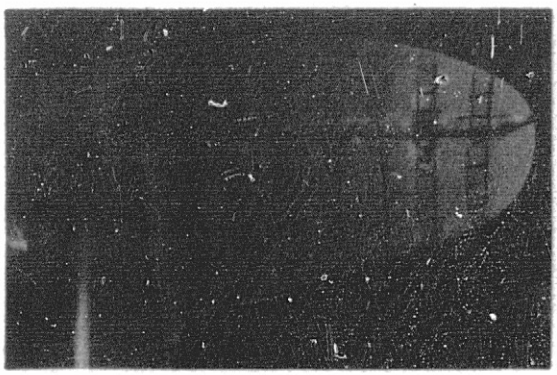

Lower surface, $\alpha_u = +5^\circ$

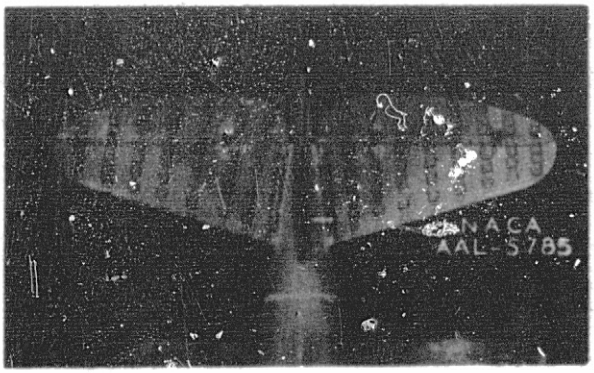

Upper surface, $\alpha_u = +5^\circ$

Figure 59.- Tuft studies of flow over the horizontal tail of the P-47D airplane model. Mach number, .291.

[redacted]

[redacted]

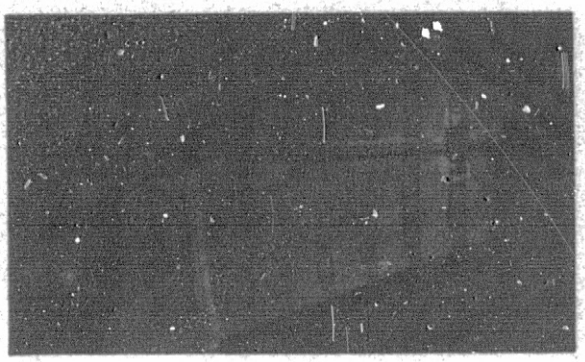

Lower surface, $\alpha_u = -2.5^\circ$

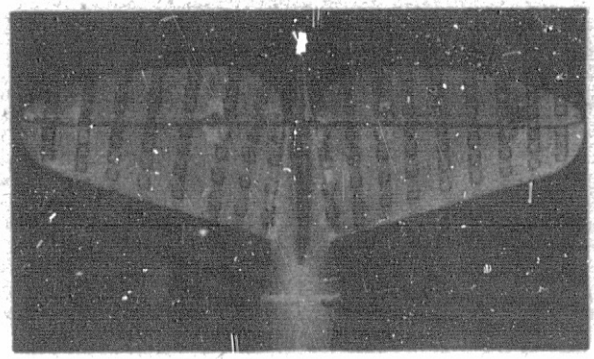

Upper surface, $\alpha_u = -2.5^\circ$

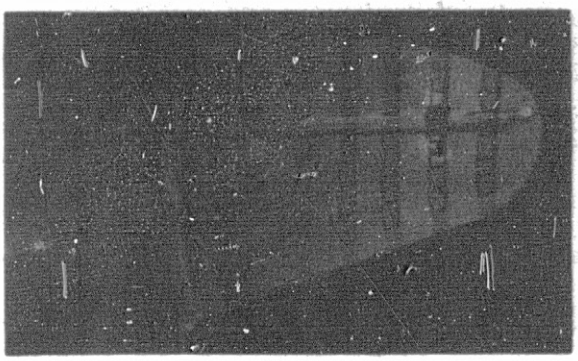

Lower surface, $\alpha_u = +.5^\circ$

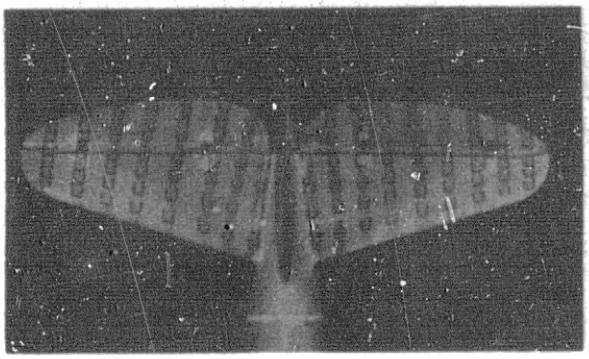

Upper surface, $\alpha_u = +.5^\circ$

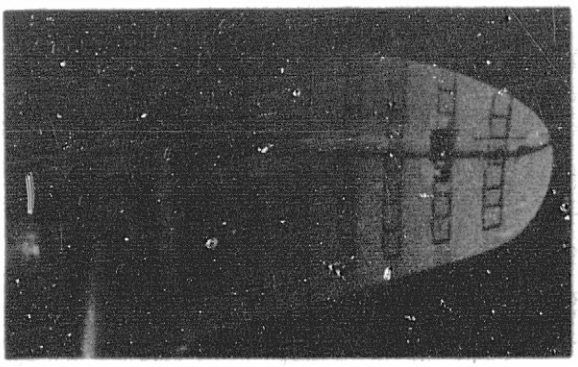

Lower surface, $\alpha_u = +5^\circ$

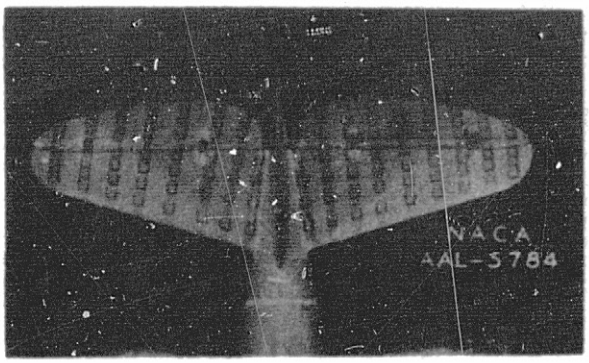

Upper surface, $\alpha_u = +5^\circ$

Figure 60.- Tuft studies of flow over the horizontal tail of the P-47D airplane model. Mach number, .591.

[redacted]

[redacted]

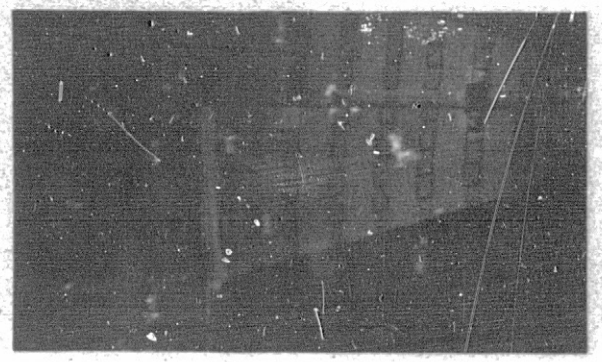

Lower surface, $\alpha_u = -2.5^\circ$

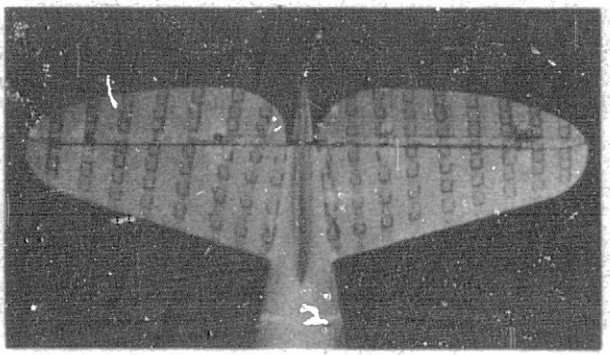

Upper surface, $\alpha_u = -2.5^\circ$

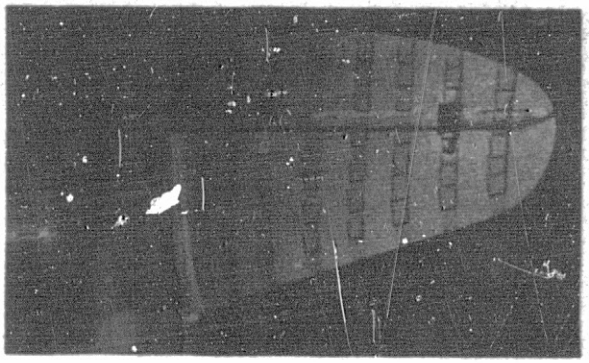

Lower surface, $\alpha_u = +.5^\circ$

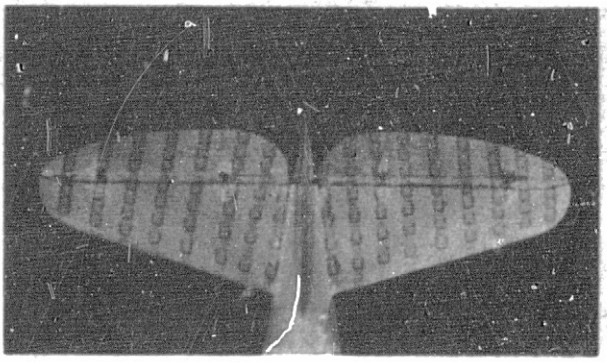

Upper surface, $\alpha_u = +.5^\circ$

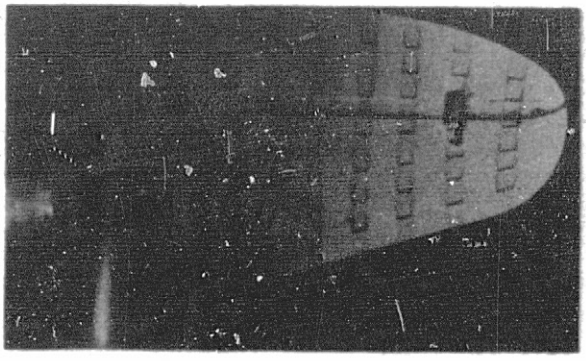

Lower surface, $\alpha_u = +5^\circ$

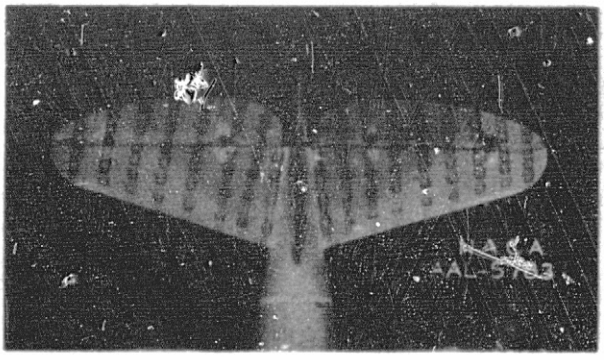

Upper surface, $\alpha_u = +5^\circ$

Figure 61.- Tuft studies of flow over the horizontal tail of the P-47D airplane model. Mach number, .731.

[redacted]

CRITERIA FOR THE LIMITING VALUE OF MACH NUMBER

(a) P_{CR} IS EXCEEDED ON ENGINE COWL
(b) P_{CR} IS EXCEEDED AT WING STATION 10.8
(c) P_{CR} IS EXCEEDED AT WING STATION 30.0
(d) MAGNITUDE OF P_{MAX} DECREASES WITH FURTHER INCREASE OF M (WING STATIONS 10.8 & 30.0)
(e) TUFTS INDICATE FLOW SEPARATES FROM WING SURFACE
(f) $(\partial C_D/\partial M)_{C_L}$ EXCEEDS 0.2
(g) $(\partial C_L/\partial \alpha)_M$ DECREASES SHARPLY
(h) SHARP INCREASE OF STATIC LONGITUDINAL STABILITY IS ENCOUNTERED
(K) DIVING TENDENCY IS ENCOUNTERED

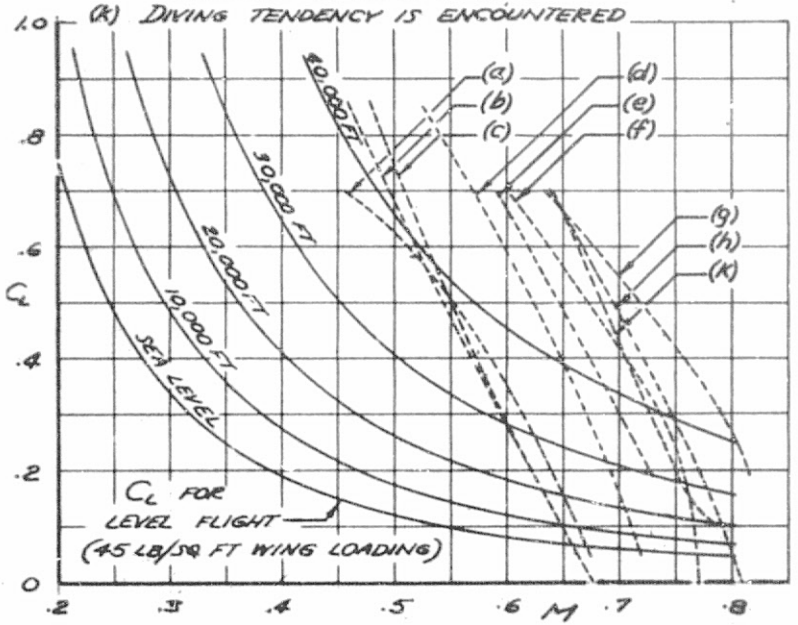

FIGURE 62.-THE LIMITING VALUE OF MACH NUMBER FOR THE P-47D AIRPLANE MODEL AS DETERMINED BY VARIOUS CRITERIA.

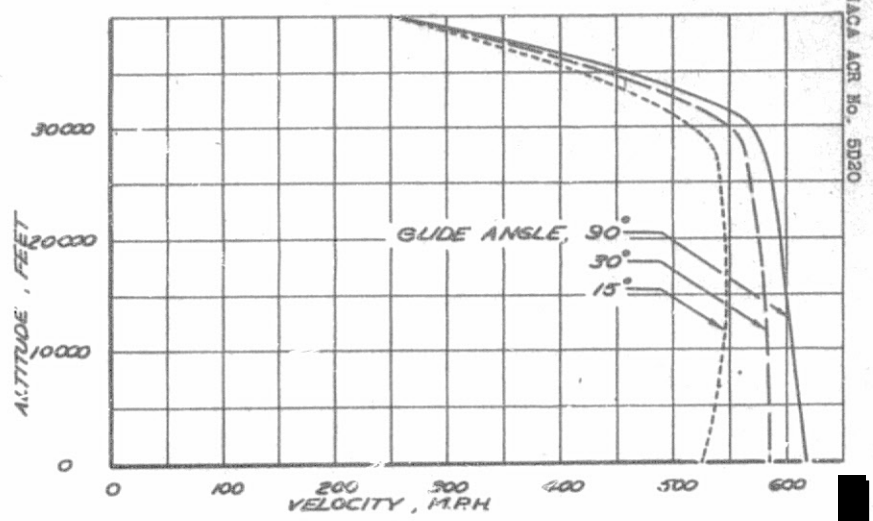

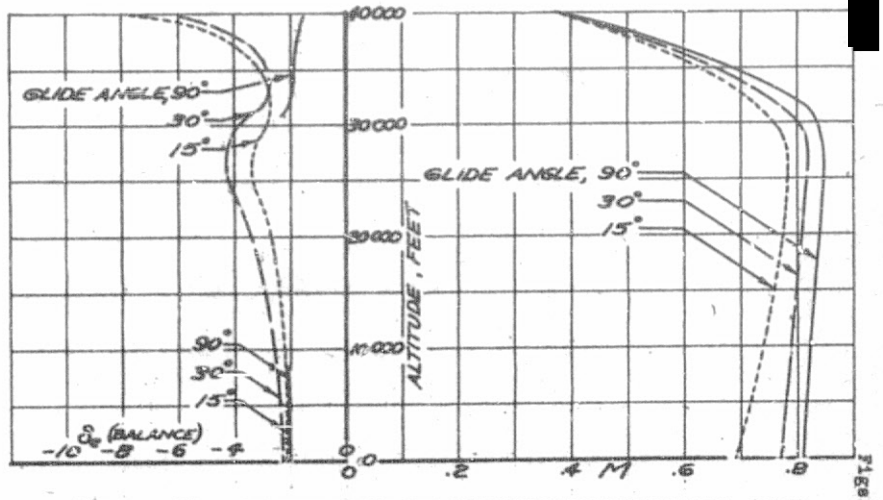

FIGURE 63.-ESTIMATED GLIDING VELOCITY, MACH NUMBER, AND ELEVATOR ANGLE OF THE P-47D AIRPLANE WITH A WING LOADING OF 45 POUNDS PER SQUARE FOOT AND WITH ZERO PROPELLER THRUST.

END